

MINOS Experiment R&D Plan: FY 1996-1998

June 14, 1996

The MINOS Collaboration

Argonne - Boston College - Caltech - Columbia - Dubna - Fermilab -
IHEP-Beijing - Indiana - ITEP-Moscow - Lebedev - Livermore - Minnesota -
Oak Ridge - Oxford - PNPI-St.Petersburg - Rutherford - Stanford -
Sussex - Texas A&M - Texas-Austin - Tufts - Western Washington

Contents

1	Executive Summary	7
2	Introduction	13
3	Physics Update	15
3.1	Status of neutrino oscillations	15
3.1.1	Experimental evidence	15
3.1.2	Sciulli Subpanel conclusions and recommendations	16
3.2	50 GeV JHP experiment in Japan	17
3.3	Possible future scenarios	20
4	Active Detector R&D	22
4.1	Introduction	22
4.1.1	Overview	22
4.1.2	Active detector selection protocol	23
4.1.3	Active detector selection technical criteria	24
4.2	Iarocci chambers	27
4.2.1	Critical issues for Iarocci chambers	27
4.2.2	Current Iarocci chamber development work	27
4.2.3	Iarocci chamber reference design	28
4.2.4	Iarocci chamber R&D plan	31
4.2.5	Iarocci chamber R&D cost estimate	34
4.3	RPC's	36
4.3.1	Critical issues for RPC's	36
4.3.2	Current status of RPC development work	36
4.3.3	RPC reference design	39
4.3.4	RPC R&D schedule milestones	41
4.3.5	RPC R&D cost estimate	42
4.4	Scintillator	43
4.4.1	Scintillator design issues	43
4.4.2	Status of liquid scintillator development	44
4.4.3	Plastic scintillator development	47
4.4.4	Photodetector R&D plan	52
4.4.5	Test beam and electronics plans	53
4.4.6	Calibration and monitoring	53
4.4.7	Plans for a full-scale module	54
4.4.8	Preliminary cost estimate for full detector	54
4.4.9	Liquid scintillator R&D cost estimate	55
4.5	Electronics	57
4.5.1	Electronics design status and issues	57
4.5.2	Current electronics development work	57
4.5.3	Electronics R&D plan	59
4.5.4	Current institutional responsibilities	61

4.5.5	Electronics R&D cost estimate	62
4.6	Test beam plans	63
4.6.1	Schedules and goals for test beam runs	63
4.6.2	Costs associated with test beam runs	64
5	Steel and Magnet Technology	66
5.1	Executive summary	66
5.2	STC Report: Introduction	67
5.3	Criteria for the magnet technology choice	68
5.3.1	Step 1: Definition of Nominal Design	69
5.3.2	Step 2: Credibility demonstration, with implied total cost	70
5.3.3	Step 3: Prototype choice(s)	72
5.4	MINOS Magnet technology options: characteristics, status and critique	72
5.4.1	Reference design	72
5.4.2	Laminated-pie design	77
5.4.3	Spiral-wound coil design	80
5.5	Recommendations to the MINOS Collaboration	84
5.5.1	General recommendations – strategic	84
5.5.2	Specific recommendations – tactical	85
5.6	Summary	86
5.7	R&D plan summary and cost	88
6	Software and Simulations	91
6.1	Introduction	91
6.2	MINOS Software System	93
6.3	The MINOS neutrino event generator	94
6.4	Active detector response simulation	97
6.4.1	Overview	97
6.4.2	Simulation development activities	97
6.4.3	Milestones and schedule	98
6.5	Detector technology and physics goals	99
6.6	Determination of neutrino mixing parameters	103
6.6.1	Δm^2 determination	104
6.6.2	Oscillation mode determination	105
6.6.3	Prospects for observing CP violation in MINOS	106
6.6.4	Future studies	107
6.7	Supplemental R&D funds for simulation work	111
7	Neutrino Beam	112
7.1	Introduction	112
7.2	Beam simulations	112
7.2.1	Oscillation tests	113
7.2.2	Contributions to beam uncertainties	114
7.2.3	Beam software tools	114
7.2.4	Plan for future beam simulation work	116

7.3	Beam options	120
7.3.1	Alternate configurations	120
7.3.2	Beam spill structure	121
7.3.3	Lithium lens development	122
7.4	The neutrino monitor detector	122
7.4.1	Neutrino monitor detector parameters	123
7.5	Near/far detector differences	124
7.6	NuMI beam design and location of the MINOS near hall	125
8	Experiment Optimization Planning at Lutsen	127
8.1	Introduction	127
8.2	Optimization for NC/CC and near-far tests	127
8.2.1	Optimization for the NC/CC test	127
8.2.2	Optimization for the near/far test	130
8.3	Optimization for CC event energy measurement	130
8.4	Optimization for electron identification	132
8.5	Optimization for explicit τ identification	133
9	Soudan Site Preparation	136
9.1	Update on recent developments	136
9.2	Schedule and cost issues	137
10	Cost Estimates and Schedules	139
10.1	Summary of FY 1996-1998 funding requirements	139
10.2	Updated MINOS cost estimate	139
10.3	Schedule	142
11	MINOS Collaboration R&D Effort	144
11.1	Current collaborator activities	144
11.2	Current MINOS collaborator effort	145

List of Tables

1	Summary of MINOS supplemental R&D and construction costs for FY 1995 (in FY 1995 dollars) and FY 1996-8 (in FY 1996 dollars). FY 1998 construction cost estimates are based on the reference detector technology.	11
2	Iarocci chamber components of the overall chamber thickness.	31
3	Iarocci chamber components of the overall chamber width.	31
4	FY 1996 funding for Iarocci chamber R&D work (actual allocations).	34
5	FY 1997 costs for Iarocci chamber R&D work (in FY 1996 dollars).	34
6	FY 1998 costs for active detector construction work (in FY 1996 dollars). This cost estimate was developed for the Iarocci reference detector, but will be similar for other detector technologies.	35
7	FY 1996 funding for RPC R&D work (actual allocations).	42
8	FY 1997 funding for RPC R&D work (in FY 1996 dollars).	42
9	Preliminary cost estimate for the liquid scintillator implementation of the full MINOS far-detector active element system (in FY 1996 dollars). Only direct costs, without contingency, "G&A," and installation, are included.	55
10	FY 1996 funding for liquid scintillator R&D work (actual allocations). Solid scintillator R&D was paid for from institutional funds during FY 1996.	55
11	FY 1997 scintillator R&D funds for solid and liquid scintillator R&D work (in FY 1996 dollars). Development of liquid and solid scintillator options will proceed in parallel during FY 1997.	56
12	Features of different MINOS active detector technologies which must be accommodated by the electronics design	59
13	Current electronics design responsibilities of MINOS institutions.	61
14	FY 1997 funding for electronics R&D work (in FY 1996 dollars).	62
15	FY 1998 funding for electronics work (in FY 1996 dollars).	62
16	FY 1996-8 funding for test beam running (in FY 1996 dollars).	65
17	FY 1996 funding for steel and magnet R&D work (actual allocations).	89
18	FY 1997 costs for steel and magnet R&D work (in FY 1996 dollars).	89
19	FY 1998 costs for steel and magnet R&D work (in FY 1996 dollars).	90
20	Major detector parameters which affect the sensitivity of tests for neutrino oscillations in the MINOS detector.	100
21	Major detector parameters which affect the capability of the MINOS detector to measure neutrino oscillation parameters.	101
22	The theoretical magnitudes of the CP violating quantity $D_{\mu e}$ for MINOS neutrino energies and baseline. Three possible mass-hierarchies have been assumed for each mixing matrix. Experimental ν_e identification efficiencies are not included.	106
23	FY 1995-8 funding for MINOS simulation work (in FY 1996 dollars except for FY 1995).	111
24	Comparison of programs used for neutrino beam simulation.	115
25	Flux of neutrinos at the center of a detector 500 m from the end of the decay pipe, broken down by source and normalized to the ν_μ flux from hadrons produced in the target.	116

26	Summary of supplemental site-related costs for FY 1995 (in FY 1995 dollars) and FY 1996-8 (in FY 1996 dollars).	138
27	Summary of MINOS supplemental R&D and construction costs for FY 1995 (in FY 1995 dollars) and FY 1996-8 (in FY 1996 dollars). FY 1998 construction cost estimates assume the reference detector technology.	140
28	Summary of the cost estimate and funding profile for the MINOS experiment, excluding NuMI beam and civil construction costs at Fermilab (in millions of FY 1996 dollars).	142
29	Current FTE effort levels at MINOS collaborating institutions.	148

List of Figures

1	Overall design and construction schedule for the MINOS experiment. The time scale shown is in fiscal years.	12
2	The relative light yield (I) data (circles) as a function of distance (x) along an unmirrored wavelength shifting fiber. The expected light yield in mirrored fibers is indicated by the curve.	45
3	A full plane of liquid scintillator modules including manifold block and photodetectors.	48
4	This cut-away (Detail 'A') shows the fiber bypass block near the central hole.	49
5	The cut-away of the endcap of a module (Detail 'B').	50
6	Error contours obtained from the energy measurements of ν_μ CC events for $\nu_\mu \rightarrow \nu_\tau$ oscillations with $\Delta m^2 = 0.01 \text{ eV}^2$ and $\sin^2(2\theta) = 0.7$. The simulated event sample includes backgrounds.	108
7	A comparison of the estimated statistical errors on Δm^2 (upper figure) and $\sin^2(2\theta)$ (lower figure) that would be obtained by fitting the E_{vis} distribution of 3000 measured ν_μ CC events for the old two-horn beam design, and the on-axis and 3 and 5 mr off-axis three-horn designs of a wide-band beam. This figure simply demonstrates how the errors change due to the different shapes of the E_ν distributions of the beams. The relative event rates (in the approximate ratios of 3:4:2:1) must be allowed for but are not included. . . .	109
8	Results of a fit of oscillation parameters to a simulated 3.3 kT-yr exposure of the MINOS detector in the two-horn wide-band beam when the true oscillation mode is maximal mixing with $\Delta m^2 = 0.0072 \text{ eV}^2$. Maximal mixing is represented by the centroid of the triangle. The vertices are pure flavor states. The matrix elements, $ U_{\alpha 3} ^2$, are the perpendicular distances of a point to the sides of the triangle.	110
9	ν_μ flux from hadrons produced in the target, and from secondary interactions, at the center of a detector 500 m from the end of the decay tunnel.	118
10	ν flux components at the center of a detector 500 m from the end of the decay tunnel.	119
11	Overall design and construction schedule for the MINOS experiment. The time scale shown is in fiscal years.	143

1 Executive Summary

This document describes the MINOS Collaboration plan to complete the design of the E-875 long-baseline neutrino oscillation experiment on a schedule which will allow data taking to begin in June 2001. This requires completion of:

- The NuMI neutrino beam and MINOS near detector at Fermilab,
- Excavation of the far detector hall in Soudan, Minnesota,
- Installation of the first third of the 10 kton MINOS far detector.

In order for these three components of the experiment, often referred to as “NuMI,” “Soudan,” and “MINOS”, to be ready in June 2001, all design work must be completed during FY 1996, 1997, and 1998. The Soudan excavation work must begin in the spring of 1998, and NuMI and MINOS construction work must start in FY 1999.

The design of the MINOS experiment was described in the February 1995 P-875 Proposal [1]. Very briefly, this reference design, which was used to calculate the physics reach and cost of the experiment, was based on a 10 kT far detector located 730 km from Fermilab in the Soudan underground laboratory. This 8-m diameter, 36-m long detector consisted of alternating planes of 4-cm thick magnetized steel and Iarocci tube detectors with an effective 2 cm transverse granularity. Since the time of the submittal of the MINOS Proposal, the experiment design has evolved as a result of interactions with the Fermilab PAC and the HEPAP Subpanel on Neutrino Oscillation Experiments [2, 3, 4, 5, 6], as well as significant R&D progress and discussions within our growing collaboration. Although the parameters of the experiment have been modified somewhat during the past year, they are still very similar to what was presented to the HEPAP Subpanel in June 1995.

Before the designs of major experimental systems are frozen near the end of FY 1997, the MINOS Collaboration and the Fermilab NuMI group will complete an intensive development program to explore the designs of the active detector technology, the fabrication technique for the steel detector planes, the neutrino beam configuration, and the near detector hall civil construction and location. The ultimate sensitivity of the experiment will be determined by how well the beam and detector designs are optimized during this period. The beam, active detector and steel plane systems are the three most expensive components of the experiment, and we are devoting considerable attention to the optimization of their designs, construction techniques and performance. This document describes our plan and funding needs for this program, as well as the procedure we have established for making key technology decisions.

Previously, the MINOS Collaboration has proposed a detailed plan for its detector R&D program, described in its FY 1996 funding request to DOE and Fermilab, “MINOS Detector R&D Plan” [7]. In the present document, we describe our detector development program in more detail, and also discuss two related activities: the initial preparations for the excavation of the new far detector hall in the Soudan mine, and the design of the NuMI neutrino beam for which Fermilab has assumed primary responsibility.

In spite of the sizable funding shortfall in FY 1996, the Collaboration has made significant progress in all areas of detector R&D. We now have much higher confidence in our active detector reference design and the development of alternative technologies has progressed to

a point that a quantitative cost and performance comparison will soon be possible. We are optimistic that the MINOS detector we ultimately build may be substantially better than the original reference design. Our understanding of technical issues related to the fabrication of the 8-m wide magnetized steel octagons is now good enough that we plan to construct at least one full-size prototype plane at the beginning of 1997. A new GEANT-based Monte Carlo detector simulation code has been developed which will allow us to calculate detector performance much more reliably.

During the next two years the MINOS Collaboration will continue to concentrate its effort in the area of active detector technology. This work will incorporate a range of activities, such as further laboratory and cosmic-ray tests of detector prototypes, more sophisticated simulations of detector performance, accelerator beam tests, and the engineering design of detector systems. In parallel, we shall continue our studies, both experimental and calculational, to determine the optimum steel plane design. We have chosen several different oscillation tests as benchmarks to evaluate the physics capabilities of different detector configurations. The goal of all these efforts is to choose technologies during the summer of 1997, to prepare a Technical Design Report in the fall of 1997, and to commence the construction of full scale prototype planes of steel and active detector elements in FY 1998.

The three active detector technologies being pursued today are Iarocci chambers (operated either in proportional or limited streamer mode), resistive plate counters (RPC's), and scintillator. These are described in Sections 4.2, 4.3, and 4.4 respectively. The three alternative steel plane fabrication techniques which are being investigated are described in Chapter 5. The MINOS Collaboration has established a management structure to provide direction and oversight for this work, to avoid unnecessary duplication at different institutions and to make the final technology selections in a timely and objective fashion. We have established formal protocols and technical criteria for selecting the optimum active detector and steel technologies. These mechanisms will work effectively only if R&D funds are disbursed in a predictable manner, consistent with the overall detector R&D plan which is described in this document. The most efficient way to achieve this is to determine the total funds available early in each fiscal year, and to distribute funds following the guidelines jointly agreed upon by Fermilab and the MINOS Collaboration.

We list below the most important schedule milestones in the MINOS detector R&D program. Although specific dates are given for technology choices, a technology may be dropped from consideration earlier if it becomes clear that it cannot satisfy the selection criteria which we have specified. Some of the key active detector milestones in the list below are one or two months later than those shown in our earlier R&D plan [7]. These delays are the result of the serious shortfall in our FY 1996 R&D funding and the slippage of the Fermilab test beam running schedule.

Mar.-June 96: SLAC test beam studies of Iarocci chambers and RPC's.

June 96: First formal review of steel engineering

Aug. 96: First formal review of active detector technologies.

Sep. 96: Release initial version of Collaboration-standard simulation software system.

- Nov. 96:** Formal review of steel engineering concepts and options; eliminate one technology if possible.
- Nov. 96:** Set dimensions of Soudan far detector hall for bid package preparation.
- Dec. 96:** Formal review of active detector technology development; eliminate one technology if possible.
- Jan. 97:** Fermilab test beam studies of EM calorimeter prototypes for all active detector technologies still under consideration.
- Feb. 97:** Assemble first engineering prototype(s) of full size steel detector plane(s).
- Apr. 97:** Formal review of active detector technologies.
- Apr. 97:** Test beam studies of full size active detector elements, including prototype electronics and readout, for all active detector technologies which are still under consideration.
- June 97:** Formal review of active detector and steel technologies
- Aug. 97:** Final active detector and steel technology decisions.
- Oct. 97:** Complete the MINOS experiment Technical Design Report.
- Oct. 97:** Complete the NuMI beam technical component Technical Design Report.
- Oct. 97:** Award contract for Soudan far detector hall excavation.
- Oct. 97:** Begin engineering design of NuMI construction at Fermilab.
- Jan. 98:** Test beam study of large prototype calorimeter with hadrons up to 20 GeV.
- Feb. 98:** Finalize details of the active detector design and fabrication methods.
- Mar. 98:** Begin excavation of far detector hall at Soudan.
- Apr. 98:** Construct and test full size engineering prototype of three planes of far detector steel and chambers.
- July 98:** Begin setup of production facilities for active detectors and steel detector plates.

The NuMI beam design is the primary responsibility of Fermilab, but several MINOS groups are also active participants in this work. Currently, an adequate beam design exists (a wide-band configuration with three horns), and software tools have been developed to study all aspects of its performance. Concurrently, we are investigating other possible wide-band beam (WBB) design choices which might increase the neutrino flux, make the beam more parallel, and minimize the near/far beam differences. Later on, these studies will be extended to optimize the narrow-band beam (NBB) design. The MINOS near hall location will be determined from these studies combined with an examination of several oscillation tests to check the sensitivity to systematic errors arising from near/far differences.

Table 1 (reproduced from Chapter 10) summarizes the FY 1995-1998 expenditures and cost estimates for the work described in this document. The FY 1998 construction costs shown in the Table are based on those for a MINOS detector instrumented with the reference detector technology. The base cost estimate assumes that all detector construction work is performed in the U.S., and then explicitly subtracts the value-equivalent contributions which are expected from overseas collaborators. The funds listed in Table 1 represent only part of the cost of the MINOS R&D program. These funds are being supplemented by substantial contributions from the home institutions and research contracts of MINOS collaborators, both in the U.S. and overseas.

Figure 1 (reproduced from Chapter 10) shows the overall schedules for the design and construction of the NUMI neutrino beam, MINOS far detector, and Soudan site work.

In summary, in this report we have tried to document both the progress we have made during the past year, i.e. since the PAC approval of our proposal, and our plans to converge on the ultimate design of the experiment by the fall of 1997. Our improved understanding of many issues, from the details of active detector technology to the control of systematic errors, has increased our confidence that the MINOS experiment can be performed within the guidelines of sensitivity, schedule, and cost which were presented to the HEPAP Subpanel on Neutrino Oscillation Experiments during the summer of 1995.

Activity	FY95	FY96	FY97	FY98
R&D funds:				
Iarocci	15	57	333	0
RPC's	25	28	259	0
Scintillator	22	28	380	0
Test beams	0	5	60	180
Electronics	12	0	150	100
Steel, magnet	26	60	513	0
Simulations	5	27	255	0
Soudan site design	13	50	150	0
Construction funds:				
Far detector systems	0	0	0	493
Near detector systems	0	0	0	164
Far detector structures	0	0	0	292
Near detector structures	0	0	0	173
Active detector factories	0	0	0	2054
Russian contributions	0	0	0	-279
Chinese contributions	0	0	0	-279
Electronics engineering	0	0	0	1272
UK contributions	0	0	0	-566
Total costs	118	255	2100	3604

Table 1: Summary of MINOS supplemental R&D and construction costs for FY 1995 (in FY 1995 dollars) and FY 1996-8 (in FY 1996 dollars). FY 1998 construction cost estimates are based on the reference detector technology.

MINOS Timelines

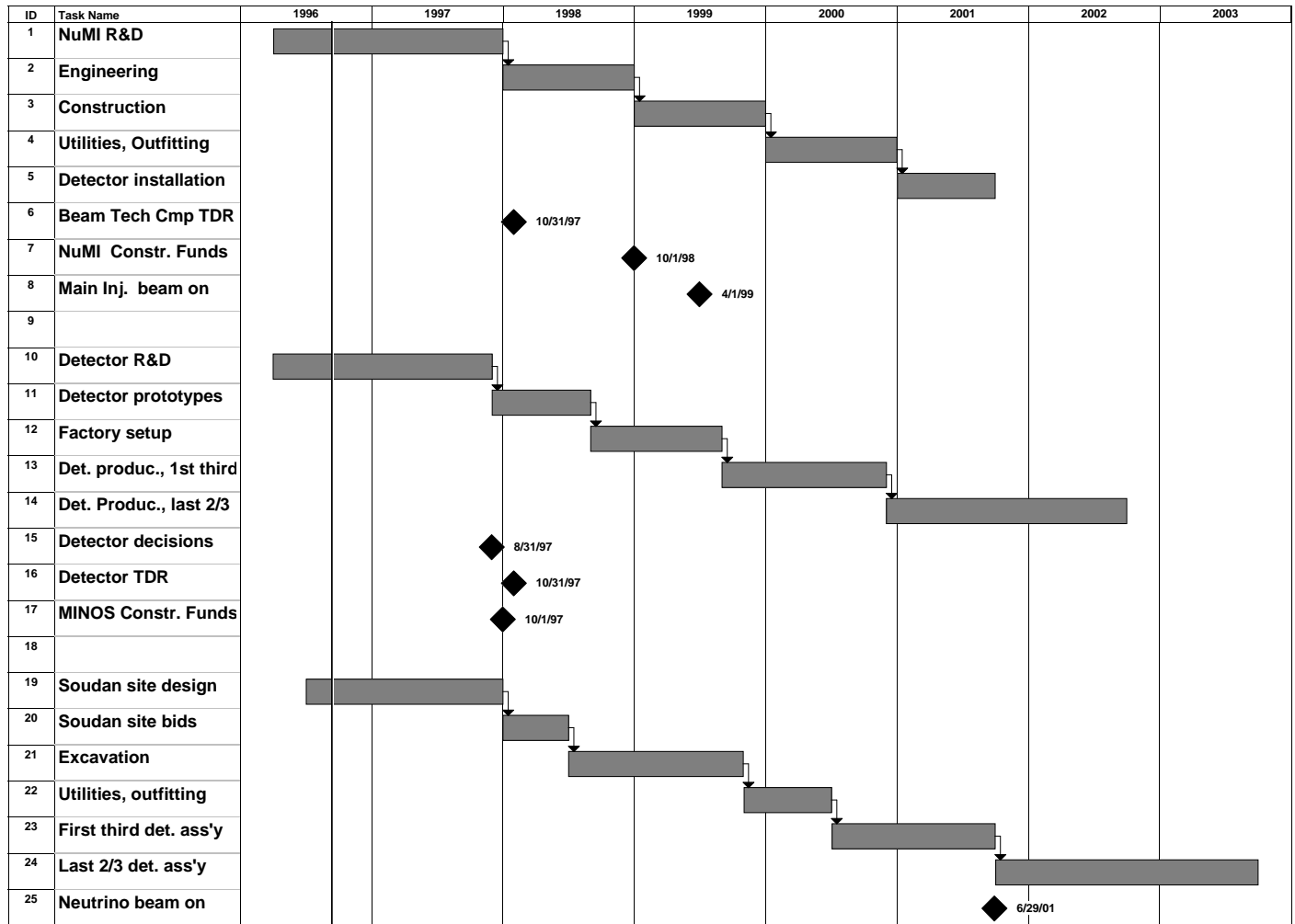


Figure 1: Overall design and construction schedule for the MINOS experiment. The time scale shown is in fiscal years.

2 Introduction

This document has been prepared at the request of the Fermilab Physics Advisory Committee (PAC) for consideration at its June 1996 meeting in Aspen, Colorado. Its primary goal is to describe the MINOS Collaboration's plan for completing the experiment optimization and design program in time for the start of construction in FY 1998. This milestone will be marked by the submission of the Technical Design Reports (TDR's) for the MINOS detectors and the NuMI beam technical components in October 1997.

The preparation of this document occurred over a time period which included a one-week long MINOS Collaboration Workshop at Lutsen, Minnesota during the second week in June. The goal of the workshop was to focus on global experiment design issues centered around the optimization, for specific oscillation tests, of the near and far detectors and the neutrino beam. Some effort at the meeting was in fact devoted to detailed planning of our R&D program and to the preparation of this document and our presentation to the June PAC meeting.

There have been a number of important developments since our last written report to the PAC in April 1995. We have updated the detailed parameters of the MINOS "reference detector," the neutrino beam design, the schedule, and the cost estimate, but the essential features of the experiment and its sensitivity to neutrino oscillations have not changed. Those developments are described in this document.

This report provides a comprehensive description of the current status of our R&D work, a statement of the most important technical issues in different areas, an outline of our proposed activities during the next few years, and a summary of the process to be used to reach key decisions. Since individual chapters are relatively self contained, the document can also be used as a reference to specific topics in our development program. This feature results in some redundancy and duplication among different chapters. To assist the reader, we give below a brief guide to the contents of the report.

In Chapter 3 we restate the physics case for our neutrino oscillation experiment. We "update" the HEPAP Subpanel report by discussing both the implications of new data supporting the LSND effect, and the competition presented by the recently proposed 50 GeV JHP proton synchrotron and its future beam directed towards the SuperKamiokande detector. We show that, in spite of the serious world-wide effort to study neutrino oscillations, the MINOS experiment will be able to make a significant impact when it begins recording data in 2001, regardless of the results of other experiments that should be forthcoming during the next five years.

Most of our R&D effort over the next two years will be focused on the development of active detector technologies. Chapter 4 addresses this central issue. We describe the current status of our understanding of the potential performance of the three competing technologies, the issues we hope to resolve with our proposed development program, and the time scale and procedures adopted by the Collaboration to make optimum choices.

Chapter 5 addresses similar issues for another key ingredient of the MINOS detector, the magnetized steel calorimeter planes. Chapter 6 describes our simulation effort, an essential component of our overall program to optimize the sensitivity of MINOS to neutrino oscillations. We give a brief overview of the collaboration's software system and discuss a representative sample of activities, both in detector simulations and physics analyses. Simu-

lation work relevant to study of the neutrino beam is covered in Chapter 7, which discusses briefly the work in progress to understand in depth the current design, the work on alternative systems which might increase the neutrino flux or decrease systematic errors, and some of the technical R&D work which we propose. This Chapter also addresses the question of the experiment's near detectors, both their design and their optimum location. At this time we have not yet resolved these issues, but we describe the relevant guiding physics principles and our plan to make key design decisions.

The report concludes with an update on the Soudan far-detector site preparation (Chapter 9) and a summary of our best estimates for the supplemental funding levels required in FY 1996, 1997, and 1998 (Chapter 10). Clearly the prognoses become less certain in the outyears because they are strongly dependent on the results of the proposed R&D work. Finally, Chapter 11 gives the most recent snapshot of the Collaboration's current manpower effort and MINOS activities.

3 Physics Update

3.1 Status of neutrino oscillations

The front line of particle physics research today is the search for phenomena beyond the Standard Model and thus for clues to the basic physics underlying it. The search for neutrino oscillations is one of the few areas where indications of its breakdown may have been glimpsed.

In the Standard Model neutrinos are massless and oscillations between neutrino species cannot occur. However, no fundamental principle requires that neutrinos have zero mass. They could acquire mass either through the same electroweak symmetry breaking which produces the quark and lepton masses or, on the GUT scale, by processes such as the “see-saw” mechanism. If these phenomena generate neutrino masses they will also in general produce mixing between neutrino flavors, giving rise to a mixing matrix analogous to the CKM quark matrix. Theory currently gives no indication of the values of the neutrino masses or mixing matrix elements. It is however popular to assume a neutrino mass hierarchy and mixing matrix similar to that found in the quark sector, i.e. with a large mass difference between the heavier members and a smaller difference between the lighter members, together with an approximately diagonal mixing matrix. Alternatively, models which postulate maximal mixing are viable both theoretically and experimentally. It is a vital feature of any experiment which discovers neutrino oscillations that it should also be able to *measure* the neutrino mass differences and mixing matrix elements, and thus provide clues to the underlying physics.

3.1.1 Experimental evidence

A number of diverse experiments have reported data that may require neutrino oscillations for their explanation. In fact it is difficult, if not impossible, for all of these experimental claims to be reconciled within a framework of a simple mixing formalism. Most of these experiments rely on the natural production of neutrinos. While these sources can give information about regions not accessible by other means, they cannot be controlled or understood as well as man-made neutrino sources. It is thus imperative to study the claimed effects at accelerators (or reactors) under controlled conditions, in order to distinguish between real and spurious effects, and to obtain a quantitative understanding of the phenomena.

The following is a very brief summary of the current evidence for neutrino oscillations and for the implied mass differences:

Solar neutrinos. The flux of solar neutrinos, measured by a number of different techniques, is consistently lower than that predicted by the standard solar model. If we do not admit to this model’s failure, the deficit may be explained by ν_e oscillations. In a two flavor $\nu_e \rightarrow \nu_\mu$ oscillation model the combination of the various experiments gives three allowed regions for Δm^2 and $\sin^2 2\theta$:

- Vacuum oscillations with Δm^2 around $10^{-10} eV^2$ and large $\sin^2 2\theta$, or
- Matter enhanced oscillations (MSW effect) with larger Δm^2 ($10^{-4} - 10^{-5} eV^2$) and either large (~ 1.0) or small ($\sim 10^{-3}$) $\sin^2 2\theta$.

Atmospheric neutrinos. Another anomaly has been observed in the interactions of neutrinos produced by cosmic ray showers in the atmosphere. The ratio of ν_e to ν_μ induced events observed in underground detectors is different from that predicted from their predominant production in the $\pi \rightarrow \mu \rightarrow e$ decay chain. If this result is not an artifact of the detectors or the Monte Carlo calculations, it is most probably due to oscillations with $\Delta m^2 > 5 \times 10^{-3} eV^2$ and large $\sin^2 2\theta$. This is one of the most important motivations for the MINOS experiment.

Dark matter. For many years astrophysical measurements have shown that a considerable amount of matter in the universe does not shine in stars: *dark matter*. Neutrinos were, of course, produced in the big bang and could account for the required hot dark matter if the highest mass neutrino has a mass of $\sim 7 eV$, or two or more neutrino masses are in the eV range. This is one of the motivations for the COSMOS experiment.

LSND results. The LSND experiment has recently reported a signal of 22 $\bar{\nu}_e$ candidate events with a background of 4.6 ± 0.6 events, arising from a beam of $\bar{\nu}_\mu$ from μ^+ decays at rest. If it is not an experimental artifact it is most likely due to oscillations with Δm^2 of the order of 0.01 to 20 eV^2 and $\sin^2 2\theta < 0.01$.

Summary of oscillation possibilities. As noted above, not all of the experimental hints can be accommodated in a three flavor neutrino mixing scheme. However, subsets of the data can be explained either by an approximately diagonal or a maximally mixed mixing matrix. An example of the latter, which highlights the power of MINOS, is the model of Harrison, Perkins and Scott [8], which can fit all neutrino data, except LSND, and which predicts equal oscillation into ν_e and ν_τ . MINOS is designed to be able to separate ν_e , ν_μ and ν_τ charged current events and to provide measurements of mass differences and mixing matrix elements. It will thus be able to substantiate or refute this complex model. This versatility will also enable MINOS to investigate other models and to respond to new experimental results as they become available.

3.1.2 Sciulli Subpanel conclusions and recommendations

The Sciulli HEPAP Subpanel was set up in 1995 to examine the US accelerator neutrino program [6]. It studied the evidence for oscillations summarized above, most of which was available at that time. The panel concluded that “*presently solar and atmospheric neutrinos provide interesting hints of oscillations*” but “*definitive tests of oscillations require more sensitive experiments than have been performed up to this time.*” Writing of the discovery of ν oscillations, they stated: “*The impact of such a discovery would be enormous; an entirely new window on physics and cosmology would open.*” They went on to recommend that “*The search for neutrino oscillations with accelerator experiments, including a single long baseline beam, should form an important part of the US high energy physics program*” and that “*the MINOS experiment at Fermilab should be supported.*” They furthermore recommended that “*The Fermilab program should remain flexible to react to new information.*”

We believe that these recommendations are just as appropriate today as they were a year ago. The MINOS experiment offers both a definitive test of some of the oscillation hints in

current data and, because of its sensitivity to all oscillation modes, it can react to any new indications of oscillations within the range of $\Delta m^2 \geq 10^{-3} \text{ eV}^2$ and $\sin^2 2\theta \geq 0.01$

3.2 50 GeV JHP experiment in Japan

After the publication of the Sciulli report, the KEK Laboratory announced plans to construct a new high intensity 50 GeV proton synchrotron (JHP) on its site. Part of the motivation for this effort is the extension of intermediate energy physics activities pursued presently at KEK and Brookhaven: rare K decays, antiproton physics, hyperfragments, etc. However, one of the principal motivations of this ambitious new project (estimated cost of \$750M) is the study of neutrino oscillations using an intense neutrino beam from the JHP accelerator and the existing 50 kT SuperKamiokande (SuperK) water Cerenkov detector some 250 km away.

In this Section we try to make an objective comparison of the JHP 50 GeV + SuperK neutrino oscillation experiment and the MINOS experiment. We are handicapped in this comparison by the absence of any "official" documentation about the Japanese project. Our comparison has to be based on oral reports and somewhat peripheral documents, and thus undoubtedly will have some deficiencies. We apologize in advance to our KEK colleagues if in this comparison we have inadvertently shortchanged their experiment.

Time scale. The Fermilab Main Injector is scheduled to become operational in 1999. It is currently on schedule and its completion date appears to be firm. The MINOS detector and the neutrino beam schedules will be determined largely by fiscal considerations. A reasonable funding scenario, however, will allow completion of the first third of the MINOS far detector and of the neutrino beam line by mid 2001; the full 10 kT far detector would be completed during the following two years.

The proposed completion date of the JHP accelerator is 2003. However this date could well be delayed, for two reasons:

- a) The KEK Laboratory is already planning a neutrino oscillation search experiment using a beam from the existing 12 GeV proton synchrotron (PS) to SuperK. This experiment is due to start in 1999 and needs at least 2-3 years of data taking at full PS intensity to reach a 3 sigma sensitivity for $\nu_\mu \rightarrow \nu_\tau$ with $\sin^2(2\theta) = 0.4$ for the Δm^2 range suggested by the Kamiokande atmospheric neutrino experiment. The existing PS tunnel will be used for the booster injector of the planned 50 GeV machine and thus this construction is likely to be delayed until the completion of the 12 GeV oscillation experiment.
- b) Annual expenditures of more than \$100-150M may be hard to achieve. Thus a minimum of 5-6 years appears necessary from the beginning of the construction until its completion.

Comparative ν_τ event rate. We try to estimate the relative KEK *versus* MINOS ν_τ event rate assuming that Δm^2 is small, i.e. about 0.01 eV^2 . Without knowing the details of the KEK beam design or their precise neutrino energy spectrum, we are limited to the use of scaling arguments. Assuming reasonable optimization at both sites, such an estimate should be correct to 25-50%. In this comparison we use the design intensities for each accelerator

at their completion times. In the ratios below, we use the convention that a ratio greater than unity favors the JHP-SuperK experiment.

Protons per pulse: $2 \times 10^{14} / 5 \times 10^{13} = 4$

Cycle time: $1.9 \text{ sec} / 3.2 \text{ sec} = 0.6$

Detector tonnage (fiducial volume): $22 \text{ kT} / 7 \text{ kT} = 3.1$

$\sigma(\nu_\mu)$: (Assume $\langle E_\nu \rangle$ scales with E_{proton}) $50 \text{ GeV} / 120 \text{ GeV} = 0.42$

$\sigma(\nu_\tau) / \sigma(\nu_\mu)$ for 6 GeV vs 15 GeV (typical ν energy): 0.33

Thus the overall factor is about 1.0. There are two additional small factors:

- a) L/E_ν dependence: neutrino flux falls off as $(E/L)^2$; however if $1.27 \times L \times \Delta m^2 / E \ll 1$, the oscillation probability goes as $(L/E)^2$. Thus for the situation in question, the L/E dependence will be very weak. Since those ratios are very similar in both cases, the L/E factor can be ignored.
- b) The s dependence of π and K production (at the same x). Assuming that this dependence goes as $s^{0.25}$, MINOS will be favored here by about 1.2.

Thus within the uncertainties of our estimates, the relative ν_τ event rate in the two experiments will be about the same.

Several additional issues need to be considered as well:

- a) If we look at quasi-elastic ν_τ interactions, the advantage of Fermilab's higher energy is less important than for DIS events. Thus the KEK experiment will have a statistical advantage for these measurements.
- b) By the year 2003 or 2004, the Main Injector will have been operational for 4-5 years. Thus its intensity at that time could be well above its design value.
- c) 2×10^{14} protons on target is almost an order of magnitude more than has been achieved to date at high energies. Difficult production target issues have been encountered at Brookhaven when 2×10^{13} protons have been delivered on target.

From the above, we conclude that MINOS will not be at a disadvantage *vis-a-vis* the JHP-SuperK experiment for measurements relying on production and subsequent decays of τ 's. There are other measurements, which are relevant for neutrino oscillations and which do not require tau production, e.g. the disappearance experiment. In that area, the KEK experiment will have an event rate advantage of a factor of 2-3. However, most of these measurements are limited by systematics. We discuss the question of systematics below.

Comparison of different oscillation measurements. Below we shall try to compare the relative capabilities of KEK and Fermilab for specific oscillation measurements. First, however, we note a very important advantage of the Fermilab NuMI program: *flexibility*. For example, to explore the very low Δm^2 region, e.g. around $0.5 \times 10^{-2} \text{ eV}^2$, we might want to reduce the mean neutrino energy by a factor of two or so to get a more favorable L/E ratio. This can be done at Fermilab without significant qualitative change; at the JHP, however, such a change would put the mean neutrino energy below tau threshold (3.45 GeV).

We turn now to specific channels:

- a) **Disappearance, i.e. near/far test.** The MINOS proposal quotes a 2% systematic uncertainty; there is some optimism within the collaboration that this might be improved. The initial LOI for the KEK 12 GeV oscillation experiment quotes the systematic error as 6%, mainly due to the contribution from fiducial volume uncertainty in the near detector, which arises from the 30 cm error on vertex reconstruction.
- b) **NC/CC test.** This is probably the most powerful measurement in MINOS, largely because it is expected to have quite small systematic errors. Previously proposed studies with water Cerenkov detectors (BNL, KEK PS) used only single π^0 NC events for this measurement. We are not aware of any studies of how such a measurement could be made at higher energies where deep inelastic scattering events contribute. Furthermore, it is our belief that the significantly different sizes of the KEK near and far detectors gives different muon identification probability in more complex events, and thus may introduce serious systematic errors into this test.
- c) **CC energy test.** This test allows MINOS to determine Δm^2 and $\sin^2(2\theta)$ in a single measurement. We do not see how the SuperK experiment can perform this test with comparable sensitivity because they measure the energies of only those muons which range out in the detector. SuperK does not have a magnetic field and a significant number of muons escape before ranging out. In addition, the different sizes of the near and far detectors will make a comparison between these two sites difficult.
- d) **$\nu_\mu \rightarrow \nu_e$ oscillation.** We believe that MINOS can reach the 1% oscillation probability level, limited by the knowledge of other sources of ν_e 's and the uncertainty in identification of electrons. Previous studies of this oscillation mode in large water Cerenkov counters used only events without additional particles. Thus it is not clear to us what the ultimate JHP-SuperK limit will be at these higher energies.
- e) **Exclusive tau channels.** We believe that tau decay modes into $\pi\nu$, $e\nu\nu$, and $\mu\nu\nu$, can potentially be identified. Clearly, the quasi-elastic channels are easier and SuperK should be able to do well here, probably better than MINOS because of their higher event rate for such events. The main uncertainty for the optimum $e\nu\nu$ mode is in their ability to distinguish electrons from π^0 's at energies higher those studied in previous water Cerenkov proposals. In MINOS, the $\mu\nu\nu$ channel identification relies on the narrow-band beam (NBB) and the measurement of muon energy. To our knowledge, NBB capability is not planned for KEK and fluxes would be low at these lower energies in any case. However, SuperK might be able to study this channel if recoil protons (in the high-energy tail of the spectrum) could be identified and measured.

To summarize, MINOS should be superior to the JHP-SuperK experiment in a number of tests limited fundamentally by systematic errors. Generally, it is these tests which allow one to perform quantitative measurements, i.e. to determine oscillation modes and their parameters. The SuperK detector will probably identify better some of the tau exclusive modes. Thus the two experiments are quite complementary.

3.3 Possible future scenarios

Results are expected from several neutrino oscillation searches over the next five years and it is important to consider what the MINOS experiment will be able to contribute as our understanding of the neutrino sector evolves.

The possible combinations of results from other experiments are too numerous for us to consider exhaustively. Instead we consider the contributions that can be made by MINOS in the case of a positive result from each of these experiments, irrespective of the results from the others. In fact some combinations of results would be contradictory and would require MINOS to resolve the contradictions. We base our conclusions on the roughly equal sensitivity of MINOS for $\nu_\mu \rightarrow \nu_\tau$ and $\nu_\mu \rightarrow \nu_e$ oscillations and the ability of the experiment to measure Δm^2 in the range $0.005 < \Delta m^2 < 0.2 \text{ eV}^2$.

1. Evidence for $\nu_\mu \rightarrow \nu_\tau$ from the CERN high-energy short-baseline experiments CHORUS and NOMAD.

Such a result would indicate $\nu_\mu \rightarrow \nu_\tau$ mixing with small mixing angles and a large Δm^2 . The emphasis of the MINOS experiment would then be on the study of $\nu_\mu \rightarrow \nu_e$ oscillations. These could explain the atmospheric neutrino anomaly and, if a positive result were found, the mixing parameters could be measured.

2. Evidence for $\bar{\nu}_\mu \rightarrow \bar{\nu}_e$ from the low energy short-baseline experiments LSND and Karman.

This is the complementary case to the observation of $\nu_\mu \rightarrow \nu_\tau$ oscillations in short baseline experiments discussed above. If $\nu_\mu \rightarrow \nu_e$ oscillations are observed in short baseline experiments the important strength of MINOS would be its sensitivity to $\nu_\mu \rightarrow \nu_\tau$ oscillations, which would then be necessary in order to explain the atmospheric anomaly. In addition, MINOS could confirm $\nu_\mu \rightarrow \nu_e$ mixing in the low Δm^2 - high $\sin^2(2\theta)$ region of LSND sensitivity.

3. Additional evidence from SuperKamiokande and Soudan 2 for the atmospheric neutrino anomaly.

MINOS would be ideally placed to confirm that this anomaly is due to neutrino oscillations, to ascertain whether the mode of oscillation is pure two generation or a mixture of the three generations (i.e. to measure the mixing matrix elements) and to measure Δm^2 . The continued observation of an angular effect in the atmospheric flavor ratio by SuperKamiokande would hint strongly at a value of $\Delta m^2 \sim 0.01 \text{ eV}^2$. If the angular effect is not confirmed, a higher value of Δm^2 would be suggested. MINOS could still provide a measurement if $\Delta m^2 < 0.2 \text{ eV}^2$.

4. The KEK-PS to SuperKamiokande long-baseline experiment obtains a $2\text{-}3\sigma$ positive result in a disappearance experiment.

The Δm^2 range of MINOS overlaps with the Δm^2 range of this experiment but MINOS has a much higher statistical power. MINOS could therefore confirm this result and measure the mixing parameters.

5. Additional evidence from SNO and SuperKamiokande that the solar neutrino deficit is explained by the MSW effect and $\nu_\mu \rightarrow \nu_e$ oscillations.

Such evidence would rule out Maximal Mixing as an explanation of the atmospheric neutrino anomaly; MINOS would confirm (or otherwise) that the atmospheric anomaly is the result of $\nu_\mu \rightarrow \nu_\tau$ oscillations.

6. ν_e disappearance is suggested by the reactor neutrino oscillation experiments at CHOOZ and Palo Verde.

As we discuss in Section 6.6, studies of ν_e and ν_μ oscillations are entirely complementary and are necessary for a determination of mixing matrix elements in a three generation model. The Δm^2 sensitivity ranges of the reactor experiments and MINOS overlap, and include the range suggested by the atmospheric anomaly. Positive results from both the reactor experiments and MINOS would therefore yield results of fundamental importance. The MINOS experiment's ability to identify ν_μ oscillation modes is crucial for the measurement of mixing matrix parameters.

These scenarios by no means exhaust the interesting possibilities for the MINOS experiment. Possible evidence for dark matter, results from neutrinoless $\beta\beta$ decay experiments, and advances in theoretical modeling can suggest scenarios that are richer than those considered so far, particularly when sterile neutrinos or gravitationally induced neutrino oscillation scenarios are considered. It is clear that MINOS will have the capability to explore and exploit a very wide range of potential neutrino oscillation parameters.

4 Active Detector R&D

4.1 Introduction

4.1.1 Overview

The MINOS active detector R&D program consists of parallel activities to develop Iarocci chamber, RPC, and scintillator detector technologies, along with associated work on electronics development and charged-particle test beam measurements. The reference detector described in the MINOS Proposal is instrumented with Iarocci tube detectors operated in limited streamer mode, and was the basis for the neutrino oscillation simulation results presented to the Fermilab PAC and HEPAP Subpanel in 1995. The extensive experience of previous experiments with large Iarocci tube arrays gave considerable confidence that the reference detector would perform as advertised, and could be constructed on the required schedule for the cost estimate presented in the MINOS proposal.

Nevertheless, the MINOS collaborators feel that two alternative active detector technologies, Resistive Plate Counters (RPC's) and scintillator with optical fiber readout, could offer potential advantages over Iarocci chambers in terms of both performance and cost. Both of these alternative technologies present technical challenges which may not be solved in the time available before the MINOS detector design must be frozen in 1997. In addition, the Iarocci tube technology itself must be adapted for use in the MINOS detector and the collaboration has to demonstrate the capability to mass produce these chambers for the advertised cost. In particular, the underground environment of the MINOS detectors makes the use of the traditional flammable Iarocci tube gas and PVC plastic unacceptable. Proportional-mode operation of "Iarocci" chambers, built with ABS-plastic and/or aluminum extrusions, may offer a natural solution to both of these requirements. Finally, the U.S. MINOS collaborators have had little direct experience in the mass production of these chambers.

In late FY 1995, MINOS collaborators initiated three parallel detector development programs to optimize each of the active detector technologies for use in the far detector. At the same time, the collaboration began to devise management structures for guiding this work and for selecting the best of the three technologies in 1997. These are described in Sections 4.1.2 and 4.1.3 below. In order to compare the cost and performance of the three active detector technologies, each one has defined an optimized reference configuration which is being used for performance simulations, conceptual engineering designs, and cost estimates. These reference designs are described for each of the detector type in Sections 4.2, 4.3, and 4.4 below.

The design of the MINOS electronics system depends to some extent on which active detector technology is chosen. Conceptual design work has begun on an electronics system for the Iarocci reference detector; the technologies required appear to be quite conventional. The collaboration has decided to delay detailed electronics engineering and prototype work as long as possible in order to take advantage of the latest technical developments in this rapidly advancing field. The electronics requirements of MINOS instrumented with RPC's would be quite similar to those of the Iarocci chamber reference detector, although some modification would be required if the fast timing information of RPC's were to be recorded. While a scintillator detector could also use similar data acquisition electronics, this might

not be optimum, and could be inappropriate for some types of photodetectors. In any case, each of the three active detector technologies would require its own unique front end electronics. MINOS electronics development work to date has focused on general system design considerations and on the prototyping of front-end electronics needed for test beam studies of the three detector types. Our electronics development plan is described in Section 4.5 below.

Although laboratory tests with cosmic rays and radioactive sources are adequate for basic performance studies of active detector prototypes, calorimeter response is best measured in charged particle test beams. Electromagnetic shower response of small Iarocci and RPC prototype chambers was measured at SLAC during the spring of 1996. These studies will be continued at Fermilab in early 1997 with all detector types still under consideration, and extended to hadrons (with a much larger calorimeter) in 1998. These measurements will determine directly the properties of calorimeter detectors based on each technology, and will also provide essential calibration data for detector response simulations. Simulations of the physics capabilities of the MINOS experiment instrumented with each of the three technologies will provide important information for the choice of the optimum detector technology. Our test beam program is described in more detail in Section 4.6 below.

The following two sections of this Introduction describe the selection protocol and the technical criteria which have been adopted by the MINOS collaboration to guide the selection of the optimum active detector technology.

4.1.2 Active detector selection protocol

The MINOS Technical Board has adopted the following protocol for making the active detector technology decision:

1. The active detector technology chosen for MINOS must satisfy the technical criteria listed in Section 4.1.3.
2. The final active detector technology decision will be made in August 1997 or before. The decision will be made by the MINOS Spokesperson, with the advice of the Technical Board.
3. An Ad Hoc Advisory Committee on MINOS Active Detector Technology will be established to provide advice to the Spokesperson, through the Technical Board, on the comparison of competing technologies.
4. The Committee will be established in close coordination with the NuMI Project Management and the Fermilab PAC.
5. The Ad Hoc Committee will make comparative evaluations of the different technologies, but does not necessarily have to recommend the final detector choice.
6. The Ad Hoc Committee will consist of six to eight members including three or four from outside the collaboration. The committee should meet every four to six months to evaluate progress and to provide advice and feedback to the collaboration in a timely fashion.

7. The Ad Hoc Committee will be appointed by the Spokesperson, with advice from the Technical Board, in early 1996. (The committee membership is now being finalized, and the first meeting is planned for August 1996 in conjunction with the next MINOS Collaboration meeting.)

4.1.3 Active detector selection technical criteria

There are four basic areas of concern which should set the criteria for selection of the active detector technology:

- A. Safety,
- B. Ease of manufacture and cost,
- C. Demonstrated operation and reliability,
- D. Physics capabilities.

Items A-C must all be “adequately satisfied.” If all technologies manage to pass these hurdles then the strongest physics capability must be the determining factor.

A. Safety:

1. Must satisfy all existing or likely-to-exist regulations of Fermilab, the State of Minnesota and any other safety agency which has jurisdiction over the Soudan mine. We must clearly identify whether OSHA, etc. have jurisdiction. “Likely-to-exist” means that safety experts from the appropriate jurisdictions advise that (in their opinions) such regulations are likely to be adopted prior to MINOS construction.
2. Risk mitigation must be considered and pursued for any “risky” technology. Estimated costs must include required safety precautions.
3. All technologies must be evaluated by a panel of safety experts, which will solicit advice from the appropriate safety agencies.

B. Ease of manufacture and cost:

1. About 50 m^2 of operating and tested chambers must be demonstrated.
2. “Industrial” production techniques must be demonstrated. Procedures for the final mass production process must be clearly described, and small scale prototype production should make use of these procedures whenever possible.
3. Reliable cost estimates must be provided.
 - (a) All required subsystems (e.g. gas handling, calibration system, safety devices, etc.) must be included in the cost estimate.

- (b) The cost of manpower must be based on Item 2. Explicit manpower profiles (what is built where) may be considered but a “fixed cost” manpower estimate (everything built under common cost assumptions with labor in the U.S.) must be provided. Evaluation of costs will be done using equivalent costs of manpower.
- (c) All significant materials from industry must have costs based on at least two actual quotes, if possible, from reliable firms. Reliability for key components should be based on demonstrated capability of firms to deliver.
- (d) Costs must include manpower for installation. An “installation board” should be formed to evaluate the installation plan for each technology.
- (e) Costs should be based on construction of a fixed cost detector with total far + near detector costs not to exceed the 1995 Lehman panel costs (using the same costing approach) under similar construction scenarios.
- (f) Detector operating costs must be estimated; low operating costs will be considered a beneficial feature.

C. Demonstrated operation and reliability:

1. 50 m^2 of chambers must be thoroughly tested. The response of individual chambers must be shown to be similar enough to each other to achieve adequate performance uniformity, and must be similar to that assumed in detector simulations of oscillation tests.
2. Results from accelerated aging conditions must be demonstrated. All chambers should be run as long as possible under nominal conditions.
3. Demonstrated previous long-term operation in existing experiments is not essential but may be considered as a feature.

D. Physics capabilities:

Although explicit physics capabilities should take precedence over generic “good features,” both should be considered. Capabilities should be based on a fixed-cost detector derived from reliable cost estimates, i.e. a far detector technology which costs more per ton must assume a smaller total detector mass than one which costs less per ton.

1. Explicit physics signatures

- (a) Reach in parameter space for the NC/CC oscillation test.
- (b) Reach in parameter space for explicit measurement of oscillation parameters based on energy spectrum differences between near and far detectors (systematic energy calibration differences will limit sensitivity).
- (c) Ability to use electron “identification” to give explicit oscillation signatures for $\nu_\mu \rightarrow \nu_e$.
- (d) Explicit tau identification signatures. In order to favor one technology, it must be understood how one technology allows a signature while another does not. It is not sufficient for an advocacy group to have a “secret result” that gives a good signature but could also apply to any of the technologies.

2. Generic “good features”

- (a) Good energy resolution in EM and hadronic showers.
- (b) Good vertex resolution.
- (c) Good shower angle resolution.
- (d) Fast timing.
- (e) Ease and reliability of calibration.
- (f) Rate capability for use in the near detector.
- (g) Stability and homogeneity in gain properties.
- (h) Previously demonstrated long-term reliability.
- (i) Minimal effect on performance from “standard” failures.
- (j) Robustness against “unforeseen” problems.
- (k) Ease of repair or replacement.
- (l) Robustness against coil heat in the center of the detector.

4.2 Iarocci chambers

4.2.1 Critical issues for Iarocci chambers

Iarocci chambers operated in limited streamer mode are the MINOS reference detector, whose design is described in detail in the MINOS Proposal. The primary goal of the Iarocci chamber R&D program is to turn this description into a fully optimized and engineered design which can be built under the cost and schedule constraints given in the Proposal and presented to the 1995 HEPAP Subpanel.

Despite the adoption of Iarocci chambers as the reference detector technology for MINOS, several critical design issues remained unresolved, and have been the focus of R&D activities during 1995 and 1996. The major issues, and some preliminary resolutions, are listed here:

a. **Is calorimetry response adequate with nonflammable gas?**

EM shower response of small Dubna prototype chambers has been measured in a SLAC test beam. Even if this response should prove acceptable, the short high voltage plateau obtained in limited streamer mode with nonflammable gas appears to be a serious problem.

b. **Is calorimetry response adequate in proportional mode?**

EM shower response of Dubna and Argonne prototype chambers has been measured in a SLAC test beam. The results of these studies, which were just completed in early June, are still being evaluated.

c. **We must identify materials to replace the PVC plastic which has been used for chamber “combs” and sheaths in the past.**

Aluminum combs appear to work well in proportional mode, but give rise to serious afterpulsing in limited streamer mode. ABS combs are expected to perform acceptably as well, but have not been tested yet. ABS sheaths will replace PVC sheaths.

d. **Mass production techniques for full size chambers must be optimized, engineered, and a proper bottoms-up cost estimate made.**

This work is just beginning. Current plans are for production to be divided among the U.S., Russia, and China, so laboratories in each country will perform independent optimization of mass production techniques to take advantage of local conditions.

4.2.2 Current Iarocci chamber development work

Iarocci chamber development work is now under way at Argonne, Tufts, JINR-Dubna, PNPI-St.Petersburg, and IHEP-Beijing. The Fermilab CMS group, which includes some MINOS collaborators, is planning an Iarocci chamber development program which will address some of the detector issues of interest to MINOS. The Fermilab and Argonne groups are also working closely with two physicists from the Dubna MINOS group who are visiting Fermilab for an extended period.

The Argonne group has concentrated its efforts on laboratory studies of prototype chambers with aluminum comb extrusions, operated with nonflammable gas (containing 9.5%

isobutane) in both limited streamer and proportional mode. EM shower response of proportional mode chambers was measured in the SLAC test beam in May, 1996. Effort is now turning to the fabrication of full size prototype chambers, constructed with components produced by local industry.

The Tufts group has concentrated its studies on the performance of Iarocci chambers operated in proportional mode with argon-CO₂ gas mixtures. They are also working with local industry to produce comb and sheath extrusions made of ABS plastic, and have provided the Argonne group with ABS extrusions for prototype chambers. The group also participated in the spring 1996 SLAC test beam run.

The Dubna group has mass produced a large number of Iarocci chambers for the LEP DELPHI experiment, and has begun R&D work on chambers for MINOS. They have developed Iarocci chambers, operated in proportional mode, for the D0 upgrade. The two Dubna visitors to Fermilab have worked on the MINOS SLAC test beam studies during spring 1996, and will also participate in the planned Fermilab test beam study of a prototype Iarocci chamber calorimeter early 1997. The group has provided a steel structure and PVC chambers for a small calorimeter whose response was studied during the SLAC test beam run. The Dubna group is coordinating its work with the MINOS group at PNPI-St.Petersburg, which is planning to provide components for MINOS chambers built in the proposed Russian chamber factory. Work at PNPI, which joined MINOS in early 1996, is just beginning.

The MINOS group at IHEP in Beijing, China joined the collaboration in early 1996. Previously, IHEP has mass produced a large number of Iarocci chambers for the LEP ALEPH detector; the group now plans to participate in both the development and mass production of MINOS chambers. They have completed the refurbishment of the ALEPH Iarocci chamber factory, have worked with local manufacturers to produce chamber components, and have built and tested small PVC prototype chambers made from all-Chinese components. Arrangements for long-term IHEP visitors at Fermilab are under discussion.

4.2.3 Iarocci chamber reference design

This Section describes our current best estimate for the parameters of the Iarocci chambers which may be used as the MINOS active detector elements. Although final design decisions have not yet been made, results from R&D work during the past year have led to a number of tentative conclusions about how the traditional design should be modified for use in this experiment. For example, PVC plastic cannot be used for the comb or sheath extrusions because of the toxic fumes which it emits when heated. We have investigated both aluminum and ABS plastic as alternative comb materials, and have had good results with aluminum prototype chambers. ABS plastic appears to be a suitable sheath material. Proportional mode operation of aluminum-comb chambers with a nonflammable gas mixture is efficient over a 1 kV anode high voltage range, without the afterpulsing which characterizes operation in limited streamer mode. Operation with negative high voltage on the combs, and the anode wires at ground (as described in the Proposal) turns out to require internal resistive covers for efficient operation. The current reference design therefore has the anode wires at high voltage, with signals read out through blocking capacitors. The Iarocci reference design described here is used for cost and performance evaluation, but is likely to change as our

R&D program continues.

The Iarocci detectors will consist of ≤ 8 m long chambers and ≤ 8 m long cathode strip boards running perpendicular to each other. They will be sized to fit the far detector steel octagons. All gas and electrical connections to the outside will occur at one end. This means that access is required only to five sides of the octagon. There will be gas jumpers from one tube to the next at the far ends of the chambers. but these can be installed during construction and will not require access.

A. Chambers

The Iarocci chambers will be made of extruded aluminum combs which are enclosed in an extruded plastic sheath. The combs will be strung with wires. The sheath will be sealed at both ends by end plugs. Gas, high voltage, ground and signals will come through the end caps.

The aluminum comb extrusions will be 16 cm wide and 1 cm high and up to 8 m long. They will have 16 channels which are open at the top and are 9 mm \times 9 mm in cross section. The aluminum walls/ribs and bottoms will be 1 mm thick. All tolerances of thickness and spacing will be 100 μ m.

There will be an anode wire strung down the center of each aluminum channel. It will be supported and centered at least every meter by a small injection molded plastic piece which will fit snugly into the channel, but not fill the channel so that gas can get around it. The wires will be tensioned and soldered to small G-10 boards. These boards will be at either end of the aluminum tube and will sit in an injection-molded-plastic wire block. The wire block, in turn, will sit in a region (~ 5 cm long) at the end of the aluminum which has had the ribs milled away. The wire block will have short "snouts" which extend into each channel to maintain alignment. The G-10 board, to which the wires are soldered, will be firmly attached to the wire block (adhesive or melted plastic) and the wire block will be bonded to the aluminum.

The whole aluminum tube will be slid into an extruded ABS plastic sheath of rectangular cross section. This sheath will have wall thicknesses of 1.25 mm and its inner dimensions will match the outer dimension of the aluminum. The sheath will provide the gas enclosure for the tube. The ends of the sheath will be sealed by injection molded plastic end caps which will be bonded or heat sealed to the sheath. The two end caps are different; one end has only a gas feed through while the other end has signals, high voltage, ground and gas. Each end cap will also have two mounting holes molded into it.

The gas fittings will be molded into the end cap during the injection molding process. Gas will flow from a supply manifold into one end of the tube, along the channels and out the far end. It will then have a short jumper to carry it over to the neighboring tube where it will flow up the length of that tube. This will daisy chain from tube to tube across the layer until it goes back to a return manifold.

The electrical connections to the tube will be made *via* a G-10 board which may be potted into a slot in one of the end caps or perhaps molded in. Traces on this board will carry high voltage, ground and signals. Inside the end cap (i.e. in the gas volume) connections will be made from the G-10 board to the anode wires and the aluminum using short soldered jumpers. Outside the end cap the board will extend far enough to hold HV blocking capacitors and current limiting resistors. The part of the board extending outside

the tube will be supported by “ears” extending from the end cap.

B. Strip Planes

The strips will be made of aluminum tape glued down to a dielectric plane. This plane will be Coroplast (an extruded polypropylene material with a structure like corrugated cardboard). The plane will be 2 mm thick (possibly changed to 4 mm after we have completed prototype tests), about 1 m wide and up to 8 m long. On one side of it there will be an aluminum foil ground plane and on the other strips of 1.8 cm aluminum tape on 2 cm centers running along the 8 m length. Connections to the strips and the ground plane will be made with aluminum solder (Solderit) which “melts” at a low enough temperature so that the plastic isn’t affected.

C. Assembly

First the strip planes and then the chambers will be attached to the steel plane while it is in the horizontal position. They will be aligned using the end cap mounting holes and studs mounted on extensions to the steel. The chambers will be supported across their large areas by double sided tape. The steel can have a slight waviness, since all the elements will have some flexibility, but it should not have sharp edges which might cut or dent the detectors. Smooth waves of <1 cm over >2 m would be acceptable. For short wavelengths (<50 cm) the detector could ride on the “crests” of the waves (as long as there is enough surface to tape to). The surface of the steel should be clean and oil free so that the tape will adhere to it. The spacing between the strip plane and the chambers should be as small as possible but no bigger than 1-2 mm.

At the outer edges of the octagon there will be a printed circuit board, probably in 1 m lengths, which will carry the signals from the wires and the strips to a connector into which an electronics card will plug. These 1 m boards will also mount to the alignment studs and possibly be bonded to the chambers and/or strip planes. Short wire jumpers will be soldered from the chambers/strips to the long board.

Since there will be exposed high voltage capacitors and connections coming out of chambers, it will be necessary to put a protective cover over the ends. This could be a sheet aluminum housing or a snap-on plastic cover, or possibly a protective coating will be sufficient.

For electrical noise reasons it will be necessary to have an external ground plane, isolated from the rest of the detector plane, but attached to it. This would be aluminized Mylar (or possibly another layer of the 2 mm Coroplast with aluminum foil). It would be attached with double-sided tape to the rest of the package.

D. Dimensions

Tables 2 and 3 summarize the dimensions of chamber components which contribute to the overall thickness and width of the Iarocci chamber reference design.

Component	Thickness (mm)
Coroplast strip plane	2
Maximum strip-tube gap	2
Sheath walls (2 sides)	2.5
Tube to sheath clearance	0.5
Aluminum comb extrusion	10
Ground planes, 2 sides (max.)	4
Adhesives, tape	2
Total thickness	23

Table 2: Iarocci chamber components of the overall chamber thickness.

Component	Width (mm)
Sheath wall thickness (2 sides)	2.5
Tube-sheath clearance	0.5
Aluminum extrusion	161
Maximum gap to next tube	1
Total width	165

Table 3: Iarocci chamber components of the overall chamber width.

4.2.4 Iarocci chamber R&D plan

The following is a summary of FY 1996-8 Iarocci chamber R&D activities. This plan is based on the assumption that the Iarocci technology continues to pass selection criteria.

FY 1996 activities in the US:

- Build small prototype chambers and test with cosmic rays and radioactive sources.
- Measure prototype chamber response to EM showers in SLAC test beam.
- Incorporate realistic Iarocci chamber response, as determined from test beam measurements, into MINOS detector simulation software.
- Consider possible changes in reference detector parameters, based on prototypes and design studies:
 - 16-channel chambers instead of 8-channel,
 - Use of aluminum comb material instead of graphite-coated plastic,
 - Saturated proportional mode operation instead of limited streamer,
 - High voltage on wires instead of on combs,

- Increase cell size to reduce sensitivity to dimensional variations.
- Design and purchase components for first chambers made of all-US components:
 - ABS plastic sheaths,
 - Both ABS and aluminum comb extrusions,
 - Injection molded end caps and wire supports.
- Set up fabrication facility for full length prototype chambers.
- Begin fabrication of first full length MINOS chambers.

FY 1996 activities in Russia and China:

- Build and test small PVC prototype chambers from existing components (Dubna).
- Complete rehabilitation of existing Iarocci factory equipment (Beijing).
- Build and test small PVC prototype chambers from all-Chinese components made specifically for MINOS (Beijing).
- Provide chambers and steel calorimeter structure for SLAC test beam studies (Dubna).
- Participate in MINOS test beam run at SLAC (Dubna).
- Investigate possible local manufacturers of aluminum comb extrusions.
- Investigate possible local manufacturers of ABS sheath extrusions.

FY 1997 activities in the US:

- Continue fabrication of full length chambers.
- Begin development of Quality Control protocols with Russian and Chinese collaborators.
- Build chambers and front-end electronics for Fermilab test beam Run #1 calorimeter.
- Study performance of prototype chambers in Fermilab test beam.
- Begin design and construction of chamber assembly machinery.
- Build and test 50 m^2 array of full length chambers.
- Test response of full length chambers in Fermilab test beam Run #2.
- Continue study of calorimeter response in Fermilab test beam Run #2.
- Write MINOS detector Technical Design Report.

FY 1997 activities in Russia and China:

- Continue construction and testing of MINOS chambers using locally produced components (especially ABS and aluminum extrusions).
- Participate in MINOS test beam runs at Fermilab.
- Test response of prototype chambers in Fermilab test beams, compare to US prototypes.
- Begin final design and prototyping of chamber assembly machinery.
- Begin tests of mass production techniques in local factories.
- Begin development of Quality Control protocols with US collaborators.

FY 1998 activities in the US:

- Continue construction of chamber assembly machinery.
- Construct hadron calorimeter chambers for Fermilab test beam Run #3.
- Assemble and test three planes of chambers on prototype MINOS steel planes using prototype factory machinery and procedures.
- Begin setup of US Iarocci chamber assembly factory.

FY 1998 activities in Russia and China:

- Continue construction of chamber assembly machinery.
- Continue mass production trials and development of Quality Control protocols.
- Begin setup of Russian and Chinese Iarocci chamber assembly factories.

4.2.5 Iarocci chamber R&D cost estimate

Tables 4 and 5 summarize MINOS Iarocci R&D activities and supplemental funding requirements for FY 1996 and 1997. In FY 1996 MINOS collaborators have paid for a substantial fraction of Iarocci R&D work with institutional and base-contract funds. The supplemental funding requirements listed in Table 5 assume that this practice will continue, although not to as great an extent as in FY 1996, when the funds received (late in the year) were much less than had been anticipated.

Table 6 shows the FY 1998 active detector *construction* cost estimate (i.e., to be paid for from MINOS construction funds, as opposed to R&D funds) which has been developed for the Iarocci reference detector technology. All FY 1998 *R&D* costs are included in Sections 4.5 and 4.6, under electronics and test beam work. Preliminary RPC and scintillator estimates indicate that their FY 1998 costs will be approximately the same as for Iarocci chambers. The costs in Table 6 will therefore be used for all three technologies until better cost estimates are completed (within the next six months).

Institution: activity	Source	\$K
Argonne: Full size prototypes	DOE	15
Dubna: Test beam prototypes	Fermilab	18
Fermilab: Prototype tests (Dubna)	Fermilab	8
IHEP: Small prototype chambers	Fermilab	8
Tufts: Prototype extrusions, test beam	Fermilab	8
Total FY 1996 Iarocci R&D		57

Table 4: FY 1996 funding for Iarocci chamber R&D work (actual allocations).

Activity	\$K
Full size prototype chambers	75
Extrusions and end cap development	59
Engineering design effort	40
Test beam prototype chambers	50
Test beam prototype electronics	25
US contrib. to work in Russia and China:	84
Dubna	32
PNPI	20
IHEP	32
Total FY 1997 Iarocci R&D	333

Table 5: FY 1997 costs for Iarocci chamber R&D work (in FY 1996 dollars).

Activity	Funds	\$K
Trial assembly, test of 3-plane prototype	Constr.	493
Tooling, assembly machines	100	
Chamber assembly (tech. effort)	40	
Note: steel planes are costed in Chap. 5		
Engineering effort	45	
Installation fixtures	122	
Detector elements	63	
Supplies	70	
Tech effort	53	
Setup of US, Russian, Chinese factories	Constr.	2054
Engineering effort	510	
Factory outfitting	226	
Production tooling	457	
Testing machines	249	
Installation	115	
Pre-production trial	497	
Expected Russian contribution	Constr.	-279
Factory outfitting	-75	
Installation	-38	
Pre-production trial	-166	
Expected Chinese contribution	Constr.	-279
Factory outfitting	-75	
Installation	-38	
Pre-production trial	-166	
Total FY 1998 active det. cost		1989

Table 6: FY 1998 costs for active detector construction work (in FY 1996 dollars). This cost estimate was developed for the Iarocci reference detector, but will be similar for other detector technologies.

4.3 RPC's

4.3.1 Critical issues for RPC's

Resistive Plate Counters (RPC's) hold promise as an inexpensive active detector alternative which will provide fast timing and potentially better calorimetric performance than Jarrocci chambers. Reduction in the active detector costs could permit finer-grained sampling (assuming fixed mass and cost) or a larger detector than otherwise possible. However, since RPC's have not previously been deployed in calorimeters, or with areas as large as proposed in MINOS, there are several crucial research and development projects which we must undertake in order to be able to realize the advantages that this technology can provide:

- Demonstrate the fundamental performance as an EM calorimeter.
- Develop full-size prototypes which are applicable to MINOS.
- Test uniformity of response in full-size prototypes.
- Develop industrial production design and techniques which will permit full realization of low-cost production.
- Study possible replacement gas mixtures which do not include Freon 13B1 and have reduced amounts of isobutane.
- Determine the optimal mode of operation.
- Test long-term stability.

We believe that with a modest R&D effort and budget, all of the above tasks can be accomplished following the program which we propose here.

4.3.2 Current status of RPC development work

RPC development for MINOS is being conducted at three institutions. The Livermore group has been developing an RPC design based on ABS plastic electrodes over the last few years. In the past year, they have continued development of this design and performed tests on alternative gas mixtures for RPC's. They have demonstrated high efficiency (92-94%) using non-ozone depleting gas mixtures containing 1% sulfur hexafluoride as a replacement for 4% Freon 13B1. This was used in our tests at SLAC. The Livermore group provided RPC's for the SLAC test and will continue work on long-term tests and full-scale prototype construction.

The Caltech group has been involved in RPC development and tests with Italian colleagues over the last few years. The focus of past work has been on construction and testing of float-glass electrode RPC's. A calorimeter test was performed at the CERN PS in November 1993 which illuminated some concerns for RPC's as the active detector for high-energy EM showers. In the last year, work at Caltech has focused on understanding ways to improve this performance and investigation of alternate gas mixtures. It was shown that the charge distribution from RPC's produced when a single muon passes through is better than that for limited streamer tubes under appropriate operating conditions. A narrow charge integration

gate is essential for this purpose and has been applied in the SLAC tests and will be used in future measurements. Work is currently underway on construction and testing of full-scale prototypes.

The Rutherford group has been involved in an RPC R&D effort focusing on new ideas for full-scale detector construction based on float-glass electrode RPC's. In addition, they have demonstrated that signals in cathode pickup strips can be propagated with negligible dispersion. Rutherford provided test chambers for, and participated in, the tests at SLAC.

Tests of calorimeter response. The calorimetric performance in MINOS is one of the most important aspects of detector response. The particular issue which we need to explore is the response to EM showers. Here the distance between particles in the shower core is relatively small compared to those in hadronic showers. In order to achieve good response to EM showers, the RPC must be capable of effectively counting the number of particles crossing the active detector gap underneath each strip of readout. If the distance between particles in an EM shower causes a saturation of response under a strip, the linearity and resolution of EM energy will be affected. Hence, it is essential to demonstrate that the response to EM showers is acceptable to the physics analyses which we need to perform.

Ultimately, the only acceptable test of the EM shower response is a full EM calorimeter test. A test in an electron beam is essential in order to understand the response to multiple particles which arrive virtually simultaneously and with small transverse separation. We have embarked on a two-tiered program of beam tests to ensure the highest probability for a successful demonstration of RPC's as an active detector element. First, we have studied the response of RPC's to EM showers near shower maximum compared to scintillator response in the same location on an event-by-event basis. We will use this information to determine the best operating conditions and to develop techniques for building a full EM calorimeter prototype.

These tests have been performed at SLAC during March and May, 1996. Each of the three institutions working on RPC development provided prototype chambers for these tests. The data from this SLAC test beam exposure are still being analysed. We anticipate that the second phase of our test program will be a full EM calorimeter performed at Fermilab starting in January 1997.

Alternative gas mixtures and operating conditions. In past applications, the "standard" operating condition for RPC's has been with a 2 mm gap and a gas mixture of approximately 60% argon, 36% isobutane and 4% freon 13B1. In this condition, good charge spectra have been demonstrated in "spark" mode. Because freon 13B1 is an ozone-unfriendly gas and isobutane is flammable we are interested in pursuing alternative gas mixtures to the standard one. We have found that a mixture of 40% isobutane, 1% SF₆ and 59% argon gives charge performance and an efficiency similar to that of the freon-based gas. We have not succeeded at this time in finding a nonflammable gas mixture which gives sufficient suppression of after pulsing in RPC's operating in spark mode. Although operation in avalanche mode may offer a way around use of flammable gas, we plan to pursue investigation of the safety precautions which will be necessary for use of such gas mixtures. Discussions with safety personnel at Fermilab and study of safety regulations indicate that for the RPC's,

the gas mixture described above should be acceptable, but may require extra precautions compared to use of a nonflammable gas.

Full-size prototype development. The development and operation of full-size prototypes is a crucial part of our development program in FY 1996. The RPC technologies being developed for MINOS have not yet been demonstrated to have the necessary uniformity of response over large-area chambers. Furthermore, the techniques required to achieve such uniformity need to be determined and factored in to the production costs of the technology. Apparently low production cost is one of the attractive features of RPC's but we must be sure that the construction remains "easy" as the size of the chambers is increased. Because of this, we think that prior to selecting the reference RPC technology we should have results not only from the SLAC beam tests but also feedback from construction and testing of large-scale prototypes.

We have two basic construction technologies that we will pursue for full-scale MINOS prototypes. For each technology, we plan to build and have tested, by September 1996, at least two chambers of 8 m length and total width of at least 1 m (8 m²). The Livermore group will build chambers based on the ABS plastic design and the Caltech and Rutherford groups will cooperate in building chambers based on float-glass inside of an outer gas envelope. (Depending on available manpower, Caltech may also build ABS-based chambers.) Tests of the optimal construction techniques will be performed at all locations. Together with the results from the SLAC tests, we will use the information gained from the construction and tests of the large chambers to choose one technology to pursue for construction of an EM calorimeter.

Front-end electronics prototypes. Front-end electronics applicable for both streamer tubes (proportional tubes) and RPC's will be built at Argonne for use in the EM calorimeter tests at Fermilab. For spark or streamer mode operation, a very short ADC gate is effective in reducing the extra charge from after pulsing. For avalanche mode operation, low gain amplifiers may be necessary to measure the small avalanche pulses.

Long-term stability Clearly, we wish to demonstrate the long-term stability as much as possible prior to making a decision on the active detector technology. Small areas of RPC's built with float glass have already been run in Italy for about three years under accelerated aging conditions (heat and radioactivity) without deleterious effects. On the other hand, there have been reports of chambers being affected by humidity. Because the construction techniques vary widely, we are performing our own stability tests. We intend to keep chambers of all construction running for as long as possible prior to any technology decisions. Livermore has set up a test rig for this purpose, and it is now in continuous operation. It uses pre-mixed gas and a simple data acquisition for continuous monitoring of efficiency, noise and charge response.

4.3.3 RPC reference design

Description. The reference plan for glass-electrode RPC's will be based on scaling up the RPC's which have already been used in tests. Each RPC will have outer dimensions of $800\text{ cm} \times 25\text{ cm} \times 1.4\text{ cm}$. An x and y view strip plane will be included in each layer. The strips will be aluminum tape on a substrate of "plastic cardboard" with a total thickness of 0.5 cm. The strips will be attached to each side of the RPC plane using adhesive tape. Hence, the total thickness of the RPC with strip plane will be:
 $1.4\text{ cm (RPC)} + 2 \times 0.5\text{ cm (strips)} + 2 \times 0.1\text{ cm (gaps)} = 2.6\text{ cm}$. The tolerance in the above numbers should be $\pm 0.3\text{ cm}$. Hence, a minimum gap between steel plates of 2.9 cm is required.

Each RPC will be built using two planes of float glass (each 3.0 mm thick) and with a 2.5 mm gap between the planes determined by spacers along the edges of the glass. The assembly of glass and spacers will be inserted into an outer plastic (ABS) envelope with rectangular cross-section with outer dimensions $25\text{ cm} \times 1.0\text{ cm}$ and with walls which are 1.5 mm in thickness. The spacers along the edge will have an "E" shape with the total width being 4.0 mm and the width of the "back" of the "E" being 1.5 mm. The center of the "E" will be 2.5 mm thick (this sets the gas gap) and the top and bottom of the "E" will be 1.0 mm thick. The spacers will run continuously along the edge of the glass. The total length of each RPC will be 8 m but each of the glass plates will have dimensions of $24.5\text{ cm} \times 200\text{ cm}$. Hence, the 8 m chamber will be constructed with a total of eight separate pieces of glass (four sections along the length of the chamber). Between each piece of glass will be a thin (1.0 mm) plastic spacer with an "E" on both sides, creating an effective dead-space of 5.0 mm along the length of the chamber.

The strip planes will have an x and y view on each detector plane with 2 cm pitch for the strips. Electronic readout of the strips may be performed on one end of the strips with no significant degradation in either timing or amplitude. The far end of strips (away from the readout) will be terminated with the characteristic impedance in order to prevent any reflections. Strips will have sufficient separation in order to reduce crosstalk to the acceptable level of a few percent.

Cost of RPC detector planes. Cost estimates for construction of RPC's are still relatively uncertain compared to streamer tubes. However, we have undertaken first cost estimates which indicate that RPC's should be relatively less expensive due to simpler construction. Preliminary estimates suggest that the cost will be between \$150 and \$200 per square meter.

Support of RPC detector planes. Although we have not addressed the support mechanism in detail, the support requirements are not very demanding. We envision a "Venetian Blind" support structure with each of the RPC's acting as an element of the (closed) "blind". Hence, with the plane lifted into place, the RPC's will be hanging from two vertical bands (steel bands for instance) with each RPC attached to the band with a loop attached to the vertical band. In addition, the bottom layer of RPC's should rest against stops attached to the steel near the bottom of steel layer. During construction, the first strip layer will be stuck to the steel using an adhesive. This is the layer with the strips running perpendicular

to the long dimension of the RPC's. Next, the RPC layers will be laid down on top of these strips with the strips running parallel to the long dimension already attached. This RPC/strip plane combination layer will be stuck to the first layer of strips using an adhesive and the banding structure will be installed as the RPC's are put into place. When lifted, the adhesive and vertical bands will keep the RPC's in place and support most of the load. The adhesive will prevent the detector plane from pulling away from the steel while the steel bands (properly tensioned) will prevent any vertical settling from occurring. Note that once planes are in place, it will be possible to install additional shimming to keep the RPC's in place, even under failure of the adhesive. Since RPC's of this design look essentially identical to streamer tubes (externally), this method of installation should be applicable to either technology.

Steel thickness and configuration. The steel plates should be spaced with gaps as small as is consistent with flatness tolerance and the above dimensions. Since the RPC's appear to offer a cost savings with respect to streamer tubes, we anticipate that the most attractive use of this "cost saving" from the presently defined reference detector will be to reduce the thickness of steel plates to 2-3 cm while keeping the same total detector mass (10 kT). Hence, we expect that the pitch of absorber/detector planes will be approximately 5.5 cm. Like scintillator planes, RPC planes carry a non-negligible total mass due to the glass plates. Each plane of detector will have a total mass of about 0.9 tons while each steel plane will have a mass of about 12.5 tons. Hence, the total mass of each detector/steel element will be 13.4 tons (3 cm thick steel) so that a total of 746 planes will be required for a total mass of 10 kT. We propose that the total mass should be reduced slightly if necessary in order to keep the total cost the same as the current reference detector.

RPC readout features and electronics. It is attractive to do precise timing with the RPC's but is not necessary for each strip in the detector. Instead, a sum of 10 strips could be used for timing purposes if this helps to realize a reduction in electronics cost compared to nanosecond timing on each strip. The minimum timing accuracy should be about 500-1000 ps. Each of the readout strips should have a charge measurement with precision of about 10%. The charge least-count should be about 0.5 pC with a maximum measurement of about 500 pC. This electronics requirement is driven by the physics demands of shower and single-particle measurement rather than any specific feature of RPC's.

4.3.4 RPC R&D schedule milestones

Nov.95-Aug.96: Continue development work on small-scale prototypes.

Mar.-June 96: SLAC test beam studies of EM shower response.

June-Oct.96: Build and test full-scale prototypes based on preferred technologies from SLAC tests. At least two chambers of 8 m length and total width of at least 1 m (8 m^2) need to be built and tested.

June-Oct.96: Develop cost estimates based on experience with full-scale prototype construction.

Sep. 96: If not already done for other considerations, choose one RPC technology for future development work.

Sep.96-Jun.97: Build and test at least 10 full-length (8 m) chambers with at least 50 m^2 of area.

Jan. 97: Fermilab test beam studies of calorimeter response with the final RPC technology.

April 97: Beam tests with full-scale prototypes at Fermilab.

Sep.96-Jun.97: Develop final industrial production techniques as much as possible in order to verify that final production cost estimates are reliable.

August 97: Final active detector technology decision.

4.3.5 RPC R&D cost estimate

Tables 7 and 8 summarize MINOS RPC R&D activities and supplemental funding requirements for FY 1996 and 1997 respectively. FY 1998 RPC construction costs will be approximately the same as those listed in Table 6 in Section 4.2.5 above. The development of detailed FY 1998 construction costs specifically for the RPC technology is now in progress.

In FY 1996 MINOS collaborators have paid for a substantial fraction of RPC R&D work with institutional and base-contract funds. The supplemental funding requirements listed in Table 8 assume that this practice will continue, although not to as great an extent as in FY 1996, when the funds received (late in the year) were much less than had been anticipated.

Institution: activity	Source	\$K
Caltech: Prototype chambers	Fermilab	18
Livermore: Gas system, gas studies	DOE	10
Rutherford: Prototype chamber studies		0
Total FY 1996 RPC R&D		28

Table 7: FY 1996 funding for RPC R&D work (actual allocations).

Activity	\$K
Gas studies, prototype chambers	24
Full size prototype chambers	93
Test beam calorimeter chambers	35
Production engineering design effort	70
Test beam prototypes, electronics	37
Total FY 1997 RPC R&D	259

Table 8: FY 1997 funding for RPC R&D work (in FY 1996 dollars).

4.4 Scintillator

4.4.1 Scintillator design issues

The use of scintillator as the MINOS active detector element could provide better electromagnetic and hadron shower resolution than gas tracking chambers, and would also give the possibility of fast timing measurements to determine track direction. Each detector plane would be constructed from a single layer of 2 cm wide, ~ 8 m long elements (either liquid-filled cells or solid plastic strips) giving one dimensional position information. Most naturally, the detector planes would alternate with 2 cm thick steel planes to optimize the electron energy resolution. Although cost considerations might require steel planes as thick as the 4 cm of the reference detector, it is unlikely that we would choose to place two planes with orthogonal coordinates in the same steel plane gap.

There are many practical advantages to using scintillator: installation would be simpler (cheaper) than for gaseous detectors since flatness of detector and steel is not critical, only a simple support system would be required, there would be no gas supply system, and overall maintenance is likely to be simpler. Initial cost estimates are comparable to those of the Reference Detector, especially when it is realized that, in such a scintillation detector, up to 10% of the total mass would lie in the scintillator material itself with a corresponding savings in the cost of steel and its installation. Scintillator technology is also highly suited to the relatively high-rate environment of the MINOS near detector.

Most of the MINOS scintillator development work to date has focused on liquid scintillator, contained in extruded plastic tubes, because our initial cost estimates showed that cast solid plastic scintillator material would be substantially more expensive than liquid. During the past year new MINOS collaborators from Fermilab and potential new collaborators from Russia have reopened the question of extruded solid scintillator because of very favorable recent experience with the D0 detector and elsewhere. This is described in Section 4.4.3 below. First, we will describe the development of liquid scintillator technology.

The liquid scintillator development work has focused on methods of efficient light collection from very long tubes containing liquid scintillator. The light produced in $2\text{ cm} \times 2\text{ cm}$ square tubes filled with liquid scintillator is converted to a longer wavelength in wavelength shifting fibers situated along their axes. This shifted light is piped to a photodetector at the end of the fiber. This scheme has the advantage that the scintillation light is very rapidly and efficiently concentrated into the small area (to minimize the cost of photodetection, which is likely the most expensive component in the system). The light collection efficiency is relatively insensitive to the position of the fiber in the cell but depends sensitively on the reflectivity of the cell walls. (The plastic scintillator option would have essentially the same geometry, and would probably have 1 cm thick \times 2 cm wide cells with a 1 mm hole down the center).

Based on a series of measurements made during the past year, we have determined that light yields are sufficient to detect minimum ionizing particles with this design. We have made preliminary choices of liquid scintillator type, fiber type, and cell materials. We have also selected a photodetector, based on cost, performance, and current availability.

During the next year, we propose to fully evaluate the relative merits of liquid *vs* plastic scintillators and to carry out two main lines of research and development in order to arrive

at an engineering cost estimate for a scintillator detector:

1. Build sufficient modules (probably $66 \text{ cm} \times 66 \text{ cm}$) to verify our simulations of the detector's response to electromagnetic showers. These measurements would be carried out during Fermilab test beam Run #2 in spring 1997, and would also be used to test prototype electronics for triggering and readout. It is likely that we will construct modules of both liquid and plastic scintillators for these tests.
2. Build at least one full-scale plane of detectors ($8 \text{ m} \times 8 \text{ m}$) to verify detector performance in both light yield and mechanical design.

4.4.2 Status of liquid scintillator development

Almost all work to the present time has been on the liquid scintillator option. We have measured the attenuation properties of fibers and light yields from various fiber/scintillator/cell wall reflectivity combinations. Both the fiber and light yield *vs* reflectivity measurements are directly applicable to the plastic scintillator possibility.

1. **Fiber attenuation lengths.** We have measured several batches and several varieties of wavelength shifting fibers manufactured by Bicron. These were found to be superior to samples we obtained from another source, Kuraray. All Bicron BCF91A (12 nsec decay time) fibers were found to have the same attenuation properties, independent of diameter and batch, single clad or multiclاد. Multiclاد fibers were found to trap a factor 1.40 ± 0.05 more light than the single clad.

The attenuation of the non-mirrored fibers can be expressed as

$$I = \exp(-x/1.35) + 0.66 \exp(-x/11.0)$$

where I is the relative light intensity measured at the end of a fiber when the source of light is x m from the end. The data are shown in Figure 2.

We have not yet made an extensive study of how to mirror the far end of fibers, although we have obtained a maximum measured reflectivity of 0.74 using an aluminizing technique. Based on these figures, the ratio of pulse heights from distances of 0.5 m to 8.5 m would be 2.4:1. This is the longest section of fiber to be used.

Based on these measurements, and also on light yield measurements, we have made a preliminary selection of 1 mm diameter multiclاد BCF91A fiber for the scintillator detector.

2. **Liquid Scintillator.** We have made measurements of light yields from fibers in $2 \text{ cm} \times 2 \text{ cm}$ tubes, up to 2 m long using several possible scintillators. Bicron BC517H yields 25% more light than BC517L; these are pseudocumene based scintillators in mineral oil. A new scintillator developed by R. Steinberg (Drexel Univ.) for use in the CHOOZ (reactor neutrino) experiment yields approximately 25% more light than BC517H. This latter has several additional desirable properties including higher density, since it uses an isopropyl biphenyl solvent rather than mineral oil, and probably

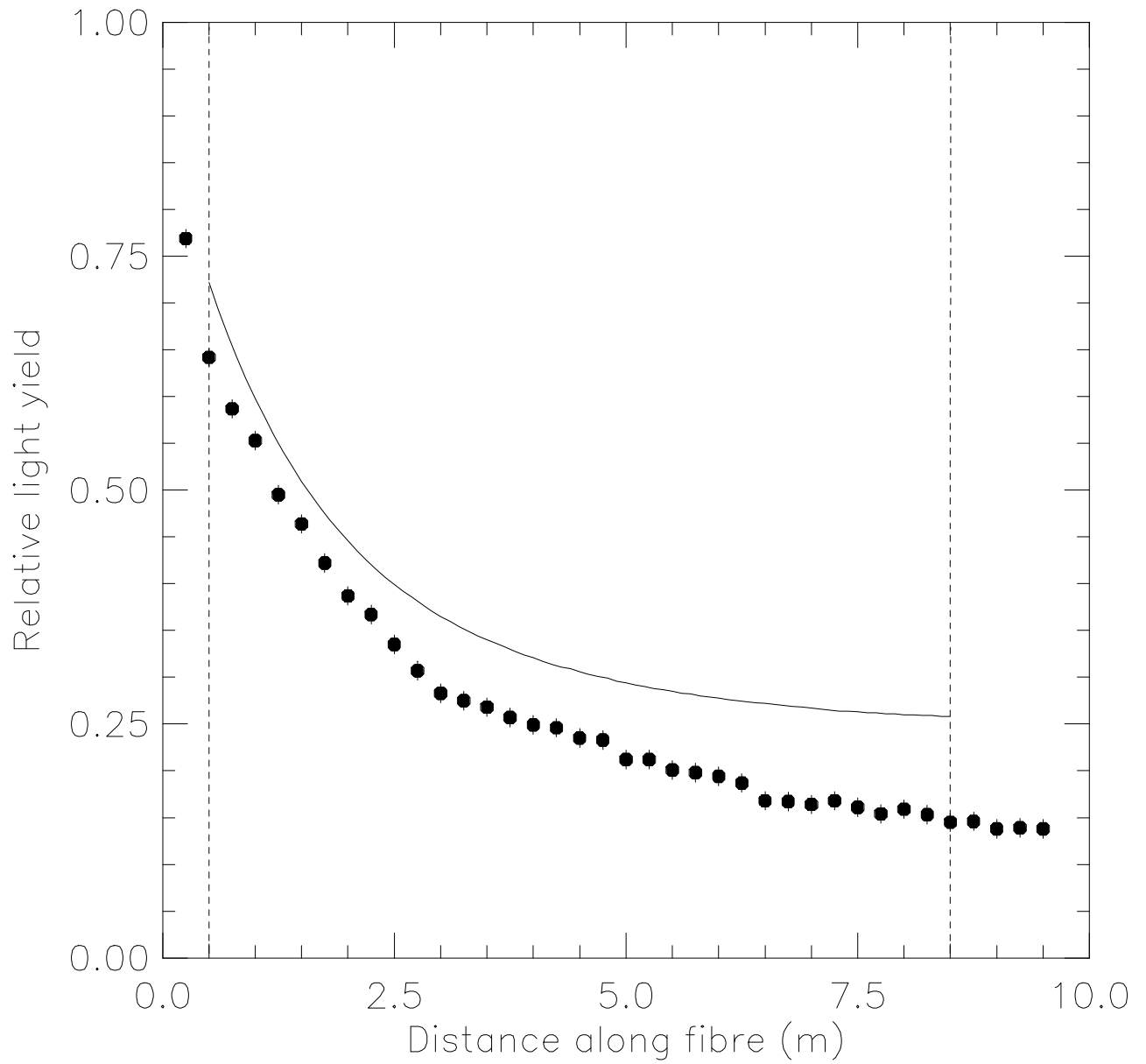


Figure 2: The relative light yield (I) data (circles) as a function of distance (x) along an unmirrored wavelength shifting fiber. The expected light yield in mirrored fibers is indicated by the curve.

less reactivity with materials used for handling and containment. It is markedly more expensive than the Bicron scintillators, however. Our studies have shown that we can obtain enough photons (> 70) from the far end of an 8 m long cell if the cell walls have a reflectivity greater than 95%. BC517H scintillator will be used in all future tests.

- 3. Cell materials for containment of liquid scintillator.** A key issue in the liquid scintillator technology is the choice of plastic, which is used both to contain the scintillator and to reflect the light which is generated. The plastic must be fire-resistant, as well as mechanically and chemically robust. Work done on prototypes by the Minnesota group leads to the requirement that the plastic must be highly reflective (at least 95%) for wavelengths above 400 nm. Because of its easy availability and low cost, PVC has been used in most prototype work. However, we plan to use an alternative material because of the potentially hazardous nature of PVC. The current choice is polypropylene, which is significantly cheaper than PVC; polypropylene also has superior heat-forming properties, which are desirable for sealing purposes.
- 4. Reflectivity measurements.** The Indiana group is investigating both polypropylene and polyethylene, each doped with varying amounts of white reflecting titanium dioxide. Indiana has a diffuse-reflecting spectrometer which they use for this work. Results to date suggest that somewhat more than 5% TiO_2 will be needed. We have recently obtained excellent results ($> 96\%$ reflectivity) with polypropylene containing 10% TiO_2 .
- 5. Other measurements in progress or planned.** There are several additional properties of the fiber/scintillator system which are being studied.

We are investigating the long-term effects of possible reaction between the liquid scintillator and the materials with which it will be in contact: the polypropylene cells and, especially, the fibers. We are carrying out tests to determine possible reaction rates at elevated temperatures in order to extrapolate to effective lifetimes at room temperature. These are difficult measurements. We have seen reaction when the polystyrene core of the fibers is directly exposed to the scintillator, but the outer cladding of the multicladd fibers is inert and we have not yet seen any deleterious effects.

The light output of most liquid scintillators falls by about 25% when they become saturated with oxygen, a process which can be reversed by bubbling nitrogen through the fluid. We are investigating oxygen take-up rates by scintillator in polypropylene cells: calculations show that the cell walls are essentially transparent to oxygen at the rate at which it is absorbed by the scintillator. We want to verify this to ascertain whether it is worth trying to completely eliminate oxygen; it is likely that we would operate with the scintillator fully oxygenated for both stability and simplicity.

We will investigate relative expansion of the scintillator fluid in polypropylene cells as a function of both temperature and humidity.

We will further investigate various mirroring techniques for the fiber ends.

6. Full scale detector engineering

Our engineering concept for the full MINOS detector is well-advanced. Each detector plane would consist of 12 individual modules manufactured from extruded polypropylene containing 10% TiO_2 , each containing 32 cells and having a width of 66 cm and lengths between 4.3 m and 8 m to accommodate the shape of the steel plates. Alternating planes are set at $\pm 45^\circ$ from vertical for two dimensional readout. A full plane of detectors is shown schematically in Figure 3. Each module is completely sealed at the bottom and fibers terminate only at the top. Modules are installed fully assembled with fibers and would be filled with liquid scintillator later. The bottom endcap is attached to the extrusion by a thermal process. It is heated in a mold to its melting point and applied to the end of the extrusion; the molten endcap is very viscous so that this process can occur with the extrusion in the horizontal position.

For modules that meet at the center hole of the detector, a special bypass block is installed that allows fibers from individual cells to bypass the hole and return to their original cells. This is shown in Figure 4.

The modules are supported at their lower edges by a series of four steel strips welded along the perimeter of the steel plates on four sides, creating a cradle. Each strip has a nominally square cross-section with a width of 2 cm and a length of approximately 130 cm. The modules are stacked in place while the steel plate is horizontal.

To the upper end of the extrusion is welded an injection molding which guides the 32 fibers to a manifold block where they are accurately positioned, glued in place, fly-cut and polished. This is shown in Figure 5. The fibers are simply inserted into the 2 cm \times 2 cm cells without regard to accurate positioning. This molding actually forms the liquid seal at the upper end and we envision that the space in the molding also acts as an expansion chamber for the fluid in case of significant temperature excursions.

The 32 fiber manifold block is connected, along with 2 other blocks, via a flexible light guide of clear fibers to a 96 channel photodetector.

Modules will be filled after their installation. Scintillator fluid will be supplied in standard 55 gallon drums; it will require four of these to fill a complete plane of detectors. The total weight of a single plane filled with scintillator is approximately 1000 kg.

4.4.3 Plastic scintillator development

There is a possibility that extrusions of polystyrene-based plastic scintillator could be sufficiently inexpensive to be comparable with the liquid scintillator in cost. Roughly, a reduction in price of at least a factor 4 from the D0 cost will be required. This could be achieved if the light yield of the plastic were sufficiently greater than that of the liquid to allow a half-thickness (1 cm) cell of a lower grade of polystyrene to provide an adequate light yield. This is a reasonable expectation because the average path length of light rays is relatively short and the attenuation of light in the scintillator itself is not critical.

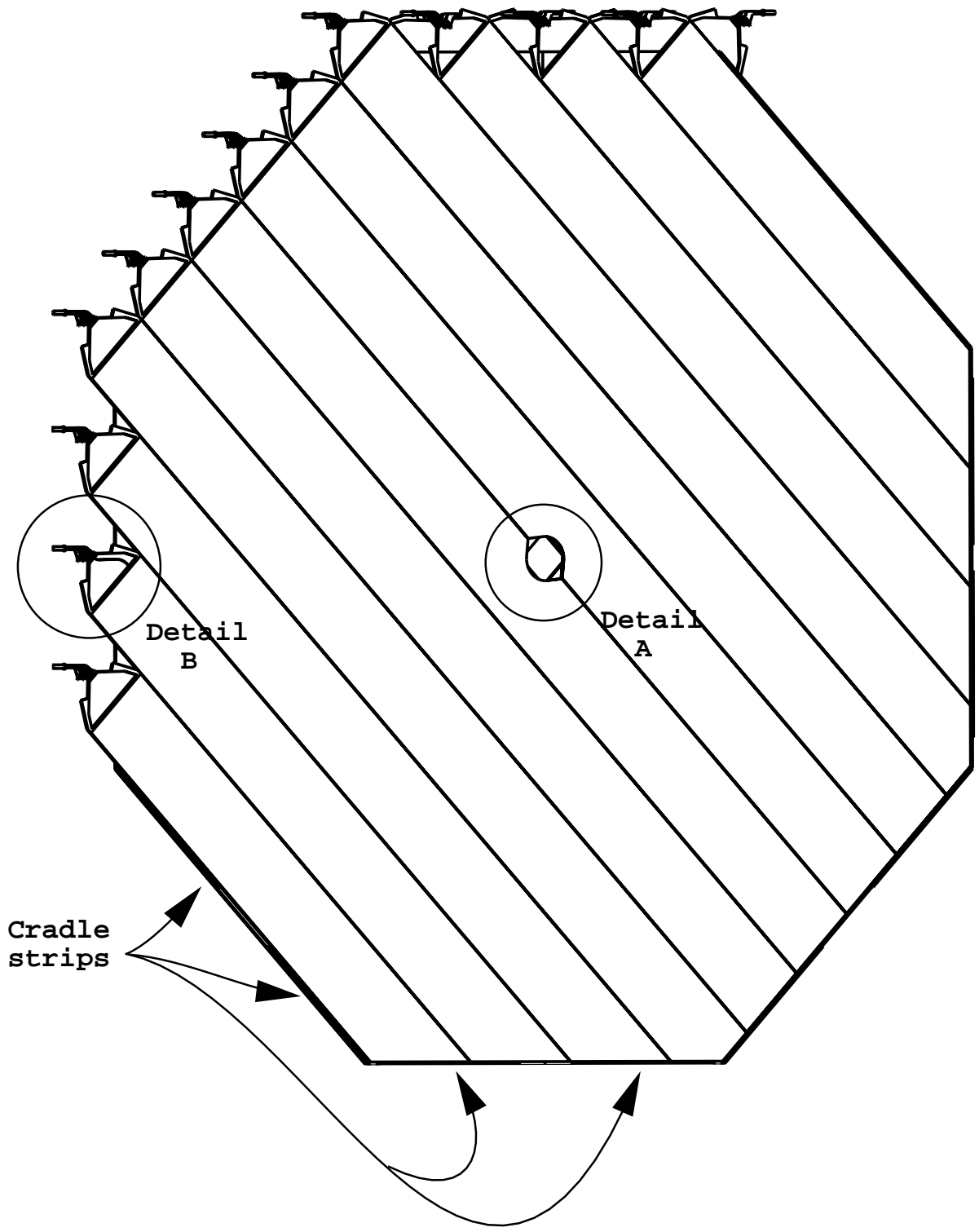


Figure 3: A full plane of liquid scintillator modules including manifold block and photodetectors.

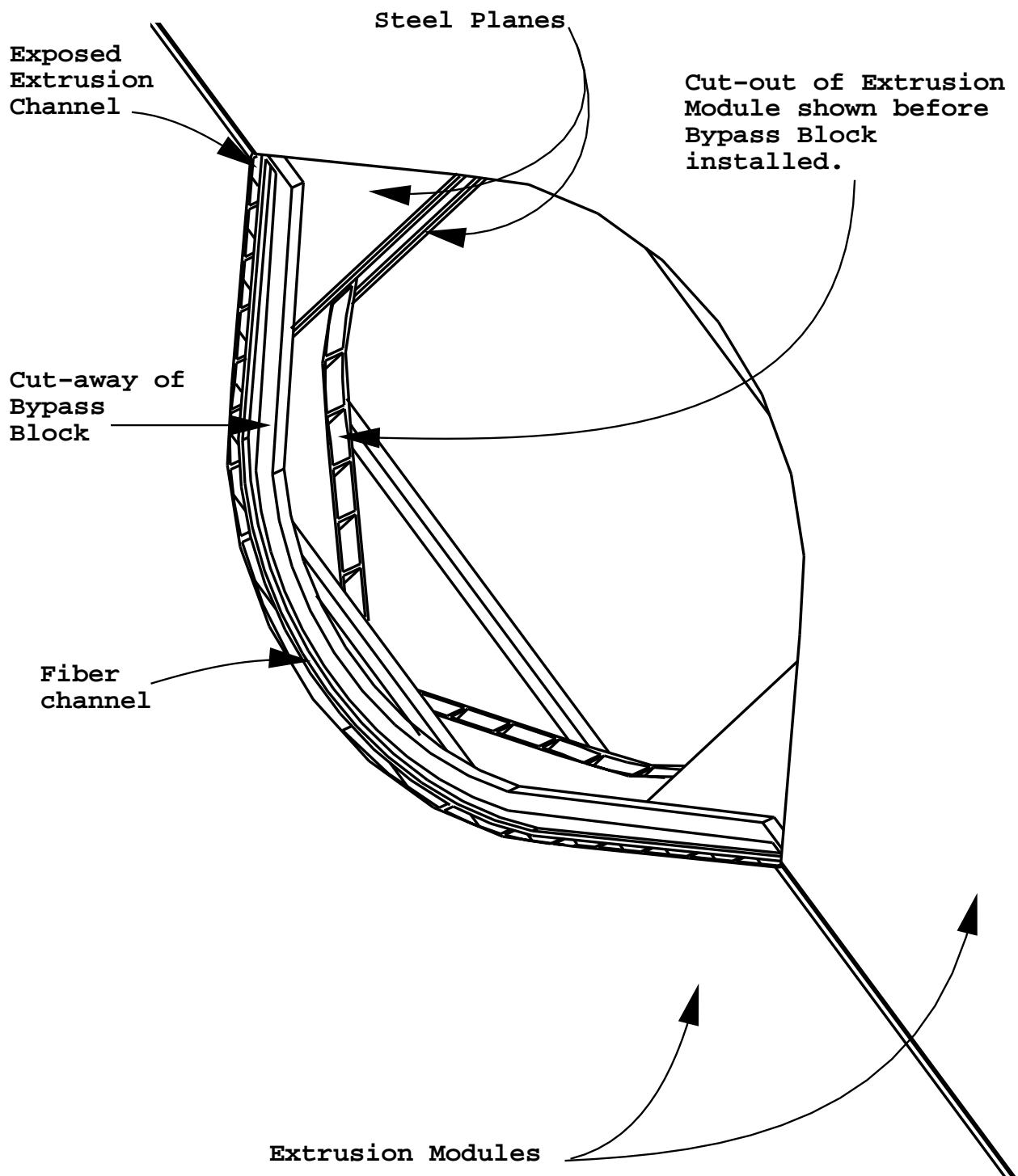


Figure 4: This cut-away (Detail 'A') shows the fiber bypass block near the central hole.

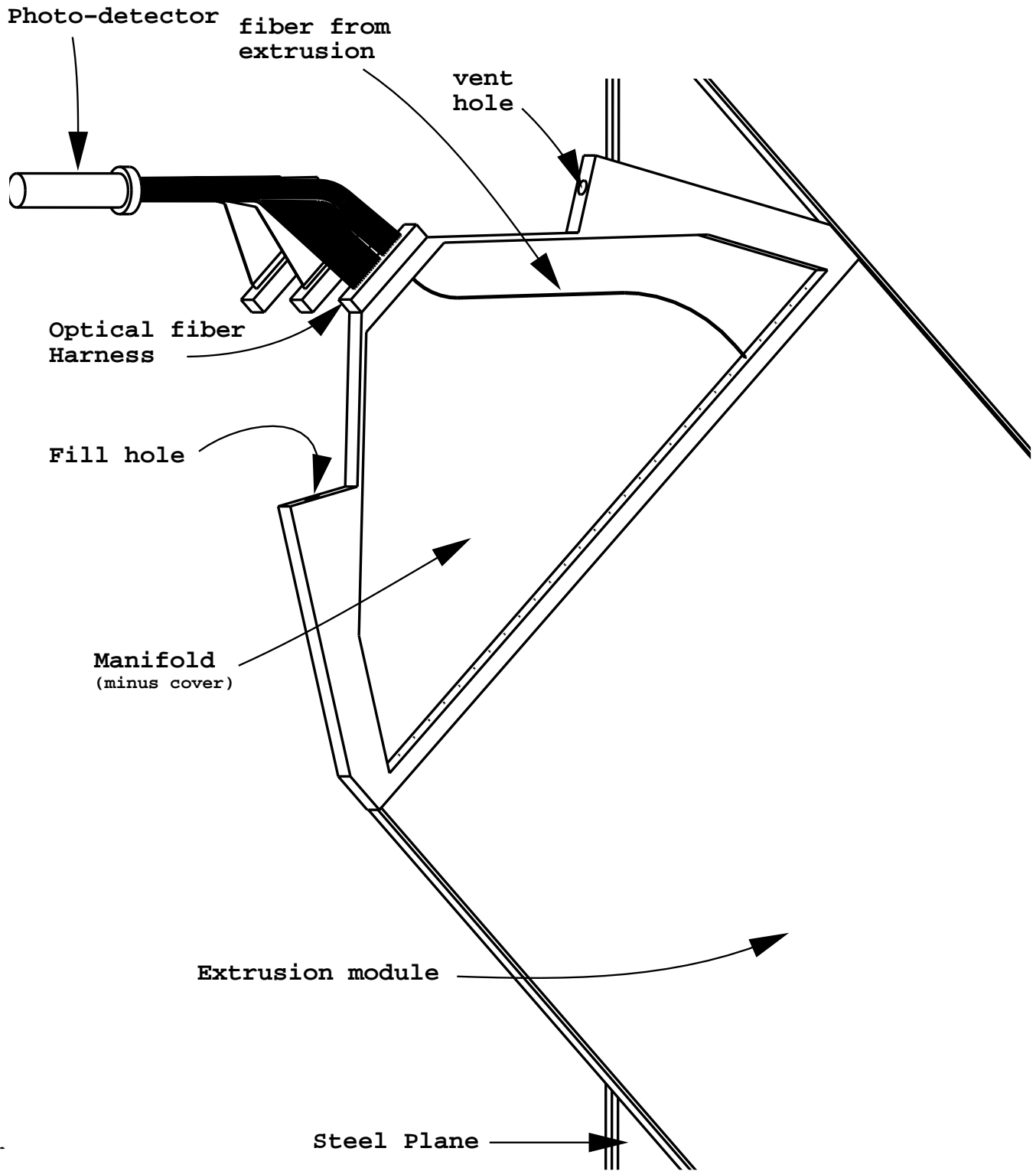


Figure 5: The cut-away of the endcap of a module (Detail 'B').

1. **Detector design:** Development of the plastic scintillator option is in its infancy, hence engineering details and cost estimates are necessarily less mature at this stage. The detector concept relies on the results of the R&D carried out for the pre-shower detectors for the D0 upgrade [9]. In this scheme, the detector would consist of planes of plastic scintillator strips 2 cm wide, 1 cm thick and up to 8 m long. The strips have a 1 mm hole in the center and light produced by charged particles crossing the scintillator is collected by 0.835 mm diameter waveshifting plastic fibers.

Detector planes will be constructed in modules with a width optimized for ease of handling, perhaps up to 160 cm wide. As in the case of the liquid scintillator, some of the strips in those modules which intersect the central hole (required for the magnet winding) will be made in two pieces. These two pieces will be read out by a single continuous waveshifting fiber which bypasses the hole.

Each module will consist of a set of scintillator strips sandwiched between 2 mm aluminum (or steel) sheets. These sheets will ensure light-tightness of the assembly and provide mechanical support. The scintillator strips will be mounted on the support sheets in a fashion to eliminate/reduce mechanical stresses, and to avoid/minimize problems due to possible crazing of the scintillator. Individual strips will be painted white to improve the light collection and to ensure optical isolation of neighboring strips. The waveshifting fibers will emerge from the modules at their upper end.

Individual modules would be manufactured at collaborating institutions and transported to Soudan for mounting into the detector. No additional assembly at the detector site will be required. Obviously, following the waveshifting fibers, the same active elements (light guides, photodetectors) are common to both liquid and plastic detectors.

2. **Cost estimate relative to liquid scintillator** As mentioned, the use of plastic scintillator is a recently introduced option, so that overall cost estimates are very preliminary. However, it is expected that most of the costs are very similar to the liquid scintillator option with the cost of the solid scintillator and its containment substituted for the cost of liquid scintillator and the plastic extrusions.

Measurements of the light yield from plastic scintillator in this configuration have been reported to give 15 photons per mm of plastic scintillator, about 1.5 to 2 times that of liquid scintillator. In that case, 1 cm thick scintillator planes may be adequate, given that there is also a small gain in light collection efficiency due to the aspect ratio of fiber diameter to cell size.

The cost of extruded polystyrene scintillator is of the order of \$4/lb (\$2.5 for the polystyrene, \$1 for the dopants, \$0.17 for the extrusion), to be compared with an estimate of \$0.7/lb for liquid scintillator: the cost of the plastic scintillator is dominated by the cost of the raw polystyrene. It is likely that scintillator produced from industrial grade polystyrene at an estimated cost of \$0.7/lb will prove satisfactory, since attenuation of scintillation light in the bulk material is not critical in this application. This factor, combined with the additional factor 2 from using a 1 cm thickness would make the plastic and liquid scintillator costs comparable.

3. **R&D projects:** We will investigate possible effects due to crazing of the plastic scintillator. Crazing could lead to a possibly significant reduction of the light yield and/or major detector nonuniformities and is one of the chief worries in this detector. We plan to investigate this problem along two lines: by investigating various scenarios for possible crazing of the scintillator (bending, pressure, stretching etc.), and by measuring any reduction in light yield.

We will investigate means of reducing the cost of the scintillator by extruding scintillator strips using industrial grade polystyrene pellets and measuring light yield and response uniformity.

As part of a study to optimize the scintillator thickness by maximizing light yield, we shall investigate effects of paint reflectivity, possibly by varying the titanium dioxide concentration.

We will also investigate possibilities of using scintillators with higher light output (such as SCSN38).

4. **Engineering studies:** To verify the feasibility of such a detector and to provide credible cost estimates several engineering studies will be undertaken. They will include:
 - (a) Detailed design of the detector planes.
 - (b) Studies of the integration of the detector planes into the absorber structure, installation, mounting etc.
 - (c) Studies of large scale manufacturing techniques. They will involve design of tooling and auxiliary equipment which will be necessary to construct and transport the detector planes (for example: fiber cutting and polishing machines, lifting and transport fixtures, etc.)

4.4.4 Photodetector R&D plan

The baseline (or reference) photodetector for both scintillator options is a 96-channel microchannel plate (MCP) photomultiplier tube manufactured by Litton Electron Devices. These tubes are a simple extension of night vision technology. Each tube will have a fiber-optic window, a three-stage microchannel plate providing a gain of 10^6 , and a pad readout on a ceramic back plate. They will operate in a pulse-saturated mode which provides a gain independent of the applied bias. As this is a well-established technology, issues such as ageing of the MCP structure or the photocathode are well understood and our requirements are well within the performance capability of these tubes.

In FY 1997 we will need to carry out some engineering design of the ceramic back plate and of special tooling for fabrication. Litton will manufacture 8 tubes for evaluation. We will conduct detailed cross-talk and destructive lifetime tests to make sure that these tubes do meet our specifications. Once these tests are complete we will make a batch of 16 tubes for use in the test beams and for further evaluation. Following this we will begin a detailed trade study with the manufacturer to optimize the device performance against the manufacturing cost to define the large scale manufacturing process.

In addition to this engineering of our baseline readout, we will be following developments in the photodetector field. We are fortunate that low cost photodetection is an area of intense activity, prompted by the needs of medical and communications technology. We will pay particular attention to the multi-channel hybrid photomultiplier tubes manufactured by DEP for the LHC experiment CMS, and to the low-cost deep-diffusion avalanche photodiodes recently patented by General Electric. Our FY 1997 cost estimate in Section 4.4.9 contains no funds for these alternative technologies.

4.4.5 Test beam and electronics plans

We propose to build a test beam detector to study the calorimeter response to electron-induced showers, in addition to muons and hadrons. This would require electrons of 1 - 30 GeV energy, both at 0° and at 30° relative to the detector axis. The scintillation detectors in this device would be shorter than, but otherwise identical to the proposed detector in all essential details. The transverse size of the test beam calorimeter would be approximately $1\text{ m} \times 1\text{ m}$. Each of the 20 steel planes would be 2 cm thick. The total number of channels would then be approximately 1000 and the weight of the detector would be approximately 3.5 tons.

1. **Mechanical.** Both plastic and liquid detector planes would be manufactured. They would be essentially identical to our proposed detector modules in all aspects except length.
2. **Electronics.** The Columbia group will provide 20 front-end cards. Each card will have 48 channels. In the card, the analog signal is integrated in a custom ASIC, digitized by a commercial ADC in real time, stored in memory, and read out to a disk/tape. An external trigger will be provided by a set of beam counters.

The custom ASIC would integrate the signals on each of 16 channels. These integrated signals would then be multiplexed to the ADCs, obtained from PREP. About $1\ \mu\text{sec}$ would be needed to digitize 16 signals with a 10 bit resolution. Timing information will be provided by the same ASIC for the first of the 16 signals to cross an analog threshold. The analog signal for the timing would be treated as an additional channel giving a total of 17 signals to digitize.

4.4.6 Calibration and monitoring

For whatever scintillator detector option is ultimately chosen, we plan to provide a calibration system which will perform the following functions:

1. Measure channel-to-channel response uniformity within the plane.
2. Measure plane-to-plane response uniformity.
3. Monitor the time stability of individual channels.
4. Enable cross-calibration of the near and far detectors.

5. Carry over the absolute calibration from the test beam to the detector.
6. Monitor/measure attenuation of the signal along the length of a strip.

We propose to employ a calibration system using a ^{137}Cs source, similar to the one employed by the CDF detector. This system was further improved and refined as a part of R&D for the SSC, and more recently for the CMS detector.

Each detector plane will have several 1 mm OD steel tubes attached to the outer walls and perpendicular to the scintillator strips. A mechanical source driver will introduce a steel wire with the pointlike ^{137}Cs source at its tip and move it across the detector. Special calibration electronics will measure the DC current of each photodetector, when it is illuminated by the source, to provide the required calibration.

One standard source will be used to cross-calibrate other sources used throughout the experiment, to provide the absolute normalization.

In addition, the electronics of the pulse height measurement chain will be calibrated using standard charge injection scheme.

4.4.7 Plans for a full-scale module

Following parallel development of both liquid and solid scintillator technologies in 1996 and 1997, one or the other will be chosen as a candidate for use in the MINOS detector. We would then construct a full-scale prototype module using that technology. This will enable us to optimize our assembly techniques and analyze the integrity of the full scale detector. It will also allow us to investigate possible construction techniques and to understand potential problems with handling such large objects. We intend to investigate various schemes for optical interconnects of fibers to photodetectors. Studies of this prototype will yield information about the uniformity of the response of a large detector. We plan to equip these prototypes with the source calibration system to conduct a full system test. For this purpose we plan to borrow one of the existing source drivers, so that no additional cost will be incurred.

4.4.8 Preliminary cost estimate for full detector

During FY 1996, the mechanical engineering and photodetector development of the liquid scintillator technology has progressed far enough that an initial cost estimate for the deployment of this system can be made.

Table 9 gives a preliminary cost estimate for the liquid scintillator implementation of the full MINOS far detector system. Only the fiber and photodetector costs are based on quotes from manufacturers. The remainder are our current best estimates based on our engineering design and preliminary discussions with potential suppliers. For this estimate we have assumed 1200 detector planes, each with 384 fibers. An 8 m wide octagonal steel plate, 2 cm thick, weighs 8.33 tons. Each scintillator plane would weigh 0.95 ton, giving a total mass of 11.1 kton.

For a 10 kton detector the overall cost reduction would be \$1.35M in the active (scintillator) detector with an additional estimated saving of \$2M for steel and installation. The resultant cost would then be \$10.2M for the active component of a 10 kton detector based on scintillator technology.

Polypropylene structures	\$1.50 M
End-cap moldings (14,400 @ \$15)	\$0.22 M
Clear fiber light guides (4,800 @ \$50)	\$0.24 M
Fibers (@ \$0.70/m)	\$2.42 M
Liquid scintillator (\$5/gallon)	\$1.32 M
Total: Mechanical Structure	\$5.70 M
Photodetectors (@ \$17/channel)	\$7.83 M
Total for 11.2 kton detector	\$13.53 M

Table 9: Preliminary cost estimate for the liquid scintillator implementation of the full MINOS far-detector active element system (in FY 1996 dollars). Only direct costs, without contingency, “G&A,” and installation, are included.

4.4.9 Liquid scintillator R&D cost estimate

Tables 10 and 11 summarize scintillator R&D supplemental funding requirements for FY 1996 and 1997 respectively. FY 1996 R&D funds are for liquid scintillator development work only; development of solid scintillator technology has begun only recently, and has used institutional funds so far. Our initial estimate for scintillator detector construction costs in FY 1998 is shown in Table 6, which applies to all active detector technologies. Development of detailed FY 1998 construction cost estimates for both the solid and liquid scintillator options is currently in under way.

In FY 1996, MINOS collaborators have paid for a substantial fraction of the liquid scintillator R&D work with institutional and base-contract funds. The supplemental funding requirements shown in Table 11 assume that this practice will continue, although not to as great an extent as in FY 1996, when the funds received (late in the year) were much less than anticipated.

Institution: activity	Source	\$K
Minnesota: Photodetector studies	Fermilab	18
Minnesota: Full length extrusion tests	Fermilab	10
Indiana: Light yield measurements		0
Texas A&M: Light yield studies, engineering		0
Total FY 1996 liquid scintillator R&D		28

Table 10: FY 1996 funding for liquid scintillator R&D work (actual allocations). Solid scintillator R&D was paid for from institutional funds during FY 1996.

Activity	\$K
Common tasks for liquid and solid:	240
Photodetectors (prototypes, engineering):	100
Conceptual design and cost engineering:	45
Light yield, reflectivity, crazing studies:	40
Light guide prototypes:	10
WLS fiber mirroring:	5
Scintillator chemistry (light yields):	10
Calibration system:	5
Electronics:	25
Liquid scintillator tasks:	90
Engineering:	15
Prototype materials:	55
Prototype detector assembly:	20
Solid scintillator tasks:	50
Engineering:	15
Polystyrene extrusions:	15
Prototype detector assembly:	20
Total FY 1997 scintillator R&D	380

Table 11: FY 1997 scintillator R&D funds for solid and liquid scintillator R&D work (in FY 1996 dollars). Development of liquid and solid scintillator options will proceed in parallel during FY 1997.

4.5 Electronics

4.5.1 Electronics design status and issues

The MINOS electronics design effort is currently focused on the evaluation of alternative conceptual designs and architectures for the detector readout. The reference design as outlined in the proposal is still valid, but several suggestions for improvements are now being investigated.

Electronics R&D is constrained by the fact that the technology of the active detector elements may not be chosen until June 1997. For the current technologies (Iarocci chambers in limited streamer or proportional mode, RPC's and scintillator with individual channel readout) there can be a common overall architecture for the readout and triggering, but each technology has its own special requirements. Extreme cases, for example the use of CCD arrays to read out liquid scintillator tubes (which is currently not favored), could necessitate completely different systems. Although we cannot proceed with the final electronics system design immediately, it is nevertheless useful to investigate some of the special requirements of the detector types under consideration to determine if they pose any particular design difficulties or costs (e.g. higher gain for APD scintillator readouts or fast timing for RPC's). In general, detector differences fall into three categories: noise rates, signal size and signal shape (not necessarily independent).

Another issue which affects the electronics design and has yet to be resolved is the structure of the beam spill. This is also outside the control of the electronics group and awaits a decision from the accelerator and beam designers.

Two subsystems which are not directly in the readout chain are the global trigger system and the pulser/calibration system. Both of these are tightly intertwined into the overall design and plans must be made for them from the beginning.

The issue of the readout system for the Soudan 2 detector, in particular for the near detector modules, must also be addressed. If a new electronics system is designed for the Soudan 2 near detector modules, perhaps the whole system currently in use for the Soudan 2 detector readout at Soudan should be similarly upgraded. Another subsystem which is included in the purview of the electronics group is the monitoring and slow control system. This must be integrated from the beginning and not be seen as an add-on at the end, since it has interfaces to the electronics which must be defined at an early stage. Finally, the electronics group will be responsible for the MINOS data acquisition system itself, consisting of a host computer, interfaces to VME crates and specialized VME cards. Almost all of these will be off-the-shelf components which do not need to be specified for several years.

4.5.2 Current electronics development work

The ultimate goal of the MINOS electronics R&D program is to produce a working readout system which will be tested and ready to operate when the detector installation begins. An intermediate goal is to have prototype electronics ready to test on the large hadron calorimeter in the January 1998 Fermilab test beam run. Although the electronics effort must be delayed until the active detector design and beam spill structure are finalized, the final design will be able to take advantage of advances in electronics technology which have occurred during this period. In addition, the actual electronics fabrication will be performed

by well established industrial procedures, and will take substantially less time than the rest of the MINOS detector production.

Current electronics design work is proceeding along two lines: investigation of possible improvements to the overall concept presented in the reference design, and consideration of how to deal with the peculiarities of the different detector technologies which are being developed.

One interesting alternative to the reference design is to use hundreds of processors to make trigger decisions and handle the readout. Each processor would have access to the data from one detector plane and would have fast data connections to the other processors, so they could look for patterns in the data which characterize interesting events (i.e. a trigger). Interesting events would then be sent to a host computer while nontriggering data would simply be overwritten. The interest in this approach is driven by its high degree of flexibility and by the availability of increasingly powerful and inexpensive processors.

Another alternative to the reference design can be characterized as “beam-driven” readout, as compared to the “data-driven” readout in the reference design. Here, short beam gates are generated and data are collected on all channels at once, providing a snapshot of the detector at the moment of each beam extraction ‘ping’. This has the advantage that all channels are on equal footing, and no hardware threshold is applied to any of them. It is also a very powerful method for reducing the accidental rate from noisy detectors since the beam gates are only open for a small fraction of the total time. A possible problem is that one must be able to predict, to better than 100 nsec, when the neutrinos will arrive at the far detector in Soudan. Of course this system only works with the ‘pinged’ beam extraction mode, and would not work with a continuous spill. In addition, a conventional trigger would be required for cosmic-ray events occurring between beam spills.

Both of these ideas are being evaluated and developed, and will eventually be costed. Work is also progressing on the reference design. Small runs of prototype chips will be produced which, while not the final ones with full functionality, will be able to test specific implementations of some of the circuits used in the reference design. This will enable us to find problems in the design, improve our cost estimates, and gain experience with practical design problems. It is our intention to establish a continual process of improving the overall design by declaring certain ideas as ‘standard’ when they are shown to be an improvement over the original reference design. This will culminate shortly after June 1997 when the final detector technology choice is made. At that time a final electronics design will be agreed upon and detailed design work will commence.

Until the final detector choice is made, we plan to investigate potential problems or advantages of specific technologies. This will enable us to prepare for the various scenarios and may provide input to the technology choice. Table 12 shows some of the ‘features’ of the various technologies as viewed from an electronics point of view.

Although it was not their direct responsibility, the electronics design group provided front-end electronics for the 1996 SLAC test beam run, and plans to support the 1997 Fermilab test beam runs in a similar fashion. A number of the people working in the electronics group are also closely involved with the detector work, and it is natural for them to assume these tasks. This provides hands-on experience in dealing with the problems associated with the detector types under study by the collaboration.

Detector Technology	Noise Rates	Signal Size	Signal Structure
Limited Streamer Tubes	Low	Large	Afterpulses Possible reflections Fairly fast
Resistive Plate Chambers	Moderately high	Large	Afterpulses Possible reflections Very fast
Proportional tubes	Low	Small	Long pulses
Scintillator w/micro channel plate	Low	Large	Very fast
Scintillator w/Avalanche photodiodes	Very high	Very small	Fast

Table 12: Features of different MINOS active detector technologies which must be accommodated by the electronics design

4.5.3 Electronics R&D plan

Oct95-Aug96 Activities:

- Evaluate improvements to the conceptual design of overall architecture compared to the reference system
- Consider how this would fit on custom chips
- Investigate possible problems with the special requirements of each technology
- Get preliminary detector signal characteristics from SLAC test beam runs

Aug96-May97 Activities:

- Board level tests of concepts
- Design, produce and test small scale runs of prototype chips (not necessarily with all functions)

Nov96-Apr97 Activities:

- Test some chips and boards with real detectors in the FNAL test beam
- Get detector signal characteristics from FNAL test beam data

August 97: Final active detector technology choice

Aug97-Mar98: Definitize final overall design:

- Final, detailed, conceptual design of chips, boards for chosen technology
- Design, produce and test runs of prototype chips to test final design

Oct97: Complete MINOS detector Technical Design Report

Jan98 Activities:

- Large scale hadron calorimeter test beam studies at Fermilab
- Supply prototype electronics for readout

Mar98-Feb99 Activities:

- Engineering of final chips, VME boards
- Final component tests

Feb99-Jan02 Activities:

- Large scale production of chips
- Large scale production of VME boards
- Testing of chips (final QA)
- Testing of boards (final QA)
- System integration tests between components
- Procurement of cables, connectors, crates,...

Aug99-Apr02 Activities:

- Installation of electronics on the detector as the planes are built
- Final system integration of readout, triggering, control and DAQ

June 01: Begin data taking with first third of detector

4.5.4 Current institutional responsibilities

Table 13 outlines the current electronics design responsibilities of MINOS collaborating institutions.

Institution	Work to be performed
Argonne	DAQ system, Iarocci, RPC problems, Soudan 2 electronics upgrade
Columbia	Investigate beam synchronized digitization and ‘triggerless’ readout, Scintillator problems
Oak Ridge	Design front-end analog chip
Oxford	Design front end digital chip, bus interface chip Investigate integrating ‘triggerless’ system into reference Design readout/trigger VME boards
Rutherford	Assist with UK chip production
Sussex	Assist with UK board production

Table 13: Current electronics design responsibilities of MINOS institutions.

4.5.5 Electronics R&D cost estimate

Tables 14 and 15 summarize MINOS electronics supplemental funding requirements for FY 1997 and FY 1998. All FY 1996 electronics R&D work was paid for from institutional funds. The FY 1997 costs in Table 14 are entirely R&D funds, while the FY 1998 costs in Table 15 consist of some R&D and some construction funds.

Activity	\$K
Prototype chip production	70
Cost estimate engineering	20
Evaluate conceptual design alternatives	20
Detailed final design	40
Total FY 1997 electronics R&D	150

Table 14: FY 1997 funding for electronics R&D work (in FY 1996 dollars).

Activity	Funds	\$K
Test beam calorimeter electronics	R&D	100
Detailed final design	Constr.	140
Tests of final design	Constr.	50
Board engineering, prototype	Constr.	60
Chip engineering, prototypes:	Constr.	1022
Monolit. chip design	922	
Chip proto., testing	100	
Expected UK contribution:		
Engineering effort	Constr.	-566
Total FY 1998 electronics cost		806

Table 15: FY 1998 funding for electronics work (in FY 1996 dollars).

4.6 Test beam plans

4.6.1 Schedules and goals for test beam runs

The response of MINOS active detector prototypes to electromagnetic (EM) showers, hadron showers, and muons will be measured in a series of charged particle test beam runs at SLAC and Fermilab. The SLAC Final Focus Test Beam (FFTB) is particularly convenient for the initial tests because it provides easy access to few GeV pure electron beams. These studies follow initial testing of prototype chambers with cosmic rays and radioactive sources, in which detector design and operating parameters have been optimized. Test beam studies will eventually be performed on all three active detector types (Iarocci chambers, RPC's, and scintillator) and will include prototype front-end electronics (which are an integral part of detector response).

While the ultimate goal of these studies is to determine the parameters of detector response to EM and hadron showers in actual steel-plate calorimeters, initial test exposures are designed to provide a first look at the response of single prototype chambers to EM showers. Later, more sophisticated tests will be used to determine calorimeter response characteristics for detector simulation software, and eventually to check detailed predictions of the simulation programs for both EM and hadron showers. Four separate test beam running periods are planned:

1. **SLAC FFTB Run: March-June 1996.** The response of Iarocci and RPC detectors was measured with few GeV electrons. The response at various depths within EM showers was compared to that of plastic scintillation counters. Initial studies of the response of an actual steel-plate calorimeter, provided by the Dubna group and instrumented with Iarocci chambers, were also performed. Issues of particular concern for this run include:
 - Effectiveness of prototype electronic afterpulse suppression circuits in RPC's.
 - Calorimeter response of different RPC types in EM showers.
 - Iarocci chamber response in limited streamer mode with nonflammable gas.
 - Iarocci chamber response in saturated proportional mode with nonflammable gas.
 - Ability to reproduce Iarocci tube calorimeter response achieved in previous experiments.

The calorimeter response of scintillation detectors is believed to be sufficiently well demonstrated in previous experiments that it does not need to be verified at this stage in our R&D program.

Prototype chambers studied at SLAC include: Iarocci tube detectors built at Dubna, operated in both limited streamer and proportional mode, Iarocci chambers built at Argonne operated in proportional mode, and RPC's built at Caltech and RAL (both with glass plates) and at Livermore (with ABS plastic plates). Data recorded during this run, which ended during the second week of June 1996, are still being analyzed.

2. **Fermilab Run #1, January 1997.** This run is planned for the "CDF" test beam at Fermilab, and will make use of the existing Dubna steel plate structure (which was first

used for the SLAC test beam run) to study the response of Iarocci chamber and RPC detectors to EM showers for energies up to tens of GeV. The shower energy and angle, and steel plate thickness will be varied to verify detector response simulation software. The tests will include ~ 300 channels of prototype front end electronics, e.g. amplifiers for proportional mode operation of Iarocci chambers, and afterpulse suppression for RPC's. Muons will be used to measure the spatial resolution of prototype detectors.

3. **Fermilab Run #2, April 1997.** This run will continue the studies of Iarocci chambers and RPC's which were started in Fermilab Run #1, and will also extend these measurements to a prototype calorimeter instrumented with scintillator detectors for the first time. The scintillator tests are described in more detail in Section 4.4.5 above. In addition, the response of full-length prototype MINOS chambers (up to 8 m long) will be measured in a test beam for the first time. By the time of this run, we hope to have learned how to obtain electrons down to a few GeV in this beam. A scheme for low energy operation has been worked out by CDF test beam users, but has not yet been tried.
4. **Fermilab Run #3, January 1998.** This run will measure the detailed response of a large prototype hadron calorimeter using the active detector technology which has been selected for MINOS. The front-end electronics used for these studies will be prototypes of the final, optimized design. Because of the large number of channels of custom electronics required (several thousand), the electronics will be one of the most expensive components of the test beam calorimeter. The steel plate calorimeter structure will be deep enough to contain hadron showers up to 20 GeV, and will have a large enough area that the response can be measured as a function of incident angle. The EM shower response and muon spatial resolution will also be measured. This run will provide a final check and calibration of the MINOS active detector response used in the experiment simulation software.

It is possible that these studies could be performed in a test beam at Brookhaven instead of Fermilab. Our decision will depend on the Fermilab test beam schedule (which depends on Main Injector commissioning) and on our success in obtaining satisfactory operation at low energies.

4.6.2 Costs associated with test beam runs

Table 16 summarizes the supplemental funding requirements for MINOS test beam running for FY 1996, FY 1997, and FY 1998. In FY 1996, \$5K was allocated by Fermilab to pay for operating supplies for the SLAC test beam run.

Activity	\$K
FY 1996:	
SLAC test beam operations	5
Total FY 1996 test beam costs	5
FY 1997:	
Fermilab test beam equipment	20
Fermilab test beam run #1 operations	20
Fermilab test beam run #2 operations	20
Total FY 1997 test beam costs	60
FY 1998:	
Hadron calorimeter construction	160
Fermilab test beam run #3 operations	20
Total FY 1998 test beam costs	180

Table 16: FY 1996-8 funding for test beam running (in FY 1996 dollars).

5 Steel and Magnet Technology

5.1 Executive summary

This Chapter contains the Report of the MINOS Steel Technology Committee (STC), which was set up by the Collaboration to provide advice on the choice of the optimum design for the fabrication of the large magnetized-steel detector planes. The current Section contains a summary of the STC recommendations. The Report itself, which is reproduced in Sections 5.2 - 5.6, outlines a procedure for choosing a specific fabrication scheme, and identifies the criteria for making the evaluation. Section 5.7, which is not part of the STC report, summarizes the costs associated with the steel and magnet R&D program.

The design optimization of the magnetized-steel planes proceeds from considering a reference design, and two alternative designs that may offer performance or cost advantages. Currently, the three designs are:

1. **Reference design.** This design consists of 8-m wide, octagonal steel planes constructed from crossed-laminate structures of 2-m wide plates. The current design [10, 11] is an optimized version of the design in the MINOS Proposal.
2. **Laminated-pie design.** This fabrication method produces 8-m diameter, circular steel planes from six laminations, each of which is composed of twelve identical triangular (pie-shaped) segments.
3. **Spiral-wound design.** This method fabricates 8-m diameter circular steel planes by winding thin steel strap material onto a central hub, to produce a structure similar to a reel of magnetic tape.

The purpose of pursuing multiple designs is to explore innovative solutions to performance and cost issues. The reference design represents a credible and documented baseline against which new ideas can be compared. The design is dynamic. It is modified, refined, or even completely changed, based on the input derived from comparing it with new ideas. The scheduled major reviews of the design concepts provide the opportunity to make large changes and set the direction for future R&D design work. Part of the charge to the STC was to conduct the first of these reviews.

The radically different nature of the alternative designs has helped to expose and clarify the major issues of constructing the far detector, for example:

- The effect of the steel shape and the geometry of gaps on magnetic field quality,
- The trade-offs between assemblies with many small pieces or few large pieces,
- The requirements on assembled plane flatness tolerance.

These issues are easy to identify, but difficult to evaluate without considering specific implementations. Many of the criteria, for example the magnetic field uniformity and flatness tolerance, may need to be verified by constructing prototypes.

The STC recommendations to the MINOS Collaboration are detailed in Section 5.5. They are, in summary:

1. We urge the Collaboration to agree as soon as possible upon the essential input parameters for the design of the MINOS far-detector magnet structure:
 - Plane thickness (e.g., 4 cm or 2 cm),
 - Criteria to evaluate the effect on physics performance of the plane-to-plane gap,
 - Constraints imposed by magnetic field magnitude and quality requirements.
2. We recommend that engineering studies be initiated to establish the intrinsic constraints imposed by mine cage and shaft limitations, including the range and cost of their potential alleviation.
3. In general, we encourage work to understand better the requirements of the passive detector layers before fully funding one, two, or three parallel efforts in FY 1997. The more decisions which can be made early, the cheaper the project will be in the long run. These decisions must be made soon, if we are to keep the goal of committing FY 1997 funds to construction of one or two prototypes. These decisions should recognize the intrinsic engineering complexities in making the thin steel planes required for the MINOS detector. The chosen design should be as robust as possible to minimize and overcome unexpected setbacks.

We also have recommended several steps to be taken in the short term which should facilitate making an early and sensible decision for support of steel plane prototype construction:

1. *Establish magnetic field quality criteria*
2. *Make design studies for both 2 cm and 4 cm options*
3. *Keep option open for two full-scale prototype planes*

5.2 STC Report: Introduction

At the April 1996 MINOS Collaboration meeting, it was decided to set up a special review committee for steel and magnet R&D work. This committee would make recommendations about future work after listening to presentations at the MINOS Workshop at Lutsen, Minnesota during the first week of June 1996.

The following committee was appointed by Stan Wojcicki, the MINOS Spokesperson:

Lincoln Read	Fermilab	Chair
Hans Courant	Minnesota	
Tom Fields	Argonne	
Jim Kerby	Fermilab	
Rick Milburn	Tufts	
Bill Miller	Minnesota (Soudan)	
Doug Wright	Livermore	

The charge to the Steel Technology Committee (STC) is as follows:

- a) The main goal of the committee is to define the optimum R&D path towards choosing the design and manufacturing method for the MINOS magnet/steel planes. The specific tasks requested of the committee are chosen so as to implement that general goal.
- b) The committee shall define the general criteria for the choice of MINOS magnet technology.
- c) The committee shall define, for each technology, the steps necessary to determine whether these criteria have been met, the time scale necessary for this task, and the resources required. The committee shall work closely with the people working on each technology in carrying out this specific task.
- d) The committee shall propose an optimum method for making the choice in this technology area.
- e) The committee shall also look at the overall funding request and evaluate its reasonableness. In addition, it shall recommend the optimum path to follow if the FY97 funds allocated to magnet R&D are only 50% or less of the currently proposed value.
- f) The committee shall prepare a written document (initial draft in time for the Lutsen meeting) of about 15 pages in length, describing their conclusions.
- g) The committee shall present its findings at the Lutsen meeting for a general discussion and critique by the MINOS collaboration and organize a review at Lutsen of the current status of the magnet R&D program with a view to determining the optimum course of action in the future.
- h) The committee shall complete the tasks defined in this charge by the time of the start of the June Fermilab PAC meeting. The issues of the continuation of the committee, its possible reconstitution, enlargement of its charge, etc. will be decided shortly after that time.

The STC met at Fermilab on 10 May 1996 and again in June at the week-long MINOS Collaboration in Lutsen, Minnesota. In addition to written documents, formal presentations and informal working group discussions about the various design efforts formed the basis for this report.

5.3 Criteria for the magnet technology choice

The following sections present a sequence of steps to select, in an efficient way, a design concept that meets the essential physics requirements at minimum cost for the MINOS far detector. A definition and description is given for each step, along with a rationale and comments summarizing the views of the STC.

5.3.1 Step 1: Definition of Nominal Design

A particular “nominal design” is defined as a complete and specific scheme to manufacture, transport to the mine, assemble and mount the steel absorber planes for the MINOS far detector. The scheme should include:

- a) Mechanical and geometrical design of each “plane”: e.g.
 - Composite thickness (2 cm, 4 cm, ? cm),
 - Material (elastic constants, density, B/H),
 - Laminated components (sizes and shapes), or spiral-wound input stock size, or whatever.
- b) Composite plane fabrication scheme (weld, bolt, winding, etc., with locations and sizes etc. specified).
- c) A specific design of the mechanical supporting structure for the planes in their final assembled configuration in the MINOS detector. For this structure a plane-to-plane (“gap”) spacing, with tolerances in spacing and flatness, should be given. Mechanical attachments and other features required to integrate the planes with the active detector elements are also very relevant here.
- d) A scheme for pre-site fabrication, transport to the mine and insertion into the Level 27 cavern, for assembly on-site, and for erection into the final structure of item c), above. The scheme must be sufficiently specific that credible costing can be carried out.

Rationale. This definition of a “nominal design” recognizes that variations in design parameters, even seemingly small ones, can have significant effects on manufacturability and costs, as well as on physics performance. (e.g. The choice 2 cm *vs* 4 cm affects the labor costs for assembly, the structural design and safety of the assembled detector, the handling mechanisms needed in the cage and shaft and (*via* flatness tolerances) the jigs, clamps, etc. for the assembly process.) Thus, to be in contention, a “nominal design” must be sufficiently specific that, were it used as the absorber for the MINOS far detector, its mechanical and magnetic properties and also its overall cost may be fairly evaluated.

We recognize that certain parameters might reasonably be varied to permit easy generation of “sub-designs.” Thus use of different kinds of steel of varying magnetic properties and costs but with similar mechanical properties *vis-a-vis* elastic moduli, machinability, weldability, etc. may enable several “nominal designs” to be developed simultaneously with but little extra effort and cost.

In general, we assume that a proposed “nominal design” will, *a priori*, be consistent with the enunciated collaboration requirements in respect to plane thickness(es), gap size(s) and flatness tolerance(s), known size and weight limitations of the mine cage and shaft (as is or as modifiable), and with minimal magnetic field requirements, as known at present or as may be determined in the future. Because a great deal of time and effort must be expended to pursue any given “nominal design,” it is *obvious* to STC that the sooner the MINOS Collaboration can resolve the several physics-related ambiguities of this sort and settle on a

specific plane geometry and tolerances, the less expensive and more rapid will be the process of developing the (one or more) surviving design(s) to the point where a sound evaluation and comparison are possible.

5.3.2 Step 2: Credibility demonstration, with implied total cost

Each Nominal Design, if it is to survive as a candidate for the construction of the MINOS far detector, should be subjected to a detailed engineering and cost analysis to prove, to the maximum degree short of actually building an accurate full-sized prototype, that the particular design is practical, that it will safely meet the physical specifications for which it was created, and that the included estimates of cost of manufacture, assembly and erection of a detector based upon it will be as believable as possible, at least *a priori*.

This analysis should include:

- a) A stress analysis of the planes as fabricated and as mounted in the final detector assembly sufficiently detailed to assure that the required gap and flatness tolerances can be met and maintained, and that the composite structure will be safe under appropriate conditions of gravitational overload, weld/bolt failure probability, etc. While this analysis will be largely theoretical (using finite element methods etc.) small-scale laboratory modeling, as of bolting or plug-welding properties, may be appropriate.
- b) Similar stress analyses for the assembly and erection process, including allowances for the problems of inducing/removing plane distortions, for the effects of stresses from welding, erection, and handling generally.
- c) A step-by-step demonstration that the primary plane components can be loaded and brought down the shaft in a feasible modification of the cage and that they can be safely unloaded and brought to the assembly area.
- d) A detailed analysis and prediction of the total cost of the steel portion of the MINOS far detector, were it to be built according to the nominal design in question. This estimate should be for everything: EDIA, raw material, labor, off- and on-site preparations, shipping and hoist charges, supporting structures, special cage modifications — everything which is relevant to making a reasonable cost estimate of the steel component of the final detector.

Rationale. The STC recommends that, prior to final determination of the steel absorber design of the MINOS Far Detector, a full-sized functional prototype plane be built and erected in its operational orientation using a supporting structure that simulates the proposed detector mounting as closely as possible. The great weight and mechanical flimsiness of the individual steel planes, together with the novel schemes proposed for their assembly to required tolerances from multiple smaller elements insertable into the Soudan mine, push against the limits of familiar techniques. In any case, once an acceptable design has been established, it will be desirable to fine-tune the fabrication and assembly techniques, and to train staff, before subjecting them to the constraints of the mine environment. The prototype will surely cost much more than the per-element cost of production-line planes as assembled

in the final detector. These costs will, however, be for “development,” not “production,” and (unless they are truly excessive) are in principle an investment in good physics.

Before proceeding to this expensive and time-consuming but essential step of fabricating a full-scale prototype according to a particular “nominal design,” we must be as certain as possible that not only the prototype but also the final assembly and erection in a stable and safe detector configuration will actually proceed as anticipated, on the required time scale and at a realistically determined cost. This requires a competent and thorough engineering analysis of each contending “nominal design” candidate for prototype. We assume that while this “credibility” analysis is underway, cost estimation will proceed in parallel and that the combined experience will lead to a dynamic evolution and refinement of the original nominal design. Further evolution may be expected from input of external information about the geometry and mounting of the active detector elements.

The output from this critical step in the evaluation process will thus be: **First**, a credible demonstration that construction of the passive detector elements according to the scheme of the nominal design is feasible *a priori* and that it will meet the specified physics requirements adequately and safely; and **Second**, that were this design chosen for the MINOS far detector the total cost can be estimated credibly as so-many dollars (with a detailed breakdown indicated).

Comments. It is evident that the work required to perform this “credibility” study on a particular nominal design is considerable, in human and computing time and thus in money also. To date, *only* the mechanical analyses of the MINOS “reference design” done at Livermore (see Section 5.4 below) appear to have approached a technical level which would justify taking the risk of actually building a costly full-scale prototype, and even this design remains not totally defined in regard to plane thickness, gap size and tolerances, assembly and mounting methods, relation to shaft and cage modifications, etc. In consequence, the cost estimates are also incomplete. In any case, competing alternative designs must be held to similar technical standards to those demonstrated in the Livermore analyses and must be costed to the level of detail outlined in the preliminary estimations presented by Miller and Alner with respect to on-site assembly and erection. It thus appears obvious that the fewer nominal designs which are submitted to this expensive and time-consuming credibility/cost demonstration cycle, the better. To achieve this, critical collaboration decisions in regard to those parameters which essentially distinguish one nominal model from another should be made at the earliest feasible moment. These include: plane thickness, gap-width and tolerances thereon, and constraints imposed by irreducible cage and shaft limitations. Possibly of comparable importance, insofar as they influence the segmentation of the elements comprising the individual planes and thus their assembly and mechanical integrity, are physics decisions in regard to the magnetic field requirements: minimum field, maximum current, and field uniformity near “cracks.” While the determination of certain parameters may turn out to be somewhat less urgent, in that they reflect primarily upon scalable cost estimations (choice of steel, precision of preliminary machining, etc.) rather than upon essential structural features, this cannot be settled until adequate field studies and tracking simulations have been carried out. The sooner these are completed, the better!

We recognize that these requested decisions are correlated with decisions about the active

detector technology, e.g. “2 cm *vs* 4 cm,” which has a major impact on the plate design and its cost. The fact remains that as long as this ambiguity exists one must either hold the steel program in abeyance, or proceed along parallel paths at additional effort and expense.

5.3.3 Step 3: Prototype choice(s)

Ideally, if one had several distinct and credible designs which would, at tolerable cost, meet the physical requirements of the MINOS detector, one would build a full-scale prototype for each. Experience suggests that revisions of design and manufacturing procedures, and of cost estimation, will flow from the actual experience of prototype construction. In several ways our detector pushes the limits of familiar technology and one hopes to avoid, but cannot absolutely rule out, the discovery of some irremediable flaw in one of the design options that would force the choice of an available alternative. Each full-scale prototype plane represents a big investment, not only for its intrinsic cost but also for the personnel costs and intellectual energy expended in any first-of-its-kind construction. The number of affordable prototypes will be limited. The goal of the preceding steps is to provide the most credible quantitative evidence for the ability of one or several designs to meet the physics requirements of the MINOS program, and of the respective cost for each to do so. This is the essential foundation for making an intelligent comparison of technologies.

The final certification of the credibility demonstrations and associated total cost implications presented by those nominal designs reaching this point should be analyzed by a suitably composed *ad hoc* committee of technical experts who will present their judgment to the collaboration. It is very important that this committee include experienced and disinterested engineers with expertise in the technology areas under review and in the sort of on-site construction problems posed by the mine environment.

5.4 MINOS Magnet technology options: characteristics, status and critique

At this writing there exist three distinctly different schemes for fabricating the steel absorbing planes of the MINOS far detector. Within each scheme are a number of variations — potential if not worked out in detail — in a plane’s external shape, thickness, segmentation, material, in techniques for fabrication, transport, assembly and final mounting in the detector. The mechanics of active detector integration and of magnetic field measurement facilities will also need to be included. In this Section we summarize the characteristics of these technology options and attempt to indicate the development status of each in the context of the proposed general criteria of the preceding Section 5.3. We also outline what should be done to bring each scheme to a level of design whose credibility can be ascertained. The material in this Section is substantially that provided by the proponents of the several technologies before and during the Lutsen workshop, edited for clarity into a common format.

5.4.1 Reference design

The current reference design [10, 11] is an optimized version of the design described in Chapter 5 of the MINOS Proposal.

Planes. 8-m octagons, 4-cm thick; each a 2-layer laminate of a minimal number of large steel sheets, rectangular and trapezoidal, crossed, welded together at various points in a compression jig for mechanical rigidity and to improve flatness tolerances.

Design variants:

- (i) 2 cm (or other) plane thickness,
- (ii) Different component dimensions for improved magnetic performance or ease of installation.

Status:

1. The subassembly of steel pieces into a full octagonal plane was examined in four ways:
 - (a) Butt joints between full thickness plates,
 - (b) Angle joints between full thickness plates,
 - (c) Lap joints between full thickness plates,
 - (d) Laminate of two crossed, half thickness plates.

The crossed laminate concept has the advantage of minimal machining, maximum strength, and improved magnetic field uniformity. Multiple laminated layers (greater than two) have also been investigated. More than two laminates may provide improved flatness tolerances, but with increased cost.

2. Two plate-attachment schemes were considered: plug welding and counterbore bolting. We determined that welding yields a much stronger attachment with less machining and overall cost. We conducted multiple sample weld tests to confirm the speed and quality of the weld.
3. We estimated the expected flatness tolerances by first examining industry standards and then we consulted directly with steel mills. This resulted in an upper-bound estimate of 1.5 mm for the flatness tolerance of an assembled plane. We also investigated the ability to flatten the plates by pressing them together before welding. We calculated that a significant amount of waviness can be removed by such a procedure.
4. To investigate the weld performance and measure the gap and flatness tolerances we constructed a 1.2 m \times 1.2 m square prototype. A pair of 2 cm plates was measured before and after being clamped together and welded. The laminate gap was measured to be below 0.5 mm with a surface flatness tolerance of approximately 1.5 mm. The plates were not pressed against a flat surface, so improved flatness tolerances could be achieved with an improved assembly setup. A large heat load (via an extremely large weld) was applied to the plates and no significant distortions were observed.
5. A full finite element analysis of the reference design steel plate configurations was conducted. The analysis incorporated the steel plate pieces, welds and minimal axial rod configurations. Both 2 cm and 4 cm thick designs were calculated for both floor support and side-rail support options. All designs were found to be within adequate safety margins for buckling and exhibited minimal deflections.

6. We find that the magnet coils can be made from off-the-shelf, inexpensive components and constructed in a conventional manner.
7. Detailed 3-D magnetic field calculations of the steel plane geometry were performed using the tolerances determined from prototype tests and other estimates demonstrating improved fields due to lamination. The integral fields were calculated and are being used to investigate muon tracking performance in the Monte Carlo simulation.
8. We obtained steel samples from a potential mill and conducted metallurgical and magnetic analysis on it. The steel was found to have the expected field strength and composition.
9. The detector cost estimates were reduced by optimizing each step in the process of manufacture, machining, transportation and assembly. We realized savings by reducing the number of different operations, performing multiple operations simultaneously and by organizing the sequence of steps in a globally minimal way.

To do: Tasks for remainder of FY 1996 and FY 1997:

The main goals are to verify the estimates of the performance parameters (e.g. flatness, gap tolerance, etc.) for full size planes, evaluate the effects of these parameters on physics analysis, establish whether stress-relieved steel is required (a potential cost savings of approximately \$1M), and improve the feasibility and cost assessment of the fabrication plan and assembly concept.

Based on the encouraging results of the 1.2 meter steel tests, we plan to measure the performance of increasingly larger plates. The main deliverables are measurements of the gap tolerances and flatness. The reasons for small (one quarter and one half size tests) are two-fold: if the parameters of smaller plates are determined to be unsatisfactory, larger prototypes are unnecessary; the cost of multiple tests can be kept low, while allowing a measure of the repeatability of the concept. These tests will also determine the weld parameters and method for the full-scale test. Ultimately a full-scale prototype will be constructed and lifted into the vertical position.

The small-scale and full-scale prototype measurements will be integrated into a single, modular test station. This test station will incorporate metrology for horizontal and vertical flatness and gap estimates. It also provides a test-bed for prototype assembly fixtures (e.g. strongbacks, hydraulics, lifting mechanisms, weld machines). The test station is, of course, not limited to measuring any one steel concept.

Summary of FY 1996-1997 tasks:

- preliminary validation of reference design
 - analysis of muon tracking with calculated magnetic fields
 - magnetic characterization of welds
 - refined plate handling plan
- physics analysis effects from steel tolerances

- muon tracking/acceptance
- event containment
- shower resolution
- refined 3-D magnetic field calculations
 - incorporate measured BH curves
 - recalculations based on new tolerance data
 - verify calculations with physical model
- active detector effects
 - attachment concept
 - mechanical loading (especially for scintillator option)
- finite element analysis of multiplane structure
- magnetic field mapping (to verify prototypes)
 - measure field in steel prototypes
 - develop plan for field mapping in final detector
- tolerance parameter tests
 - site preparation
 - test station construction
 - quarter and half scale tests (multiple versions)
 - full-scale partial tests
 - stress relieving investigation
- full scale prototype
 - upgrade test station
 - plane assembly and metrology
 - magnetic field mapping
- near detector conceptual design and small-scale prototypes
- refine cost estimates and fabrication plan

Tasks for FY 1998:

Following the choice of the steel technology in mid 1997, the final design and eventual prototype production would begin in FY 1998 with construction funds. A complete systems test of at least three full planes of the detector would be constructed. The system test would include installation of prototype active detectors and assembly of the planes in the vertical support. Installation procedure and plane-to-plane separation would be studied.

Summary of FY 1998 tasks:

- far detector tests
 - assembly test station construction (or upgrade of full-scale test station)
 - vertical supports and strongback construction
 - steel machining
 - plane assembly and metrology
 - magnetic field mapping
 - plate handling study
 - prototyping of automated tooling or special fixtures
 - survey and alignment systems tests
- near detector full scale prototypes and system test

Mounting. On floor, or by various schemes of hanging including edge mounting. For rigidity and stability, the planes are tied to one another at the central hole, at points on the periphery, and possibly at intermediate radii as well. At section ends the assembly is to be tied to the cavern wall or to “bookend” frames.

Status: The engineering design of the mounting of the planes in the detector assembly remains at the conceptual level, except for the above-mentioned studies of the longitudinal “tie-bolting” required to keep 4 cm planes adequately, and safely, rigid.

During FY 1995 and early FY 1996, the design evolved from examining the physics and engineering trade-offs and cost of numerous alternatives. Four support options were considered for the far detector:

- Floor mounted with shims on a narrow base plate,
- Raised from floor on a cradle,
- Suspended from above via a superstructure,
- Suspended from side rails.

The floor mounted option was selected as the simplest and least expensive choice. The side-rail concept offers significant installation advantages with an increased cost.

To do: A basic structural design of the plane mounting should be drawn up to a detail which permits stress analyses, and also which will permit a realistic procedure for erection of assembled steel planes and active detector elements into this structure to be devised, and costed. In particular, the notion of “edge mounting” the 15-ton planes from side rails, like files hanging in a drawer, requires a careful stress analysis of transverse stability at the hanging attachments. If these attachments are to permit rolling the plane longitudinally into the detector assembly, this fact must be included. Design of these attachments, in turn, requires some limiting definition of the inter-plane gap size, and also of the active detector geometry in the vicinity. Designs for the 2 cm and 4 cm planes will likely differ in significant detail.

Assembly and erection drill. A multistation (5) assembly line in the cavern is proposed (in a draft by Bill Miller and John Alner) in which the large components of the individual planes in the “4 cm Reference Design” are flattened and welded together on “strong-backs” and then raised to vertical for erection in the detector. A number of variations in the thickness and shapes of the laminae are discussed, along with different methods of fastening the pieces into a plane (with welding, pins, etc.) The primary purpose of the draft report was to organize a process for analyzing the cost and time factors for the actual construction of the detector planes from materials brought into the mine, and for their assembly, along with active counter elements, into the MINOS detector.

Status: This draft study is a first effort toward a detailed analysis of the assembly process, and contains many variables, including plane thickness, segmentation, interconnection, and mounting which remain to be specified. The cavern length is another variable of critical importance. The study does serve a valuable purpose as an outline to indicate the level of detail that will be essential for demonstrating the credibility of any particular “Nominal Design,” and especially of its purported cost. It is also a witness to the urgent need to pin down the more critical variables as soon as possible.

To do: A variable crucial to the mine-insertion and assembly process is the limiting capacity of the cage and handling facilities at both ends of the shaft. Until this has been evaluated by mine professionals who can design and cost an optimum cage system, it would be prudent to be conservative by having at least one fall-back design which limits steel segmentation to that proven to be transportable by the present cages or trivial modifications thereof. Thus, one should at this juncture:

- (i) Focus on detailing a “baseline reference design” whose cost can serve as a comparison standard for alternatives requiring major cage and shaft amendments.
- (ii) Establish the actual extent and cost of enhancements to the cage and shaft which would enable larger plane segments to be handled so giving possible improvements in performance and economies in assembly.

5.4.2 Laminated-pie design

This design has been proposed and primarily studied at Argonne as a possible alternative to the reference design. Potential advantages (over the reference design) include:

- flatness tolerances may be easier to achieve,
- ease of handling without cage or shaft modifications,
- more efficient use of hoist trips,
- uniformity of segment manufacture,
- relaxed tolerances on edge machining,
- improved magnetic field uniformity at gaps and in azimuth.

Planes. 8-m diameter circles, 4-cm thick; each is made up of 4 or 6 layers of steel sheets. Each layer consists of 12 pie-shaped segments of 30 degrees azimuthal width. All of these steel segments are identical (except for counterbores), with the machining and hole drilling done in stacks. The individual segments are less than 4-m long and the number transported at a time in the mine cage will be limited only by weight. The layers are offset in angle so that the radial gaps in a layer do not line up with those in any other layer. The segments will be tied together using special (bolt+nut)-in sleeve sets in counter-bored holes requiring no tapping. Although there will be 12 radial gaps, two-to-three times the number in the reference design, each gap will affect only 1/4 (or 1/6) the plane thickness, thus providing better magnetic shunting at fields near saturation which should yield less stringent joint tolerances and smaller local field dips near the joints.

Status: The initial engineering design of this technology has been carried out for 4 cm planes and the magnetic field size and homogeneity have been computed. Several design options regarding gap size and number of laminations have been analyzed.

To do: Further study of the countersunk bolts is needed to better understand the required tolerances and to find ways to decrease the cost of the bolting. In addition, welding should be investigated as an alternative approach.

A comparably detailed mechanical design and cost estimate for a 2 cm thick plane also needs to be carried out.

Mounting. The structure for mounting the planes into the detector will likely be somewhat different from that for the octagonal, reference detector of comparable thickness. One can argue that the former, for which each radial gap region is backed up by 3/4 (or 5/6) of integral plates, would be more rigid than the reference design in which the ratio is only 1/2. On the other hand, the two layers of the latter would be welded tightly together, whereas the stiffness of the laminated pie will rely upon bolt-hole tolerances and number, and upon interlayer friction. The effective elastic properties, including yield points, of each design as assembled will probably need to be confirmed empirically.

Status: The mounting structure has not yet been designed in detail. However, supporting the installed plates at the bottom is not advocated by the Argonne group because this scheme may require the use of many axial tie rods. These rods may seriously interfere with active detector installation. Still needed are engineering studies leading to the possible elimination of tie rods.

To do: Make a detailed mechanical design of the mounting, as described in the preceding paragraph.

Assembly and erection drill. The assembly and erection options for the laminated-pie design are similar to those for the 4 cm thick segments of the reference design. In either case one strongback for steel assembly and erection could be used if the active detector elements were assembled separately. Of course the details of handling the many more but lighter

segments, and also of flattening and bolting them together in lieu of welding, will require a quite different set of steps with different costs; but in either case one assembled steel plane can be produced per day.

Status: A detailed fabrication and assembly procedure has not yet been presented.

To do: Since this “laminated pie” design offers some potential magnetic and installational advantages over the reference design, its cost needs to be carefully compared with that of the latter. Building a full scale prototype during FY97 would provide valuable information on all of the key issues, particularly cost and how to minimize it.

Summary of Proposed R&D Program on Laminated Pie Design

Remainder of FY 1996:

- Make a detailed design and cost estimate for the 2 cm system;
- Investigate cost reduction possibilities for the countersunk bolts;
- Make an initial mechanical design of the mounting;
- Measure B/H curves for some candidate steels;
- Complete the gap effect magnetic calculations;
- Continue to make field calculations available to simulation groups.

FY 1997:

- Determine field perturbations due to bolts and/or welding;
- Build a full scale prototype plane, either 2 cm or 4 cm;
- Mount the prototype plane in a vertical position;
- Make initial measurements of the mechanical and magnetic properties of the prototype plane.

FY 1998:

- Based on the results of the above R&D work and of progress on other steel options, a final design would be chosen by the MINOS collaboration; then bid packages for full scale production would be prepared.

5.4.3 Spiral-wound coil design

The proposal is to fabricate 8 m circular planes, 2 cm or 4 cm thick, by winding a continuous soft iron strip, approximately 1-cm thick, into a tight flat spiral of 4-m radius with a central hole 30 cm in diameter. The spirals would be wound on mandrels in the MINOS cavern.

Spiral-wound plates offer the potential for attractive physical properties at low cost. Steel spirals are likely to exhibit an azimuthally uniform magnetic field due to the elimination of radial gaps. Larger fields per Ampere-turn may be realizable from use of more suitable iron stock than is available in steel plate form. Winding the spirals nearly eliminates machining costs. Little assembly is required beyond winding. Handling problems in bringing very large and heavy plates down into the mine are eliminated in favor of transporting palletized coils of supply stock. The fabrication plan requires neither a “strongback” for lifting the planes nor a press for maintaining flatness.

However, we are not aware that spirals of the proposed magnitude have been wound previously. The novelty of the design raises its risk factor. Engineering and testing is required to accurately compare the cost and integrity of the design with the reference design.

The plan proposed below is based on the time frame necessary for trial assembly of full-scale planes during 1998. The plan contains several checkpoints to assess the viability of the spiral-wound plate as engineering data are accumulated. The plan is designed to minimize loss in the case that insurmountable problems are discovered at any checkpoint. While the plan requires a short-term investment of development funds at risk, success would result in lowering overall steel costs for the detector while simultaneously improving its magnetic field.

Planes. Circular, of 8 m diameter, and 2-cm or 4-cm thick. Each plane is made of a spiral of iron strip wound in the mine cavern using a special rewinder. The rewinder unwinds the strip from the supply coils and rewinds it on a mandrel into the final spiral.

The spiral design does not utilize a press to ensure flatness; rather, flatness is maintained by controlling the tracking of the strip entering the spiral. Winding can be accomplished in a near-vertical plane, eliminating the need for a strongback to rotate each plane from the horizontal to vertical positions, thus simplifying the handling in connection with assembly. In addition, winding near-vertical rolls reduces the floor space requirements of the rewinder.

The rewinder would wind the spiral under sufficient tension to ensure tight radial contact between the layers. A portion of the winding energy is stored in the roll, as in any roll. This energy is required to deform the constitutive strip, which in turn generates in-roll stresses sufficient to realize a self-supporting roll.

The low bending strength of the low carbon steel utilized in the spiral coil is not likely to result in an explosive release of energy in the case of catastrophic roll failure (as would be associated with fracture of a high strength tempered clock spring). Rather, the failure mode of concern is passive collapse — a simple disassembly — of the roll. The development plan proposed below is focused on minimizing the possibility of such collapse.

The unusually high aspect ratio between diameter and thickness of the spiral-wound coils presents the greatest challenge to successful winding. Calculations and experiments are based on 2 cm thick planes, as 4 cm thick planes are less demanding. Otherwise, plane thickness is not expected to significantly impact the spiral-wound plate design. The rewinder will be

costed for fabricating both 2 cm and 4 cm planes, as the power requirements are twice as high for the thicker planes.

The overall mechanical and magnetic simplicity of this design remains the main feature of the spiral.

Status: Engineering studies involving a computer-simulated model spiral have resulted in prediction of in-roll stresses. The calculations are based on the assumption that the radial modulus of the helically wound strip is $0.1 \times$ the circumferential modulus (see e) in "1996 development plan" below), and that the strip is wound at constant torque. The viability of the spiral winding technique is supported by the results.

To do: Available winding models are limited in their capacity for modeling second-order effects such as tracking of the incoming strip, variations in the thickness of the strip, bending stresses in the strip, and inter-layer friction. Therefore, experiments are essential to confirming theoretical predictions made to date. Additionally, detailed costing of the planes, their mounting, and a full-scale rewinder is necessary to definitively compare spiral-wound coils with the reference design.

The development plan proposed below realizes considerable savings by winding scaled rolls early on, thus generating critical engineering data without the expense of full-scale winder construction. Winding a miniature demonstration roll is scheduled to begin immediately, followed by winding 50% scale rolls in late 1996 and early 1997. The 50% scale rolls are likely to be within the capacity of an existing winder at Livermore. The 50% scale rolls are expected to resolve questions on magnetic quality, maintaining flatness, causes and extent of gaps, and whether inter-wrap binder is necessary to guarantee roll integrity. Improved theoretical modeling is integrated with experiments to leverage improved parameter windows defined by the experiments.

Some winding parameters do not scale proportionally. Therefore, scaled rolls do not definitively resolve full-scale roll parameters. Nevertheless, success in winding scaled rolls should provide sound justification for continuing spiral coil development. Inversely, unjustifiable failure at any step is likely to warrant termination of spiral coil development while avoiding full-scale prototyping and development costs.

Spiral-coil: 1996 Development Plan:

(Approximate completion dates included in parentheses. Items marked by asterisks for 1996 are included in previously-proposed \$10,000 seed funding budgeted for FY 1996. Unmarked items are to be funded by additional support requested for FY 1996: see Table 17.)

- a) Perform initial design of spiral coil plane concept (February)*.
- b) Theoretically determine in-roll stresses developed by winding spiral coil at constant tension and constant torque using linear winding model (April)*.
- c) Perform initial theoretical roll integrity analysis based on ability of roll to support its own weight in horizontal configuration (April)*.
- d) Perform initial parameter definition and conceptual design for full-scale coil winder (June)*.

- e) Verify the radial modulus of spiral by performing stack test (June).
- f) Wind miniature test roll (July)*.
- g) Perform initial theoretical analysis of strip thickness and bending effects (August)*.
- h) Resolve 50% scale spiral winding parameters, and set up actual winder (August).
- i) Wind first 50% scale spiral for initial testing of set-up and roll integrity (September).
- j) Develop full-scale roll support concept and detector attachment plan (December)*.
- k) Wind second 50% scale spiral to refine parameter windows (December).

Spiral-coil: 1997 development plan:

(Approximate completion dates included in parentheses)

- a) Wind third 50% scale spiral and perform detailed study of integrity, gapping and magnetics (February).
- b) Identify and cost material and mounting schemes for full-scale spiral (March).
- c) Obtain detailed costing on full-scale rewinder (June).
- d) Complete detailed designs of full-scale spirals, plane mounting, detector attachment, rewinder and detector attachment workstation(s) (September).
- e) Complete construction of full-scale rewinder (October).
- f) Test full-scale winder (December).

Spiral-coil: 1998 development plan:

- a) Perform 3-plane trial assembly.
- b) Refine winding parameters and installation plan.

Mounting. The finished circular planes may stand on a quarter-cylindrical cradle on the cavern floor, fabricated from concrete or simple steel weldments. Alternatively, the planes may be supported by hanging them from steel straps, where the straps wrap underneath each plane and are in turn hung from supports positioned slightly above the centerline of the planes. Basic axial positioning is realized through manipulating the base and core. If required, axial spacing can be provided by way of axial bars mounted radially outside the periphery of the spirals and threaded through tabs spot welded to each spiral.

Status: The mounting schemes are conceptual at this time.

To do: The mounting scheme must be developed in sufficient detail for engineering stress analyses to be based upon it, and so that an assembly and erection program also based upon it can be developed and costed.

Assembly and erection drill. An attractive feature of the spiral coil design is that little assembly is required beyond winding the coil. Therefore, the key to using this proposed steel technology lies in the winding machine itself. After winding, erection consists of attaching a detector layer to a finished plane, presumably at a separate workstation, then transporting the finished assembly to its installation position, presumably by overhead crane. Due to winding the finished roll in the vertical position, scaffolding is likely to be necessary to provide access to the total surface area of the plane at the detector attachment workstation.

Status: The winder can be conceptually divided into five modules: main torque generator, strip tensioner, tracking apparatus, welder for connecting supply strips, and mandrel attachment mechanism. Available technologies are likely to be adapted to each module. Preliminary calculations indicate that only one horsepower developed at the spiral mandrel should suffice to wind a full-scale spiral in 10 hours or less. (Note: Only a portion of the input energy is stored in the roll; the majority is consumed by the winding brake.)

To do: A 5 m diameter winder available in the Livermore magnet shop is likely to be used for the 50% scale roll winding. The 50% scale rolls will preserve the challenging aspect ratio of the final spiral. Once appropriate strip stock is obtained, set-up and winding the first spiral will take approximately two weeks. Approximately one month has been scheduled between the winding of each of the three 50% scale spirals to allow for appraisal of experimental results and refinement of parameters and equipment for use in the next wind.

Scaling of the rewinder from the 50% scale roll test apparatus to the final design is expected to be straightforward. However, a plan must also be developed for moving finished planes from the rewinder to a detector attachment workstation, then moving and aligning the instrumented plane to its final installed position.

5.5 Recommendations to the MINOS Collaboration

The following recommendations emerge from Section 5.3 and from the collaboration review of the STC Report draft as presented to the Lutsen meeting and from the numerous discussions relevant to the several technologies: their state of development, plans for installation in the mine, and cost. These recommendations are intended to guide collaboration policy in setting priorities for performance of R&D in other areas with significant impact on the selection of magnet technology and the timely construction of one or more prototype planes.

5.5.1 General recommendations – strategic

1. We urge the Collaboration to agree as soon as possible upon the following parameters for the MINOS far detector magnet structure:
 - a) The plane thickness (2 cm, 4 cm, ? cm).
 - b) Establish criteria to evaluate the effect on physics performance of the plane-to-plane gap.
 - c) Plane internal component segmentation as constrained by the physics requirements on magnetic field magnitude and quality, the latter to be established by Monte Carlo study of tracks from MINOS neutrino events and the discrimination of the desired oscillation signals.
 - d) The plane's role in supporting the active detector elements.

In other words, the collaboration should work hard to gain the best possible understanding of the segmentation issues associated with the detector. The segmentation choice should also be driven by installation issues including the integration of the active detector elements. For example, taking the targeted assembly rate as one per day for 4-cm thick planes, if this rate were limited to one per day independent of thickness, then adding more planes to the detector would make the overall MINOS assembly and installation time frame too long. The collaboration should also work hard to fix the gap spacing (distance from steel plane to steel plane) and flatness tolerances. Obviously these depend on the active detector choice, but they also depend on the flatness and thickness tolerances on the steel and from the assembly method. The effect of cracks in the passive detectors should also be understood. This encompasses magnet design, magnetic field quality, and depends strongly on physics issues.

2. We further urge the Collaboration to establish firmly as soon as possible the practical geometrical and weight constraints upon the transport of plane elements/winding stock or whatever. To the extent that cage and shaft modifications can be envisioned to handle various problems, credible costs should be developed for inclusion in the cost estimates of those specific designs requiring such modifications.

Bill Miller and others are obviously starting to consider the assembly and installation issues, and these need to be thought through as they limit the maximum size of items which may be lowered into the mine as well as the rate at which things occur. If the

assembly were really limited to one plane per day, the segmentation of the detector would be limited by the assembly time.

3. As a general recommendation, we encourage work to understand better the requirements of the passive detector layers before fully funding two or three parallel efforts. In a resource limited project, as MINOS is evidently going to be, the more decisions which can be made early, the cheaper the project will be in the long run. These decisions need to be made in the short term, if we are to have the goal of committing FY97 funds to construction of a prototype.

Anticipating that the goal is to produce very few prototype passive layers, perhaps only one, we propose that the technical design review be focused primarily on the mechanical issues of the layers – the planes. To do this, we need a choice of the thickness, an understanding of the tolerance issues, and a plan for assembly and handling. Each group proposing a particular design should be encouraged to understand their design to the best of their ability at a level such that a technical review panel would be able to judge their relative merits. This may include scale models such as that performed by Livermore on the “reference” design to prove an understanding of the engineering issues. This review would also include cost issues, and each design should be judged on an equal basis, such as the cost per layer to the completion of steel plane assembly in the mine. Incremental costs such as a reworked cage (if necessary for one design as opposed to another) should be included. That is, “compare apples with apples!”

The earlier decisions can be made, the more savings in resources and money will result for the collaboration in the long run. These decisions, and planning generally, should recognize the intrinsic engineering complexities in fabricating hundreds of relatively flimsy steel absorber plates into a ten kiloton detector assembly. This assembly and the overall design should be as robust as possible to aid in overcoming unexpected setbacks.

5.5.2 Specific recommendations – tactical

At Lutsen the status reviews of both the steel and the active detector technologies made it evident that certain activities should be given a high priority for near-immediate completion to accelerate collaboration ability to make timely and sensible decisions about full-scale prototype construction.

1. *Establish Magnetic Field Quality Criteria.* The knowledgeable collaborators should quickly agree upon a relatively simple and specific set of quality criteria which, when calculated for the several competing nominal designs, will enable them to be compared on a common and meaningful basis. Criteria might include: spatial homogeneity, field magnitude/Ampere-turns, field predictability (as for the manufacture of a field table for analyses, etc.) but need only represent current best judgment, not necessarily an ideal. Reference to these criteria should then be an item in the “credibility demonstration” for each design. These criteria should be established well in advance of the August 1996 MINOS meeting so that status reports on the several designs can include compatible predictions of magnetic field structure.

2. *Make Design Studies for both 2 cm and 4 cm Options.* It is evident that the R&D on the active detector systems is not yet at a stage which would permit the essential decision to be made concerning choice of the steel plane thickness (2 cm, 4 cm, other). As described under Step 2 of Section 5.3, the study for each option should include all relevant aspects of the design, including plane manufacture, assembly and erection in the mine, the magnetic field performance, and the full-detector cost.

Doing this will obviously involve significant extra effort on the part of technology proponents, especially in dealing with those elements of the technology which do not scale simply with plane thickness, for example mechanical fixturing. We nonetheless encourage this effort, and the provision of necessary resources, on the basis that it is a wise investment toward a good detector. The rationale for making both studies prior to defining the plane thickness is that the latter decision depends upon the selection among options for the active detector elements — e.g. scintillator, RPC's, etc. — which in turn depends not only upon physics considerations but also upon cost. To the extent that the cost of a particular thickness of the steel plane elements can be known *a priori*, the more readily can a prudent choice of active detector technology be made when other relevant information becomes available. For the steel plane costs of the 2 cm *vs* 4 cm options to be used in this critical way, they must be comparably credible and based upon comparably complete understanding of the two distinct designs, including fabrication and mounting in the detector. To rely upon “guestimates” extrapolating a well-studied thickness design by a factor of 2 (1/2) to the alternative is intrinsically risky. (On the other hand, interpolating *between* 2 cm and 4 cm thicknesses will likely be much safer!)

3. *Keep Option Open for Two Full-scale Prototype Planes.* The present candidate technologies each are of such a nature that many features, especially manufacturability and assembly and thus ultimately the cost, cannot be predicted in confidence without the practical experience of constructing a full scale prototype under conditions simulating the actual assembly in the mine. In particular, the Reference Design and the Laminated Pie Design have much in common but involve quite different details of plane segmentation. On the other hand, experience gained in prototyping either one of these designs — e.g. in fixturing for hanging the planes, integrating the laminates, or attaching the active detector elements — can in principle be of direct and perhaps very useful application to the other.

5.6 Summary

We have proposed a sequence of steps to be followed for the development of the several competing technologies to a level at which a prudent and efficient selection of the final design and manufacturing method can be made, consistent with meeting essential physics requirements at minimum cost for the MINOS far detector. Implicit in this sequence is the expectation that during the process of development of the necessary detail of design a good deal of internal optimization will occur in both mechanics and costs.

The first step involves the recognition that, even within a particular “technology,” variations in certain input parameters — especially the plane thickness — can result in different

“nominal designs” having sharply different mechanical characteristics and costs. For a proper comparison each nominal design in contention must be developed separately.

The second proposed step is that this development be carried out for each nominal design to the level of a persuasive “credibility demonstration” showing that a MINOS detector could be built in this way and would meet the required specifications at a predictable overall cost for the steel as manufactured, assembled and mounted in the final structure.

The development of the different “nominal designs” involves independent stress analyses and other engineering procedures, each taking time and money. We emphasize that the sooner the MINOS Collaboration can resolve the several physics-related input ambiguities including plane thickness, gap width and tolerances, magnetic field inhomogeneity limits and mine cage and shaft limitations, the less expensive and more rapid will be the progress of the surviving designs through the credibility demonstration and the estimation of total costs to the point where a sound comparative evaluation is possible.

For the third step we recommend that for each design surviving Step 2, or at least for each of those designs offering the best prospects after a comparison based on the results of Step 2, a full-sized functional prototype plane be built. Each plane should be erected in its operational orientation using a supporting structure that simulates the corresponding proposed detector mounting as closely as possible. The great weight and mechanical flimsiness of the individual steel planes, together with the several novel schemes proposed for their assembly to required tolerances from multiple smaller elements insertable into the Soudan mine, challenge our current experience. Prudence requires that realistic prototypes be tested under conditions where repairs and adaptations can be easily made and their safety assured. This experience is also essential for estimating a believable cost prediction for the full detector. Afterwards, it will be useful for fine-tuning the fabrication and assembly techniques and staff training, for studying the mating process with the active detector elements, and for verifying the magnetic field predictions.

We have attached no time line to this progression of steps, believing that the Collaboration needs to make some crucial simplifying decisions before such a schedule can reasonably be established. At this writing there exist three distinctly different schemes for fabricating the steel absorbing planes of the MINOS far detector, and within each scheme are offered a number of variations in essential input parameters. Many of these “nominal designs” are not worked out in detail and only in one of them has the methodology and cost of assembly and mounting in the detector structure been worked out at all. These details must be worked out. Different schemes may have significantly different time lines. Each time line will also depend totally upon the availability and strategic allocation of R&D funds.

We have summarized in Section 5.4 of this report the three general technologies presently in contention. The “Reference Design” has been pursued in by far the greatest detail of the three by our Livermore colleagues, and their analyses and specifics provide a sort of standard for the other designs to meet. Even this Reference Design suffers from the uncertainties of the input specifications (plane thickness, etc.) and plans for the associated mounting structure, and for the plane assembly into them, are just getting underway. The “Laminated Pie” design of our ANL colleagues offers some alluring potential advantages in way of magnetic field size and quality, and in the manufacture and handling of components, but requires considerable additional engineering development and analysis of the planes themselves, and for the assembly process and mounting structure. As a variant of the comparable reference

design it is similarly conservative mechanically, but its differences may affect the final cost significantly. The "Spiral-Wound Plate" design from our Minnesota colleagues is ingenious and novel, and is radically different from the conventional lamination of smaller flat components into a whole, and it offers a very attractive quality of magnetic field as well as almost total plane fabrication on-site in the mine. However, many features of this design remain to be proven as practical and considerable engineering development remains to be done.

Our recommendations to the MINOS Collaboration are summarized in Section 5.1.

End of Steel Technology Committee Report

5.7 R&D plan summary and cost

In the remainder of FY 1996, a detailed analysis and conceptual tests for the reference design, and the initial analysis of the alternative concepts, will be completed.

In FY 1997, small-scale tests and, if warranted, full-scale prototypes will be constructed to evaluate the reference design and possible alternatives. This will address construction issues as well as fabrication tolerances and magnetic field quality. Multiple small-scale tests will be conducted to address issues of repeatability. The large-scale prototypes will be magnetized with a test coil and the magnetic field will be mapped and benchmarked against 3-D calculations.

Part of the evaluation process of the steel design is to ascertain the capabilities and cost of industry and the limitations imposed by underground assembly at the mine. We also plan to investigate the possibility of large cost savings using foreign fabrication. This involves travel of various MINOS collaborators to the Soudan site, and to U.S. and foreign steel mills and fabricators.

Much of the R&D effort has concentrated on the large far detector system. As this system becomes better defined, increased effort will be allocated to develop a comparable near detector steel and magnet system.

In FY 1998, using construction funds, we will build production prototypes and conduct a complete system test of three full-size planes (for both the near and far detectors), including prototype support structures. The prototype far-detector planes will be fully instrumented with active detectors. The cost for the prototype steel planes is included here as part of the FY 1998 budget; the cost of the associated prototype active detector planes is given in Section 4.2.5.

Tables 17, 18, and 19 summarize MINOS steel and magnet R&D activities and supplemental funding requirements for FY 1996, 1997, and 1998 respectively. In FY 1996 MINOS collaborators have paid for a substantial fraction of steel R&D work with institutional and base-contract funds. The supplemental funding requirements listed in the tables assume that this practice will continue, although not to as great an extent as in FY 1996, when the funds received (late in the year) were much less than had been requested.

Institution: activity	Source	\$K
Argonne: Magnetic field calculations	DOE	20
Minnesota: Spiral coil structural analysis	Fermilab	10
Livermore:	DOE	30
Finite element analysis		
Fabrication engineering		
Spiral coil fabrication plan		
Small-scale steel tests		
ED&I: ref. test station, eng. oversight		
Total FY 1996 steel/magnet R&D		60

Table 17: FY 1996 funding for steel and magnet R&D work (actual allocations).

Activity	\$K
Reference Design Parameter Tests	60
Spiral Coil Engineering	50
Full Scale Prototype Planes	263
Engineering	48
Plane Materials, Gases	96
Support Fixture	58
Coil	7
Gap, Flatness Metrology	23
Magnetic Measurements	31
Magnetic Field Calculations	50
Travel to Site & Vendors	40
Near Detector Concepts, Prototypes	50
Total FY 1997 steel/magnet R&D	513

Table 18: FY 1997 costs for steel and magnet R&D work (in FY 1996 dollars).

Activity	Funds	\$K
Far detector: 3-plane trial assembly:	Constr.	292
Engineering	40	
Steel, fabrication	117	
Fixtures, support	54	
Technical effort	41	
Magnet coil	40	
Near detector: 3-plane trial assembly:	Constr.	173
Engineering	27	
Steel, fabrication	58	
Fixtures, support	34	
Technical effort	27	
Magnet coil	27	
Total FY 1998 steel/magnet R&D		465

Table 19: FY 1998 costs for steel and magnet R&D work (in FY 1996 dollars).

6 Software and Simulations

6.1 Introduction

A large amount of simulations work was performed for the MINOS Proposal. This work made use of several different Monte Carlo programs which were modifications of software already developed for other purposes by MINOS collaborators. This approach, dictated by time constraints, was satisfactory for demonstrating that the MINOS reference design provided good sensitivity to neutrino oscillations in several possible modes. The first step in our MINOS Simulations R&D plan has been a shift into a coordinated, organized Collaboration approach to the software and simulation issues which confront us.

This Chapter describes the status of the Collaboration's work to provide an integrated system of standard simulation software for a variety of detector design tasks. We focus here on the description of the overall software system and its application to the optimization of detector parameters. Chapter 7 describes the neutrino beam simulation software which will be an integral part of the system. The present Chapter is organized around the following topics:

1. MINOS software system

An immediate goal for MINOS is to choose the active detector technology. It is essential that a single simulations package be created which allows all technologies to be evaluated on the same footing by the various collaborators doing the simulations. In addition, the subsequent optimization of the chosen technology must use a common, integrated simulations package.

The basic code management package is largely completed. Our GEANT-based simulation structure, called GMINOS, will use GEANT-ADAMO software tools for the beam and detector. The software will be maintained on various system platforms, and will be relatively easy to use by non-experts. The utility program CVS (Concurrent Versions System) has been chosen as the primary software tool for program distribution and for revision control during code development. GMINOS uses the VINES event display program.

The first phase of the implementation of the MINOS system will be completed by September 1996. A more detailed description of the system which is currently being used for the simulations development is contained in Section 6.2.

2. Technology choice

We will use GMINOS to compare the ability of the three candidate technologies to achieve the MINOS physics goals. The neutrino event generator is a central part of the simulation code, and is described in Section 6.3. Detailed models of the response of each active detector technology are being developed in close collaboration with the proponents of each technology. Models will be modified to be compatible with test beam data generated by each technology prototype as required. This effort will continue as long as test beam data are collected and analyzed. Section 6.4 describes this work in detail.

Using these technology models, we will address the core question of how each technology can do the physics. This is an ongoing process which will begin with the present technology models, and will be improved as these models are developed and refined. This work, described in Section 6.5, is central to the selection of the MINOS technology. Major issues of complete event reconstruction and pattern recognition will need to be addressed. This process will be completed in August 1997 when the experiment technology is chosen.

3. Optimization

Finally, after the technology is chosen, we will optimize the design of this technology. In Section 6.6 we describe in detail some examples of how neutrino oscillation parameters may be determined, demonstrating how the MINOS physics goals drive the optimization process. The final optimization will entail an investigation of the sensitivity of the oscillation tests to the parameters of the MINOS beam (energy distributions for each neutrino species) and near and far detectors. Some detector issues include granularity (lateral and longitudinal), magnetic field, steel thickness, aspect ratio (length *vs* width) and tonnage. Section 6.5 discusses this in more detail. This work will begin in early 1997, even though the technology choice will not yet have been made. It will continue in earnest once the technology is chosen and will last until February 1998 when the MINOS design is finalized.

This will end the simulations R&D phase. However, the analysis package developed for this work will serve as the foundation for the construction of the final MINOS data analysis software.

Section 6.7 summarizes the supplemental funding requirements associated with MINOS software and simulation work.

6.2 MINOS Software System

A central source code repository for the development and distribution of collaboration standard simulations programs has been established at Indiana University. The Free Software Foundation utility program CVS (Concurrent Versions System) has been chosen as the primary software tool for program distribution and for revision control during code development. Several elements of the envisioned MINOS simulation package are now available from the Indiana University CVS repository, including the GEANT-based GMINOS detector simulation, the NEUGEN neutrino interaction event generator, and the VINES event display program. Several member institutions, including SLAC, FNAL, Oxford, and the University of Minnesota, have now installed the CVS program and have successfully accessed the Indiana repository. These sites have also reported success with building the GMINOS executable program from the source code files.

CVS is a tool for version management and code distribution during the software development phase. Built on top of the older RCS (Revision Control System), CVS adds the flexibility of allowing multiple developers to work on the same source files concurrently. Each programmer/user checks out copies of the desired files from the central repository into a personal work area on his/her home computer. The system accommodates both users who wish to modify the source code, and also those who merely want to build an executable program for their studies.

There are several important steps yet to be accomplished before a complete MINOS simulations package becomes available for general collaboration use. By ‘complete package’, we mean the set of programs necessary to allow the user to simulate all physical elements of the experiment, from the neutrino beam, through interactions in the detector and the detector response, to the display of the detector and events within it. First, the program elements which are now being developed at independent sites must be incorporated into the central repository and integrated with the rest of the system. This integration will be accomplished in part by the definition of common data structures. The ADAMO Entity-Relationship programming system, developed by the Programming Techniques Group at CERN, has been adopted for defining tabular data structures and providing the means for manipulation and validation of the structures.

Several features of ADAMO suggest that it is and will continue to be a good tool for the MINOS software applications. The ADAMO system works with FORTRAN, C, or other programming languages. Although the programming being done for MINOS short-term simulations studies employs FORTRAN almost exclusively, it is conceivable (even highly probable) that much of the MINOS software will evolve into a more object-oriented approach, for which C++ or other languages are much more suitable than FORTRAN. Having an adaptable data structures system will facilitate such an evolution. ADAMO also provides flexibility in the choice of input/output formats, so that transportability of files across different computing platforms can be easily accomplished when necessary. Finally, since an ADAMO record carries not only the data itself but also the data model, changes in the model do not cause problems with accessing older versions of the output files.

In the MINOS software which now exists, ADAMO data structures have been defined for several aspects of the GMINOS detector simulation, including geometry specifications, GEANT parameters (materials definitions and tracking media, cuts, physics processes, ro-

tation matrices), neutrino event kinematics, and output hits and digitizations. The data structures describing the neutrino event kinematics will be shared with the event generator and neutrino beam portions of the simulations package, while the detector geometry, hits, and digitizations structures will be shared with the event display and physics analysis programs.

6.3 The MINOS neutrino event generator

The Fermilab wide band neutrino beam spectrum spans an energy range where a number of neutrino scattering mechanisms are important. This ‘medium’ energy range is somewhat problematic because it lies at the transition region between two models for neutrino interactions. At low energies, which are well understood phenomenologically, neutrino scatterings are predominantly quasi-elastic, in which the target is taken to be an entire nucleon. At high energies, neutrino interactions are mainly deep inelastic scattering (DIS), where the target is one of the constituent partons inside the nucleon. Again in this region the theoretical and experimental situations are well in hand. In the medium energy (≈ 10 GeV) range, the concept of a well-defined ‘target’ is more tenuous, as quasi-elastic, resonance production and DIS interactions can occur.

The details of the physics models which form the basis of the MINOS neutrino event generator (NEUGEN) are described elsewhere [12]. In this section we shall describe some of the uncertainties involved in simulating neutrino interactions at these ‘medium’ energies, and outline our plans for quantifying and minimizing these uncertainties.

1. Nuclear effects

Since the nucleons which participate in the scattering are bound inside nuclei, there may be many-body interactions (that necessarily depend upon the type of nucleus) which modify the cross sections. Of concern is the fact that low energy measurements of quasi-elastic scattering have primarily been made on deuterium targets, while we are interested in these processes on heavier targets, primarily iron. Nuclear target effects will necessarily change both the x_{Bj} and Q^2 distributions as well as cross sections.

For quasi-elastic neutrino scattering, the Fermi gas model of the nucleus accounts for the main modifications in scattering from heavy targets: Fermi motion of the nucleons ($P_f \approx 200$ MeV/c for iron) and suppression of scattering at low Q^2 due to the Pauli Exclusion Principle. This model is incorporated in NEUGEN.

Nuclear effects can also produce substantial changes in the differential cross section for deep inelastic scattering in particular regions of phase space. Nuclear shadowing, anti-shadowing and EMC effects have been measured in muon-nucleus scattering experiments and can produce as much as a 20% reduction in the deep inelastic scattering differential cross section at very low x_{Bj} (shadowing at 10^{-3}) [13] and again at higher x_{Bj} (EMC effect at 0.5). These effects have not been measured very accurately in neutrino scattering [14]. Work is in progress to incorporate these effects as well as possible.

Nuclear effects on neutrino scattering in the low to medium energy range have been studied in a number of bubble chamber experiments which have used both light (deu-

terium) and heavy (neon or Freon) targets. Requiring that the nuclear models employed in our Monte Carlo reproduce the measured differences between these experiments provides a fairly strong constraint on the parameters of these models.

2. Resonance production

There is not a uniform treatment of neutrino induced resonance production in the literature. The model used in NEUGEN is from the work of Rein and Seghal, and employs the Feynman, Kislinger, and Ravndal model of baryon resonances [15, 16]. This model describes resonances in terms of excited states of the 3-quark system bound by a relativistic harmonic oscillator potential. The corresponding Hamiltonian is solved for the bound state wave functions, which are then associated with the observed resonances. The resonance wave functions are then used to calculate the weak transition amplitudes directly.

Besides the Rein and Seghal model, several other phenomenological descriptions of neutrino resonance production have been described in the literature. Methods involving calculation of dispersion relations, or isobar models in which the resonance is treated as an elementary particle have also been investigated by several authors [17, 18]. Resonance production is dominated by the $\Delta(1232)$, and while these different models generally agree on their predictions for this lowest mass resonance, they differ in their predictions for higher mass resonances.

Numerous experiments have measured the total cross section, invariant mass distributions, and Q^2 distributions of hadronic final states consisting of a single pion and a nucleon. These states are dominated at low energy and medium energy by baryonic resonance production. The predictions of NEUGEN have been compared to this data and reproduce it well.

3. Forming σ_{tot}

There is no consensus as to the best way to combine the quasi-elastic, resonance, and deep inelastic scattering cross sections at a fixed energy to form the total cross section. A number of different approaches have been suggested in the literature or used in practice. Recent preprints have discussed the effects that different prescriptions would have on calculations of rates of stopping and throughgoing neutrino-induced upward going muons [19]. Again the prescription used in NEUGEN agrees with the available data.

4. Deep inelastic scattering at low Q^2

Deep inelastic scattering cross sections are calculated in terms of the nucleon form factors F_2 and F_3 which are in turn determined from the parton distributions. One difficulty is that the simple DIS expressions can acquire large corrections for scattering at low Q^2 , since the assumptions which underlie the parton model assume large Q^2 . Because of the difficulties at low Q^2 , many parametrizations of parton distributions only fit to data in a region where these assumptions are valid, $Q^2 > Q_0^2 \approx 4 \text{ GeV}^2$. Fortunately, the situation has changed somewhat in the last two years, and sets of parton distributions have been released which incorporate fits to data down to much

lower Q^2 than were previously available. Nonetheless, there are still a number of ‘grey areas’, including the size of the longitudinal form factor and the relative contribution from higher twist (nonperturbative) terms. These have not previously been included in our simulations.

Measurements have been made (mainly at higher energies) of the contributions of such effects to the total cross section. Although the experimental situation is not unambiguous, requiring that our simulations be consistent with the experimental results at higher energies provides a very valuable boundary constraint for the more difficult medium energy regime.

5. Hadronization

The Soudan 2 Monte Carlo uses a hadronization scheme which is based on KNO scaling [20, 21]. We are in the process of incorporating the JETSET library of routines, which use the Lund string model for hadronization, into NEUGEN as well [22, 23, 24]. Once this has been done, studies of final state multiplicities and the dynamics of the hadronic system can be conducted.

These different fragmentation models can then be compared to the considerable body of data which exists on final state multiplicities in neutrino scattering.

6. Charm production

Charm production will account for around 1% of the charged current events in the MINOS experiment. Neutrino production of charm has been measured at high energies with opposite sign dimuon data and at lower energies in bubble chamber studies of $\mu^- l^+$ final states [25, 26]. Sizable experimental uncertainties exist in these cross sections, particularly at low energy. These uncertainties can be parametrized as an uncertainty in the charm quark mass in the slow rescaling model [27]. Calculations have been made of the effects these uncertainties will have on the MINOS analyses [1, 28], and charm production is being incorporated into our event generator at the present time.

It is the aim of the collaboration that within the next few months we will assemble a Monte Carlo which is capable of running under any of the different physics models previously mentioned. The detailed differences between different hadronization schemes, resonance production models, nuclear models, or parton distributions can then be studied.

Of course the predictions of any simulation should be consistent with existing measurements. The collaboration plans to extensively test the event generator by detailed comparisons to data. To this end, the collaboration has been given access to the DST’s from the BEBC experiments, which took nearly 750,000 bubble chamber pictures in runs from 1977-1983 involving both Ne and H targets. We hope to have access to other experiment DST’s which will allow us to further test our simulation in this and other energy ranges.

We are confident that the NEUGEN generator is now sufficiently accurate to enable the decisions on detector optimization to be made, based on the simulations carried out in the next few months; we expect these decisions to be insensitive to the finer details of the generator. In the longer term the studies and improvements discussed above will enable us to use the generator as a sensitive tool in the analysis of MINOS data.

6.4 Active detector response simulation

6.4.1 Overview

One goal of the MINOS detector simulation effort is to assist with the choice of detector design parameters that optimize the sensitivity of the oscillation tests described in the MINOS Proposal. In particular, the simulation effort will provide performance comparisons of the detector instrumented with alternative active detector technologies. It is likely that simulations will play a major role in the detector technology decision.

The simulations effort complements the hardware development work on the three candidate active detector technologies: Iarocci chambers (operated in either limited streamer or proportional mode), scintillator, and RPC's. Realistic, detailed models of the physical characteristics and responses of each technology, including trigger logic and electronics response, will be developed in close collaboration with the proponents of each technology. Input assumptions about detector response and the resulting sensitivity of the different oscillation tests will be thoroughly checked and documented for use in the active detector technology choice.

6.4.2 Simulation development activities

The MINOS Monte Carlo program (GMINOS) will incorporate sets of standard input assumptions and parameters which will be used in common by all active detector technology simulations. These include the wide-band and narrow-band beam energy distributions, the neutrino interaction event generator, and the magnetic field model. The use of such standard assumptions is essential for a fair comparison of the different active detector technologies. At present several choices for detector geometry and component materials have been defined in GMINOS.

Our most immediate development goal is to incorporate detector response functions into the simulation. Simple implementations of Iarocci tube response and scintillator response based on previous experimental results have already been included. Future improvements will be based on the results of the beam test program currently underway. However, there is no simulation as yet of the RPC response. The plan is to add a simple response algorithm in the near future and then improve upon it as beam test data become available.

Once the detector responses of the different technologies have been modeled, the detector hits will be digitized. For the scintillator option, this work has already begun. These digitized hits will then be used to create Monte Carlo data records that mimic the response of MINOS to electron and hadron test beam particles, as well as cosmic ray muons. More accuracy in the simulation will be achieved by including detector inefficiencies and noise. Test beam data from prototype detectors will be compared with the Monte Carlo simulations in an iterative process to improve the simulation.

Different oscillation tests will then be analysed separately for each technology to determine physics capabilities and the sensitivity of the active technology options to oscillations. This comparison will be based on a fixed-cost far detector (using reliable cost estimates) with granularity and total mass optimized for each technology.

6.4.3 Milestones and schedule

June 1996 milestones:

- Model RPC performance.
- Decide on standard event generators, fragmentation functions, and GEANT controls.

July 1996 milestones:

- Prepare standard beam profiles for wide-band and narrow-band beams in conjunction with the Fermilab NUMI beam group.
- Incorporate realistic magnetic field maps into detector models.

Summer 1996 milestones:

- Interact with hardware contacts to develop realistic detector models.
- Simulate anticipated prototype data. (As real data become available, this process will be iterated until the simulations agree with the data.)
- Prepare standard near and far detector configurations.
- Decide on data format.

September 1996 milestone:

- Release initial version of collaboration-standard simulation software system.

Fall 1996 – Winter 1997 milestone:

- Calculate muon, electron, and hadron energy and angle resolutions (including shapes, tails of Gaussians, etc.) for each of the three technologies.

Winter – Spring 1997 milestones:

- Compare oscillation-test sensitivities of different technologies.
- Do mass versus granularity optimization for each viable technology.

August 1997 milestone:

- Active detector technology decision

6.5 Detector technology and physics goals

The initial goal of the MINOS experiment is either to exclude the possibility of ν_μ oscillations over as wide a range of parameter space as possible or, more positively, to provide unambiguous evidence for their existence. In the event that evidence for ν_μ oscillations is indeed found, the goal of the experiment will be to measure the mixing parameters.

The first objective, to establish or refute the existence of oscillations with the maximum sensitivity, requires that the near and far detectors be as similar as possible, thereby reducing systematic errors to a minimum. (See Section 7.5.) Ideally the two detectors would be identical, and in identical environments, however cost considerations mean that the near detector will be substantially smaller in all dimensions than the far detector. It will also be situated in a higher rate environment. These two important differences place constraints on the active detector technology that is finally chosen.

The difference in size of the detectors means that the different responses of different length active detectors must be fully understood for the three technologies (scintillator, Iarocci or RPC). It must be demonstrated that the responses are correctable and do not result in different thresholds, or different calorimetric behaviors of the two detectors. Uncorrected differences would increase the systematic errors and reduce the sensitivity of the experiment to ν_μ oscillations.

The different environments of the two detectors will also influence the choice of detector technology. The near detector will be in an environment where the rate from genuine ν_μ interactions and cosmic rays is relatively high; the far detector will be in a quiet environment where the principal rate will be due to a low cosmic ray flux, radioactive decays, and singles from the detector elements or electronic noise. The detector technology, and electronics, must respond as identically as possible to neutrino events in both environments. In particular, the rate of overlapping events in the near detector will constrain the timing properties of the active elements; the noise properties (singles rates) of the elements will determine the threshold of the far detector for neutral current events.

Table 20 lists some of the detector parameters which are critical to each of the principal oscillation tests discussed in the Proposal.

The second objective, to measure the neutrino mixing parameters, requires the detector to be ‘flavor sensitive’ for a determination of the mixing matrix elements, and to be able to measure neutrino energy to determine Δm^2 .

As we discuss in Section 6.6, a measurement of the visible energy of CC events is a measurement of E_ν . Both ν_μ and ν_e CC events can be used to determine Δm^2 , although the use of ν_e CC events is practical only if the oscillation is $\nu_\mu \rightarrow \nu_e$ or a three-flavor mode. Simulations have already shown that measurements of the ν_μ CC event rate spectrum for a modest exposure of the reference detector allow a determination of $\Delta m^2 = 0.01 \text{ eV}^2$ to be made to a statistical accuracy of a few percent. The same simulations have also shown that the reference detector can achieve flavor separation on a *statistical* basis, allowing the mixing matrix elements to be measured. A more demanding challenge is explicit ν_τ appearance based on, for example, events with missing p_t , or missing p_l using the Narrow Band Beam.

Further simulations are required to understand how much the accuracy of parameter measurements is determined by the components of the detector, and how much by the raw neutrino energy spectrum and the underlying physics of neutrino interactions in the detector.

Test	Basis	Sensitive to	Detector Parameter
T	$N_{cc}/\text{Total events}$	NC event threshold CC event length cut	1 Steel thickness: • longit. granularity 2 Event overlap rate: • pulse shapes • timing properties • transv. granularity 3 Trigger threshold: • singles rate • electronic noise
Z	$E_\nu = E_{\text{had}} + E_\mu$ (ν_μ CC events)	Hadronic energy calibration and resolution P_μ measurement	1 Steel thickness 2 Sampling medium: • gas or liquid/solid 3 Pulse height: • attenuation • dynamic range • calibration 4 Inefficiencies: • monitoring 5 Magnetic field: • uniformity • calibration 6 Quantization errors: • transv. granularity • interpolation 7 Near detector size
ν_e appearance	Electron ‘identification’ by longitudinal energy deposition profile	Hadronic and electromagnetic energy measurement	1 Steel thickness: • longit. granularity 2 Sampling medium: • gas or liquid/solid 3 Pulse height: • as for Z above 4 Pattern recognition • transv. granularity

Table 20: Major detector parameters which affect the sensitivity of tests for neutrino oscillations in the MINOS detector.

Physics Parameter	Basis	Requirements	Detector Parameter
Δm^2 ($\nu_\mu \rightarrow \nu_x$)	Energies of ν_μ CC events	E_{had} P_μ	1 As for Z test in previous table
Δm^2 ($\nu_\mu \rightarrow \nu_e$)	Energies of ν_e CC events	E_{had} E_{electron} <i>separately</i> <i>if</i> <i>possible</i>	1 As for Z test in previous table 2 Steel thickness: • longit. granularity • transv. granularity Sampling medium • gas or liquid/solid
Statistical flavor identification	Longitudinal energy deposition	Pulse height profile and event length	1 Steel thickness • longit. granularity 2 Pulse height • as for Z test
Explicit ν_e appearance	Identify electron shower	Separate hadron and electron showers	1 Spatial resolution • transv. granularity • interpolation 2 Pulse height
Explicit ν_τ appearance	Missing P_t	$P_t(\text{lepton})$ $P_t(\text{hadrons})$	All of above

Table 21: Major detector parameters which affect the capability of the MINOS detector to measure neutrino oscillation parameters.

Table 21 shows some of the detector parameters which will influence the ability of MINOS to measure mixing parameters. It is clear from Tables 20 and 21 that the critical detector issues are:

1. The *longitudinal granularity* of the detector,
2. The *transverse granularity* of the detector,
3. The *magnetic field*,
4. The *sampling medium* of the active detector planes¹,
5. The *pulse height properties* of the active detectors, and
6. The *event rate capabilities* of the active detectors and electronics.

It is unrealistic to imagine simulations of the entire spectrum of different detector granularities and types of active detector. In fact it would be misleading to place too much reliance upon simulations of the active detectors until prototypes have been constructed and their behavior thoroughly studied in the laboratory and in test beams. To a large extent, however, the issues of granularity and magnetic field are independent of the issues associated with the active detector technology. We therefore plan a top-down approach where, initially, the specific physics goals discussed in Chapter 8 are used to specify the *general* properties of the detector. This will involve a study of how the granularity and magnetic field configuration affect:

1. The threshold, in terms of E_ν , for neutral current events,
2. The acceptance for ν_μ charged current events,
3. The muon momentum resolution of the detector,
4. The hadronic energy resolution of the detector,
5. The electromagnetic energy resolution of the detector,
6. The relative electromagnetic and hadronic energy scales,
7. The statistical flavor identification properties of the detector, and
8. The possibility of explicit neutrino flavor identification.

We expect to have to develop new event reconstruction algorithms in the course of this study.

The specific technology items which must be understood, and their influence on the physics capabilities of the detector, are mentioned briefly in Tables 20 and 21. To reiterate, these include:

¹Calorimeters based on proportional gaseous detectors are reputed to have a worse energy resolution than those using liquids or solids, probably because of the broad ‘Landau’ distribution characteristic of thin layers of gas.

1. The sampling medium,
2. The reproducibility of, and correction for, attenuation of pulse height in long detector elements,
3. The uniformity of response of the large number of elements,
4. The stability of response with time and external changes,
5. The linearity (or not) of response to particles giving different ionization densities,
6. The response to closely separated pairs of particles,
7. The dynamic range of pulse heights, and consequent requirements on the readout electronics,
8. The ease of calibration and monitoring,
9. The potential inefficiencies associated with constructional techniques,
10. The possibility of interpolation of the position of a hit by pulse height measurements from adjacent channels,
11. The pulse shape and timing properties of the active elements, and
12. The single channel counting rate and electronic noise rate.

Simultaneously with our studies to define the general properties of the detector, results from laboratory studies and test beam running will allow us to develop reliable models of each active technology to be incorporated into the detector simulation. The veracity of the simulation program incorporating these models will be checked by comparing the results of simulations with results of the exposure of large scale prototypes to test beams, as described in Section 4.6.

6.6 Determination of neutrino mixing parameters

In the MINOS Proposal [1] the sensitivity of the experiment to neutrino oscillations was quantified in terms of the exclusion limits that the experiment could establish in the absence of oscillations. We have now extended our studies to investigate the capability of the experiment to measure neutrino mixing parameters if conclusive evidence is found for oscillations. Some preliminary results were presented to the HEPAP Subpanel [4], [5] in the summer of 1995. The possibility of observing CP violating effects by comparing the results of running with $\bar{\nu}_\mu$ with the results of an initial run with ν_μ has also been studied [29] and is discussed briefly below.

We have not considered neutrino oscillations arising from exotic or sterile neutrinos but have confined our studies to a scenario consisting of mixing between the three conventional flavors, ν_e , ν_μ and ν_τ . Six parameters are required to describe generalized three-flavor mixing. These are two Δm^2 's, and the complex matrix elements $U_{\alpha i}$ which relate the flavor eigenstates, α , to the mass eigenstates i . These matrix elements can be expressed in terms

of three mixing-angles and a CP violating phase. FORTRAN code has been written, and will be incorporated into the Monte Carlo program, which can be used to calculate oscillation probabilities for any desired set of three-flavor oscillation parameters. It is, of course, of interest to be able to determine all of the mixing parameters but analysis in this general six-dimensional space is difficult and intractable to display. We have therefore so far limited our studies to the simplified ‘one mass scale dominance’ model [30, 31] which assumes a hierarchy of neutrino masses such that $\Delta m_{32}^2 \gg \Delta m_{21}^2$ and where we assume $\Delta m_{32}^2 L/E_\nu \sim \mathcal{O}(1)$ for the MINOS range of E_ν .

In this simplified model the oscillation probabilities become

$$P_{\mu\mu} = 1 - 4|U_{\mu 3}|^2(1 - |U_{\mu 3}|^2) \sin^2(1.27\Delta m^2 L/E_\nu) \quad (1)$$

$$P_{\mu e} = 4|U_{\mu 3}|^2|U_{e 3}|^2 \sin^2(1.27\Delta m^2 L/E_\nu) \quad (2)$$

$$P_{\mu\tau} = 4|U_{\mu 3}|^2|U_{\tau 3}|^2 \sin^2(1.27\Delta m^2 L/E_\nu). \quad (3)$$

Unitarity requires that $|U_{e3}|^2 + |U_{\mu 3}|^2 + |U_{\tau 3}|^2 = 1$. The ν_μ disappearance probability given by Equation (1) has the same form as the two flavor ν_μ disappearance probability with the substitution $\sin^2(2\theta) = 4|U_{\mu 3}|^2(1 - |U_{\mu 3}|^2)$. If the oscillation probabilities are measured, these equations can be solved to find the matrix elements $|U_{\alpha 3}|^2$. If the oscillation probabilities are measured as functions of E_ν , then Δm^2 may also be determined.

The full set of matrix elements, $U_{\alpha i}$, in any three flavor mixing scheme, *cannot* be determined using a neutrino beam of a single flavor; reactor experiments are entirely complementary to MINOS. It is therefore desirable that accelerator ν_μ experiments and reactor ν_e experiments overlap in the coverage of Δm^2 .

6.6.1 Δm^2 determination

Equation (1) for $P_{\mu\mu}$ shows that the ν_μ disappearance probability, in this simplified scheme, is independent of the mode ($\nu_\mu \rightarrow \nu_e$ or $\nu_\mu \rightarrow \nu_\tau$) of oscillation, furthermore the total visible energy, $E_{\text{vis}} = E_\mu + E_{\text{had}}$, of ν_μ charged current events is a measure of the energy of the interacting ν_μ , within the resolution of the detector. As we have shown in the proposal, a cut on event length selects ν_μ CC events with little background from other types of interaction. The ν_μ CC energy spectrum can therefore be used to simultaneously determine Δm^2 and $\sin^2(2\theta)$ (*i.e.* $4|U_{\mu 3}|^2(1 - |U_{\mu 3}|^2)$) by fitting the observed E_{vis} distribution to a function which is the product of the expected E_{vis} distribution and $P_{\mu\mu}(\Delta m^2, \sin^2(2\theta))$.

Figure 6 [5] shows the error contours from such a fit to the ν_μ CC E_{vis} distribution for true values $\Delta m^2 = 0.01 \text{ eV}^2$ and $\sin^2(2\theta) = 0.7$. An exposure of $\sim 3.3 \text{ kT years}$ in the original wide-band two-horn beam was simulated. We expect to obtain this sensitivity in an initial 9 month run with an incomplete far detector. Our final exposure will be at least a factor of 6 greater. The size of the *statistical* error ellipse at low Δm^2 depends on the number of events and the shape of the E_{vis} distribution. The MINOS baseline of 730 km and $\Delta m^2 = \mathcal{O}(0.01) \text{ eV}^2$ produces a relatively long oscillation wavelength on the E_{vis} distribution and thus the error depends rather little upon the detector resolution. The size of the error ellipse in the $\Delta m^2 - \sin^2(2\theta)$ plane can therefore be *estimated* for small

²This mass hierarchy is suggested by the fit of Harrison, Perkins and Scott to all atmospheric and solar neutrino data [8]. These authors assume maximal mixing and find a value of $\Delta m_{32}^2 = 0.0072 \text{ eV}^2$.

values of Δm^2 (< 0.05 eV²) from the interaction rate distribution without recourse to many full Monte-Carlo simulations of the detector [32].

At low Δm^2 the first minimum of the oscillation approaches the low end of the MINOS beam energy distribution. The new three-horn beam design has a higher flux of neutrinos at lower energies and the error ellipse at low Δm^2 is therefore expected to be smaller. An enhancement of the low energy flux is also obtained by using an off-axis beam. Figure 7 shows a comparison of the difference in the size of the error ellipses, $\sigma(\Delta m^2)$ and $\sigma(\sin^2(2\theta))$, arising from the different shapes of the E_ν spectrum, for the old two-horn beam, and the on-axis, and 3 and 5 mr off-axis three horn designs. For this *shape* comparison these estimates assume an arbitrary sample of 3000 fully measured CC interactions in each case. The absolute interaction rates are, of course, different in the four cases, being in the approximate ratios of 3:4:2:1 respectively. The statistical errors will scale as the square root of the number of events. The three horn design of beam, therefore, seems to offer an increase in precision in the determination of Δm^2 , at low Δm^2 , of approximately a factor two over the two-horn design for the same exposure. When the lower event rates are allowed for there seems to be no obvious advantage in using the off-axis designs. These estimates must be confirmed by full simulations of the experiment.

6.6.2 Oscillation mode determination

Some preliminary studies have been made of the capability of MINOS to determine the mode of neutrino oscillation. These studies use the simplified ‘one mass scale dominance’ model described above. For a specific example we show results assuming that the oscillation mode is the maximal mixing scheme of Harrison, Perkins and Scott [8] with $\Delta m^2 = 0.0072$ eV² as suggested by these authors. So far very simple longitudinal cuts, similar to those described in the proposal, have been used to identify the flavour of neutrinos interacting in the detector. Events are classified exclusively as ‘long’, ‘short’ and ‘electron’-like. These classes attempt to select ν_μ CC events, NC events and ν_τ CC events, and ν_e CC events respectively.

For a given set of oscillation parameters, $U_{\alpha 3}$ and Δm^2 , the numbers of events expected in each class can be calculated by numerical integration over E_ν of the product of the ν_μ flux, the oscillation probability ($P_{\mu\alpha}$), the NC or CC cross section for a neutrino of flavor α , and the probability that the interaction is observed in each of the three classes. A χ^2 based on the difference between the observed and expected numbers in each class can then be calculated as the parameters are varied about their true values.

Figure 8 shows the $\chi^2 = 1, 4$ and 9 contours expected from such a fit when the true mode is maximal mixing with $\Delta m^2 = 0.0072$ eV² (*i.e.* the HPS mode) for a 3.3 kT-yr exposure of the detector in the two-horn ν_μ beam³. In the figure the vertices of the triangle represent pure flavor states. The values of the matrix elements ($|U_{e3}|^2$ etc.) are represented by the perpendicular distance of a point to the sides of the triangle [29, 33]. Maximal mixing is represented by the centroid of the triangle.

Two χ^2 minima are found. The minimum at the center represents the true maximal mixing mode. The second minimum, close to the ν_μ vertex, is expected. It results from a

³These results assume that the value of Δm^2 obtained from the analysis of the CC E_{vis} distribution is equal to the true value. The effect on the determination of the matrix elements due to an error on Δm^2 is being evaluated.

fundamental quadratic ambiguity in Equation (1) for the ν_μ disappearance probability. As we remarked above, an experiment using a ν_e beam which covers the same range of Δm^2 would be required to resolve this ambiguity.

6.6.3 Prospects for observing CP violation in MINOS

If it is established that the three neutrino flavors are mixed, complementary runs made with neutrino and antineutrino beams would allow the differences,

$D_{\mu e} = P(\nu_\mu \rightarrow \nu_e) - P(\bar{\nu}_\mu \rightarrow \bar{\nu}_e)$ and $D_{\mu\tau} = P(\nu_\mu \rightarrow \nu_\tau) - P(\bar{\nu}_\mu \rightarrow \bar{\nu}_\tau)$ to be measured. By the CPT theorem $D_{\mu e} = -D_{\mu\tau}$. If CP is conserved each of these quantities should equal zero. A significant non-zero result would indicate leptonic CP violation arising from a complex T-violating phase in the neutrino mixing matrix. There is no such phase if only two generations of neutrinos are mixed; the mixing of at least three generations is required for CP violation to be observable.

The size of any CP violating effect depends on several factors. The difference, $D_{\mu e}$, can be written as

$$D_{\mu e} = 4J_{CP} \left(\sin(1.27\Delta m_{21}^2 L/E_\nu) + \sin(1.27\Delta m_{32}^2 L/E_\nu) - \sin(1.27\Delta m_{31}^2 L/E_\nu) \right) .$$

The CP violating parameter, J_{CP} , depends entirely on the mixing-matrix elements. The maximum possible value of $|J_{CP}|$ is $1/6\sqrt{3}$ and occurs for threefold maximal mixing. If one $\Delta m^2 = 0$ then $D_{\mu e} = 0$ and no CP violation is expected.

Two factors therefore determine whether leptonic CP violation could be observed; the magnitude of J_{CP} and the values of $\Delta m_{32}^2 L/E_\nu$ and $\Delta m_{21}^2 L/E_\nu$. Because CP violation arises from interference between these two Δm^2 -dependent phases, an experiment must be sensitive to the *smaller* of the two Δm^2 's to observe a large effect. CP violation will be observable in MINOS only if the smaller Δm^2 is of order 0.01 to 0.1 eV², and J_{CP} sufficiently large.

Δm_{32}^2	10	0.01	0.01 eV ²
Δm_{21}^2	0.01	0.01	10 ⁻⁵ eV ²
Maximal three-flavor	0.29	0.41	5 × 10 ⁻⁴
Weak three-flavor	3.1 × 10 ⁻³	4.5 × 10 ⁻³	6 × 10 ⁻⁶

Table 22: The theoretical magnitudes of the CP violating quantity $D_{\mu e}$ for MINOS neutrino energies and baseline. Three possible mass-hierarchies have been assumed for each mixing matrix. Experimental ν_e identification efficiencies are not included.

Possible values of the mixing parameters are, as yet, too poorly known to be able to make any very definite predictions of the amount of CP violation to be expected. We have therefore made calculations for some example cases. These calculations assume perfect efficiency for the identification of ν_e CC events. Table 22 shows calculations of $D_{\mu e}$, averaged over the neutrino energy spectrum, that could be observed in MINOS for two possible mixing matrices

and three mass hierarchies. The ‘weak mixing’ matrix is representative of a type that could simultaneously explain the LSND [34] result and the atmospheric neutrino deficit. For this matrix $|J_{CP}| = 10^{-3}$ and a maximal CP violating phase of $\frac{\pi}{2}$ has been enforced. Maximal CP violation is a natural consequence of maximal three-flavor mixing.

In all but two of the six cases the magnitude of $D_{\mu e}$ is $\sim 5 \times 10^{-3}$ or less. Since $D_{\mu e}$ represents the *difference* of the ν_e appearance probabilities between neutrino and antineutrino beams, CP violation would never be observed in MINOS for the third mass hierarchy. Work is continuing to understand for what range of parameters MINOS would be able to observe CP violation, and what constraints this places on the design of the detector.

6.6.4 Future studies

The preliminary studies presented in Sections 6.6.1 and 6.6.2 indicate that MINOS has a good capability to measure mixing parameters in the low Δm^2 region. These results were obtained from simulations of the reference detector described in the Proposal and assume a granularity of 4 cm of steel, a 2 cm transverse granularity and a modest pulse-height capability. Items for future study include:

1. To understand how the choice of the active detector technology will influence the measurement of mixing parameters.
2. To understand how the longitudinal and transverse granularity of the detector will influence parameter measurement.
3. To quantify the possible systematic errors on measured parameters associated with any residual uncorrected near-far beam difference.
4. To further quantify the gains, in terms of the errors on measured parameters, of the new three-horn wide-band beam design.
5. To consider the relative merits of running with an on- or off-axis wide-band beam, or a narrow-band beam from the point of view of parameter measurement.
6. To understand how to combine Δm^2 and mode identification in a global analysis of data from the detector. Use of all the events in a simultaneous fit should reduce the errors on both Δm^2 and the mixing-matrix elements.
7. To develop a better method (than simple cuts) of using the information from the detector for parameter determination. This could be based, for example, on a likelihood estimator which uses the longitudinal and transverse pulse-height profiles of events in the detector. It is unlikely that this study, which is extremely Monte Carlo intensive, will be undertaken before the active technology is chosen.

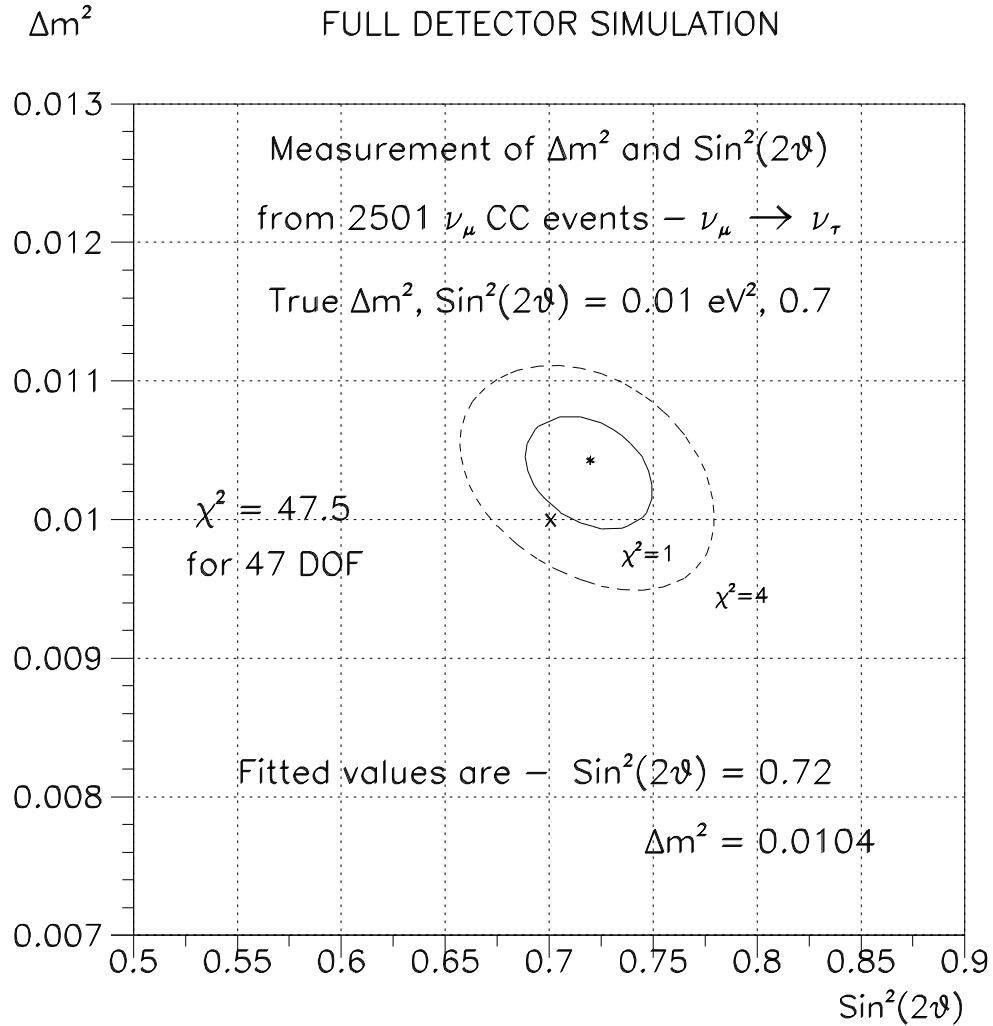


Figure 6: Error contours obtained from the energy measurements of ν_μ CC events for $\nu_\mu \rightarrow \nu_\tau$ oscillations with $\Delta m^2 = 0.01 \text{ eV}^2$ and $\text{sin}^2(2\theta) = 0.7$. The simulated event sample includes backgrounds.

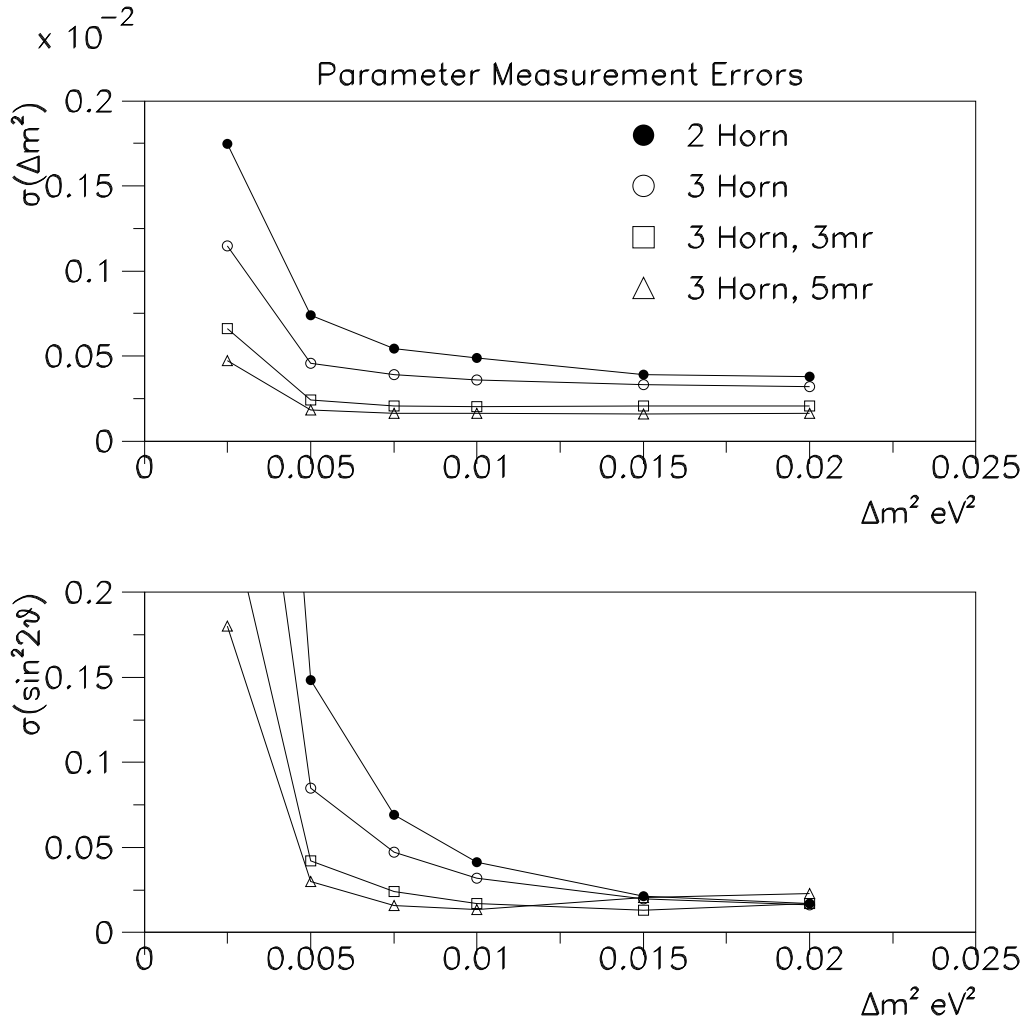


Figure 7: A comparison of the estimated statistical errors on Δm^2 (upper figure) and $\sin^2(2\theta)$ (lower figure) that would be obtained by fitting the E_{vis} distribution of 3000 measured ν_μ CC events for the old two-horn beam design, and the on-axis and 3 and 5 mr off-axis three-horn designs of a wide-band beam. This figure simply demonstrates how the errors change due to the different shapes of the E_ν distributions of the beams. The relative event rates (in the approximate ratios of 3:4:2:1) must be allowed for but are not included.

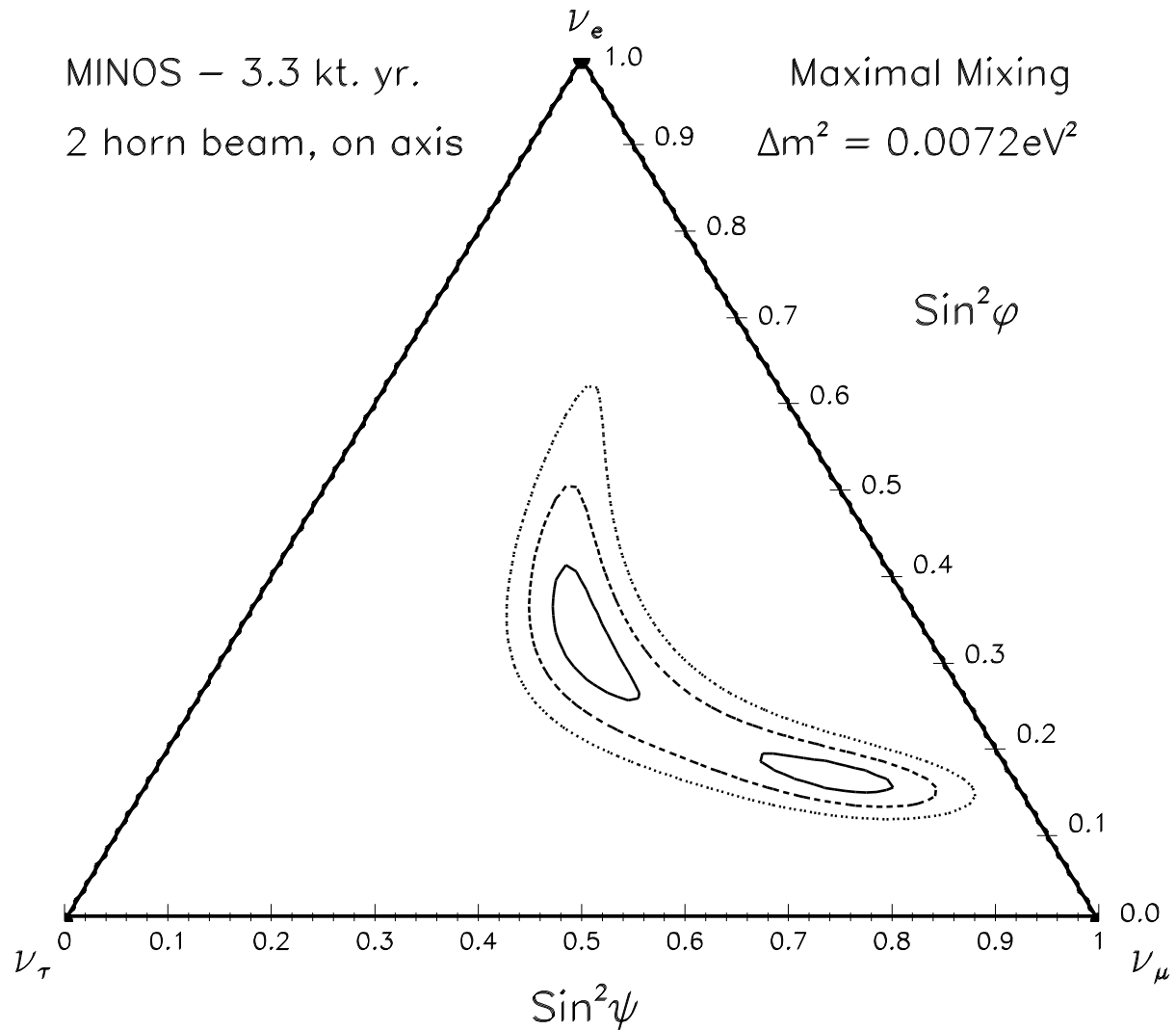


Figure 8: Results of a fit of oscillation parameters to a simulated 3.3 kT-yr exposure of the MINOS detector in the two-horn wide-band beam when the true oscillation mode is maximal mixing with $\Delta m^2 = 0.0072 \text{ eV}^2$. Maximal mixing is represented by the centroid of the triangle. The vertices are pure flavor states. The matrix elements, $|U_{\alpha 3}|^2$, are the perpendicular distances of a point to the sides of the triangle.

6.7 Supplemental R&D funds for simulation work

Most of the costs associated with MINOS simulation work are associated with physicist and programmer effort, and are paid for by the collaborating institutions' base contracts and grants. In January 1996 however, the collaboration requested direct DOE and NSF support for one-year "bridging" postdoctoral appointments at Caltech, Indiana, Minnesota, and Stanford. These funds would have allowed new MINOS postdocs to be hired one year earlier than an existing position was scheduled to be vacated by a postdoc currently working on another project [7]. Only a small fraction of the requested funds were supplied (to Indiana) in FY 1996, so we have "rolled over" the balance of the original \$280K request into our FY 1997 funding request.

Two small computer hardware items were purchased with MINOS R&D funds allocated by Fermilab: a personal computer for the ITEP-LPI (Moscow) group for use in test beam calibration simulations, and a memory upgrade for the Indiana computer which hosts the collaboration CVS system, as described in Section 6.2 above.

Table 23 summarizes the supplemental funding allocations and requests.

Activity	\$K
FY 1995: (actual allocation)	5
PC for ITEP-LPI group	5
FY 1996: (actual allocation)	27
Indiana computer memory upgrade	2
Indiana postdoctoral support	25
FY 1997: (request)	255
Caltech postdoctoral position (DOE)	80
Indiana postdoctoral position (DOE)	40
Minnesota postdoctoral position (DOE)	65
Stanford postdoctoral position (NSF)	70
FY 1998:	0

Table 23: FY 1995-8 funding for MINOS simulation work (in FY 1996 dollars except for FY 1995).

7 Neutrino Beam

7.1 Introduction

This Chapter describes the ideas that guide the NuMI beam design, and gives the current status of this design activity. We also touch briefly on the question of the optimal location for the MINOS near detector hall.

Our NuMI neutrino beam design work to date has concentrated on maximizing the flux while understanding its spatial and energy distributions in detail. Large neutrino flux is essential for a long baseline experiment but the ultimate sensitivity of the experiment may be determined by our understanding of neutrino events at the far detector while using the near detector as a reference. Differences between the beams at the near and far detectors must be minimized, but those arising from easily calculated effects such as time dilation or decay kinematics are of secondary importance. The differences to be minimized are those caused by the *background* neutrinos which are difficult to calculate or even to measure.

Another important beam criterion for MINOS is flexibility. The ideal way to verify the presence of oscillations is to change conditions in such a way that the result is predictable, and dependent on whether an initial oscillation signal is real or is caused by some unforeseen effect. For that reason both wide band and narrow band beam capabilities are being pursued.

Even though we have no radically new solutions to propose for the NuMI beam design, our current studies indicate that development work to push some technologies beyond the region of previous experience may be required in the future.

From a more general perspective, the beam question can be viewed as the task of optimizing the physics capabilities of the experiment by varying three general “components:”

- The beam itself,
- The location of the detector site at Fermilab,
- The nature of the near detectors,

all under a constraint of reasonable cost. Our general strategy here is to identify the most interesting oscillation channels and then to determine the different ingredients which enter into the various measurements used to test for the presence of oscillations. We can then evaluate the effect of the uncertainties in these ingredients on the results of the oscillation tests for different design choices.

7.2 Beam simulations

Our current designs for the NuMI neutrino beam produce high fluxes of neutrinos which are sufficient to give, in a few years running time, relatively small statistical errors in different neutrino oscillation tests. Thus understanding and reducing systematic errors acquires special importance. The near term goal of the beam simulation work is, therefore, not further optimization of the flux, but deeper understanding of the potential systematic errors caused by beam effects on neutrino oscillation tests. One effort, primarily at Fermilab and Argonne,

is to finish work on the modeling of systematic effects for the current baseline 3-horn wide-band beam (WBB) design. Another effort, primarily at Columbia, is to study alternative designs of beam line optics which may reduce systematic errors.

We will discuss the simulation plans in terms of:

- The oscillation tests and their systematic errors,
- The effects which cause uncertainty in the beam calculations,
- The development and applicability of specific software tools,
- Our plan for future beam simulation work.

7.2.1 Oscillation tests

The bottom line for the beamline simulation work is the effect on the oscillation tests. Four tests have been selected as general MINOS benchmarks:

- NC/CC test,
- The ν_μ CC total energy spectrum test,
- Identification of electron events from $\nu_\mu \rightarrow \nu_e$ oscillations,
- Tau identification from ν_τ events.

The NC/CC test is the one that has received the most attention so far, and descriptions of systematic error calculations for this mode can be found in the MINOS Proposal and follow-on documents. Plans to optimize the detector design for the NC/CC (or “T”) test are outlined in Section 8.2. In this test, oscillations to ν_e or ν_τ produce interactions which look like “NC” events in the far detector. This test is rather insensitive to beam effects which cause near/far spectrum differences because it uses the detected ν_μ CC events to normalize the expected number of ν_μ NC events both in the far detector and the near detector. The systematic beam-related effects that have been studied so far are uncertainties in hadron production, other-flavor neutrino backgrounds, and how near/far spectrum differences convolute with uncertainties of neutrino cross sections and detector response. All of these systematics appear to be well under control. The systematics left to study are the effects of tertiary hadron interactions in the decay tunnel and beam element misalignments.

The ν_μ CC energy spectrum test, on the other hand, relies completely on the transference of the ν_μ energy spectrum from the near detector to the far detector, and is thus *a priori* more sensitive to near/far spectrum differences. This mode has received less attention so far, but detailed studies of its systematics are planned. Detector optimization for the CC energy spectrum test is described in Section 8.3.

For the electron identification test, where the $\nu_e, \bar{\nu}_e$ backgrounds and their near/far differences are especially important, the software tools for the proper studies are just becoming available. Plans to optimize the detector design for electron identification are outlined in Section 8.4.

Each of the ν_τ identification modes requires study of different aspects of the beam. When using $\tau \rightarrow e$ identification, ν_e backgrounds must be well known. The neutrino from τ decay produces missing energy, which may be measured in $\nu_\tau \rightarrow \tau \rightarrow \mu$ events if the initial ν energy is known, i.e. in the narrow-band beam (NBB). The energy spread and low energy tails of the NBB are then important. The NC event energy distribution is also sensitive to $\nu_\mu \rightarrow \nu_\tau$ oscillations, but near/far differences must be well understood. All of these require further study. Plans to optimize the detector design for tau identification are outlined in Section 8.5.

7.2.2 Contributions to beam uncertainties

The general thrust of the systematic error calculations is to determine how the oscillation tests are affected by variations in the following:

- Hadron production spectrum,
- Beam line alignment, including magnetic field variations,
- Secondary interactions in horns, tunnel walls,
- Neutrino cross sections,
- Neutrino event generation,
- Detector response, acceptance,
- Reconstruction and identification cuts.

Other effects, such as hadron decay kinematics, also contribute to near/far differences but are exactly calculable. The uncertainties in hadron production, beam alignment, and secondary interactions are specifically part of the beam simulations, but proper understanding of systematic effects requires simultaneous understanding of beam, detector and physics aspects of the simulations. For instance, in the NC/CC test, ν_μ induced charm events contribute directly to the CC channel, but to the NC channel only through event misidentification. If the ν_μ beam spectrum were exactly the same in near and far detectors, the effect would cancel out in the near/far NC/CC ratio. The calculation of the systematic error is the convolution over the near/far difference and the uncertainty in the charm cross section.

7.2.3 Beam software tools

Three beam simulation packages are currently being used in the systematic error studies. These trade off speed versus range of effects that are included, as shown in Table 24.

NUADA generates a matrix of production angles and momenta for π^\pm and K^\pm at the target, and tracks this “mesh” through the focusing system. At each step along each track, it integrates a neutrino flux at the detector which combines the production probability for that angle and momentum, the decay probability for that track, and the acceptance of the detector. Continuing care is required to ensure that the granularity of the mesh is fine enough.

PBEAM generates π^\pm , K^\pm , and K^0 in a Monte Carlo fashion, and tracks them through the focusing system. Absorption of hadrons in the horns is taken into account, but secondaries are not generated. Each hadron is then decayed at one position. PBEAM contains the option of generating neutrino fluxes two ways, either selecting random decay angles (i.e. unweighted Monte Carlo), or calculating the weight for that decay to produce a neutrino in the detector acceptance.

GBEAM generates neutrino fluxes in a manner similar to PBEAM. It differs from PBEAM in being GEANT based, and in the larger number of effects that it includes. GBEAM was developed specifically for NuMI beam design work over the past six months, and is designed to interface to the MINOS detector simulation program, GMINOS.

The alignment studies will be done primarily with NUADA and PBEAM. Background studies require the use of GBEAM.

	NUADA	PBEAM	GBEAM
Typical run time	0.2 hr	2 hr	200 hr
$\pi^\pm, K^\pm \rightarrow \nu_\mu, \bar{\nu}_\mu$	yes	yes	yes
$K_L^0 \rightarrow \nu_\mu, \bar{\nu}_\mu, \nu_e, \bar{\nu}_e$	no	yes	yes
$\mu^\pm \rightarrow \nu_\mu, \bar{\nu}_\mu, \nu_e, \bar{\nu}_e$	no	yes (ignores polarization)	yes
3 body decay model	none	phase space	V-A
Hadron absorption by horns etc.	yes	yes	yes
Secondary interactions from horns etc.	no	no	yes
μ (for monitor chambers)	no	yes	yes
Baryons (monitor chambers, radiation)	no	no	yes

Table 24: Comparison of programs used for neutrino beam simulation.

Progress since January in the development of the software tools includes:

- The creation of the GEANT-based GBEAM package, which allows us to calculate for the first time the flux of neutrinos created by secondary hadronic interactions in the horns and decay tunnel walls.
- The creation of code to properly handle the effect of polarization in the $\pi \rightarrow \mu \rightarrow \nu$ decay chain, including the angle and energy correlations.
- Linking of the software chain, so that the neutrinos generated from GBEAM or NUADA can be read in directly by GMINOS (the detector simulation program described in Chapter 6).

As an example of the recent progress in modeling the beam, we show in Figure 9 the ν_μ flux from interactions occurring outside the target compared to the flux from hadrons produced in the target. Here the GEANT/FLUKA hadron production model is used in GBEAM. Secondary hadron interactions are a significant source of neutrinos only at the lowest energies. The sources are further broken down in Table 25. Neutrinos from secondaries produced in the

decay tunnel walls, which had previously been an area of considerable uncertainty, appear to be a fairly small contribution. Figure 10 shows the wrong-flavor neutrino backgrounds. The inclusion of secondary interactions and muon polarization have not significantly increased these backgrounds over the numbers given in the MINOS Proposal.

SOURCE	ν_μ	$\bar{\nu}_\mu$	ν_e	$\bar{\nu}_e$
π^\pm, K^\pm, K^0 produced in target	100.00 %	0.76 %	0.14 %	0.02 %
μ^\pm decay	0.00 %	0.36 %	0.38 %	0.00 %
Secondary decay, e.g. $K \rightarrow \pi \rightarrow \nu$	1.73 %	0.11 %	0.00 %	0.00 %
Aluminum focusing horns	2.47 %	0.14 %	0.01 %	0.00 %
Concrete shield, tunnel walls	0.00 %	0.00 %	0.00 %	0.00 %
Target area steel	0.03 %	0.02 %	0.00 %	0.00 %
Decay pipe window	0.20 %	0.12 %	0.00 %	0.00 %
Decay pipe walls	0.51 %	0.35 %	0.01 %	0.00 %
Hadron absorber	0.01 %	0.01 %	0.00 %	0.00 %

Table 25: Flux of neutrinos at the center of a detector 500 m from the end of the decay pipe, broken down by source and normalized to the ν_μ flux from hadrons produced in the target.

7.2.4 Plan for future beam simulation work

By October 1996 we expect to have completed the propagation of variations in beam element alignment, production model uncertainties, and near/far spectrum differences through the benchmark oscillation tests, although this will continue to change as detector simulation and analysis code evolves. However, we also need to calculate how accurately various beam monitoring devices will be able to determine actual beam parameters. For example, the radial dependence of the energy spectrum in the near detector will be a strong constraint on production model variations. Ion chambers in the decay tunnel and muon chambers after the hadron absorber could also turn out to provide useful information. But the correlation and limits of constraint need to be quantified. Thus we expect that beam simulation work will continue for an extended period of time, as outlined in the following list of milestones:

Milestones for NuMI simulation of the Baseline Beams:

- **July 1996:** Finish study of variations of hadron production in GBEAM for WBB.
- **September 1996:** Finish studies of effects on beam flux of beam line element misalignments for WBB.
- **October 1996:** Have analysis code integrated so that variations from beam uncertainties can be propagated through to variations in oscillation tests for WBB.
- **November 1996:** Finish study of effect of field variations on beam flux for WBB.
- **January 1997:** For WBB, understand how much the radial dependence of the neutrino interaction energy spectrum in the near detector pins down variations in the near/far difference due to (a) variations of hadron production models, (b) misalignments of beam elements, (c) variations in beam line fields, and (d) uncertainty in contribution from secondary interactions.
- **March 1997:** For WBB, understand how much beam monitor devices (ion chambers in decay tunnel, muon chambers after hadron absorber) pin down variations in the near/far differences.
- **March 1997:** Answers to (a) how systematic uncertainties vary with location of the near detector (e.g. 250 m versus 500 m from the end of the decay tunnel), (b) how systematics vary with shape of the decay pipe, and (c) how sophisticated a set of monitoring systems is required.
- **April 1997:** Complete Technical Requirements Document for the WBB design.
- **July 1997:** Finish similar studies for NBB.
- **October 1997:** Complete the Technical Design Report for beam technical components.

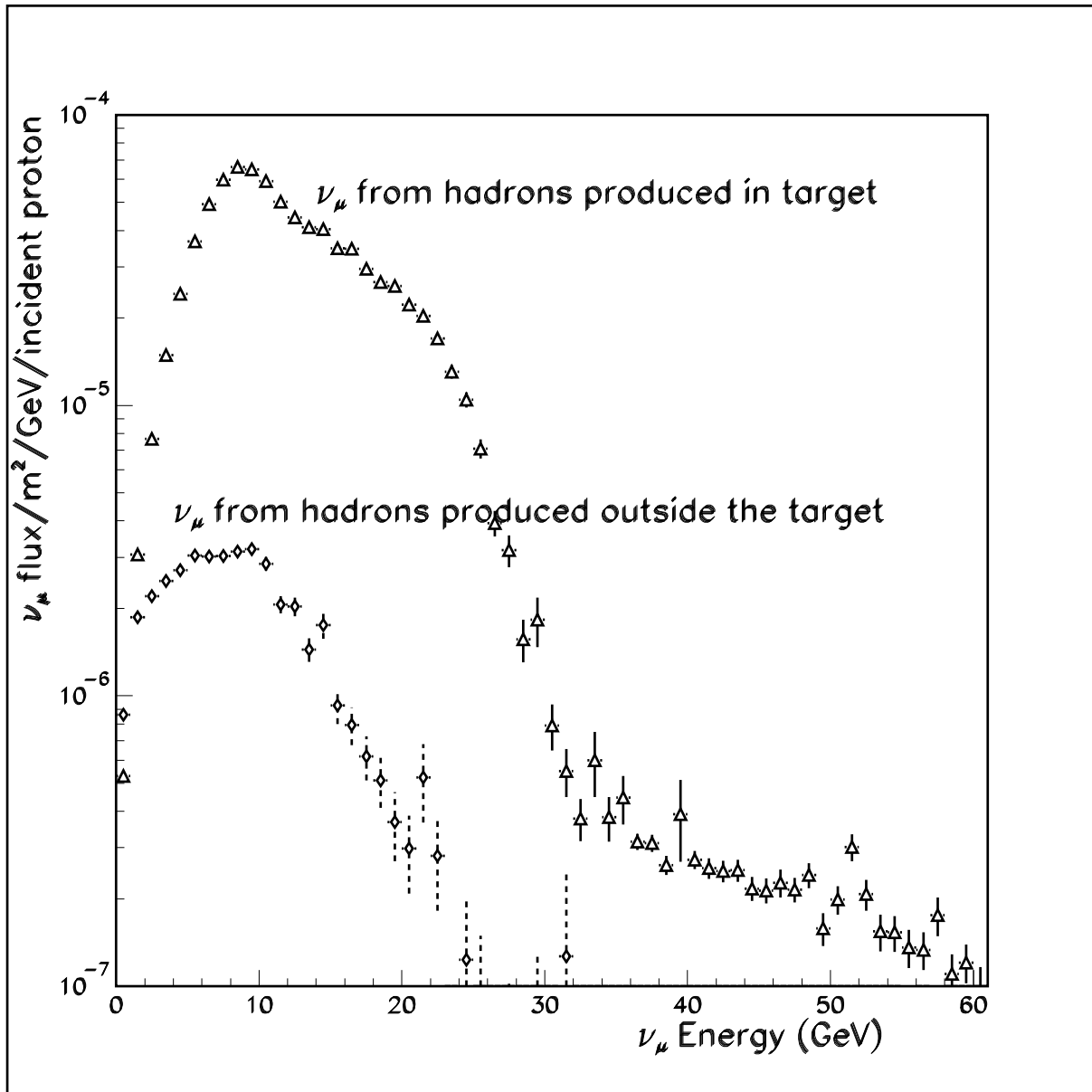


Figure 9: ν_μ flux from hadrons produced in the target, and from secondary interactions, at the center of a detector 500 m from the end of the decay tunnel.

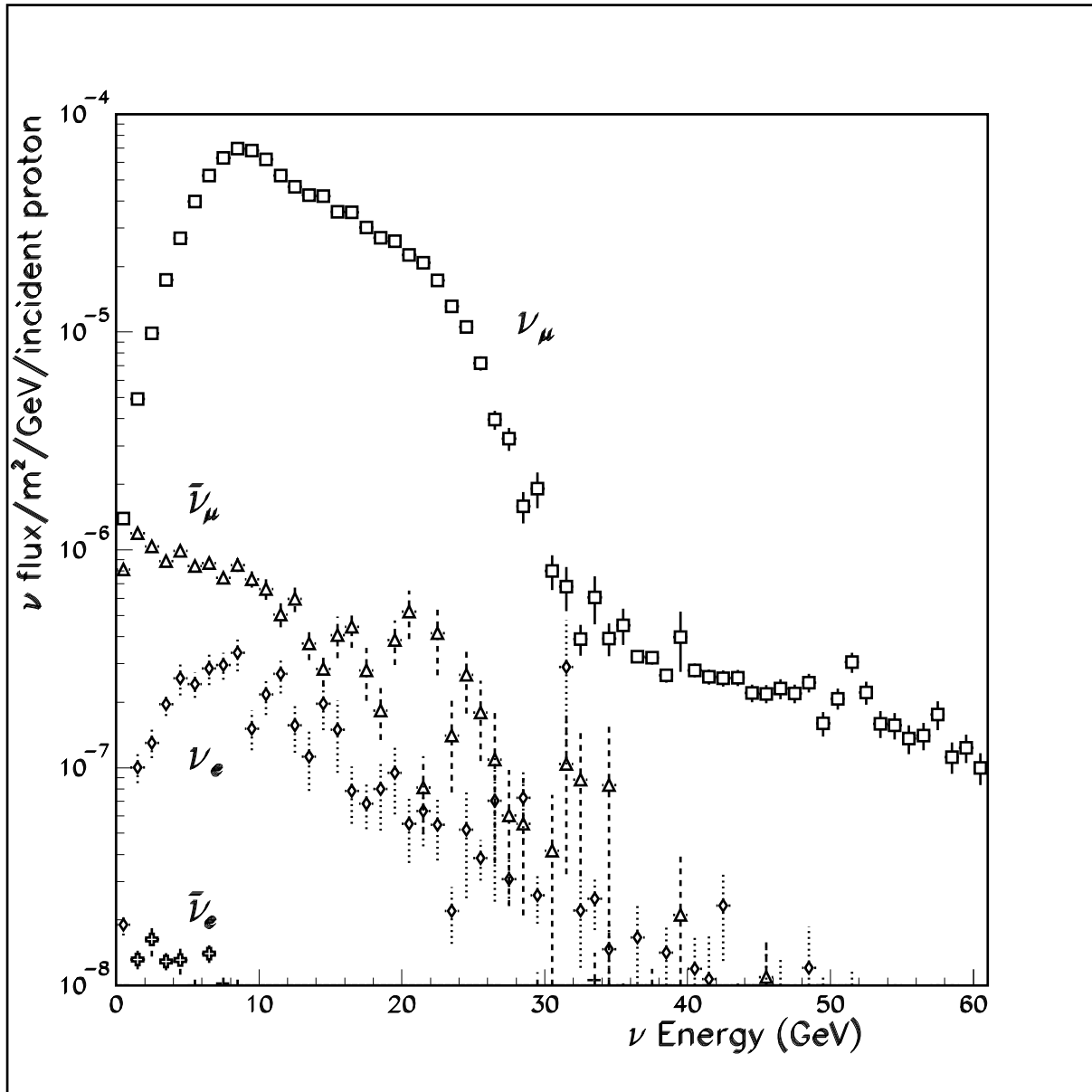


Figure 10: ν flux components at the center of a detector 500 m from the end of the decay tunnel.

7.3 Beam options

7.3.1 Alternate configurations

One of the important premises underlying the MINOS experiment is that the NuMI beam will have the capability of running in several different configurations. Thus it is important to design multi-beam capability from the outset, since it will be difficult or impossible to implement some types of changes later on when the beamline civil construction is completed.

There are at least three different arguments for having this variety of options:

- a) If a neutrino oscillation signal is thought to be detected, it is important to be able to change conditions, so that the expected new results will be significantly different in a predictable way. Changing the neutrino beam parameters appears to be a very powerful way to do this.
- b) Pursuing the positive signal scenario, once the approximate range of Δm^2 and $\sin^2(2\theta)$ parameters is known we would want to run in that beam configuration (or those configurations) which would give the best opportunity to measure precisely the mode(s) of oscillation and the oscillation parameters.
- c) It is quite possible that new information, obtained during the next few years from other neutrino experiments, would argue for a different initial beam configuration than a wide band beam optimized for maximum number of neutrino interactions. Maintaining such flexibility is in the spirit of Recommendation 4 of the Sciulli Subpanel [6].

Because of the arguments given above, the MINOS Collaboration's experimental scenario included from the beginning both the WBB and the NBB options. The beam design work performed over the last year or so has demonstrated that retaining these two options is feasible and does not increase the cost significantly. As a result of this work, adequate WBB and NBB designs now exist, the latter for hadron beam energies from 20 to 45 GeV.

As part of our continuing process of optimizing the experiment, with special attention to minimizing systematic errors, we have investigated a number of variants on these two basic options. This work is still very much in progress. Most of the results are not crucial to the critical-path decisions that have to be made during the next year. The main variants, very briefly, are:

- a) Different elements in the WBB. The current baseline WBB design is a three horn system. Arguments have been made that the systematics from a run in a WBB would be improved if the first horn were replaced by a lithium lens. Detailed studies of such a design are being pursued and results should be forthcoming in the next few months.
- b) A WBB optimized for lower neutrino energies. The neutrino oscillation parameters suggested by the results of the Kamiokande experiment would give 6-10 GeV as the optimum neutrino energy for the Fermilab-Soudan distance. It is our plan to investigate this option during the next six months. Clearly, whether such an option is or is not interesting will depend on developments in the field during the next few years.

- c) An alternative way to achieve high flux in the low E_ν range is to orient the beam so that the MINOS detector looks at a finite neutrino emission angle (with respect to the hadron beam direction). There are a number of variants on this scheme, i.e. what angle (3 and 5 mr have been investigated) and what primary beam parameters (standard WBB or NBB, and if the latter, at what energy). The studies so far have focused on flux calculations and indicate that a rather monochromatic high intensity, 6-10 GeV neutrino beam can be obtained by this means. Changing from an on-axis to an off-axis configuration after the beam is built would be a major undertaking, however. Thus the choice of this option would have to be decided on early, based on solid physics arguments.

In addition, there are a number of other, minor variants that also need to be pursued as part of these optimization studies. The general philosophy in these studies is always the same: the three horn wide band beam design is the reference design; small variants on this particular scheme have to demonstrate improved performance at no, or small, additional cost. “Improved performance” would be determined by considering both the predicted neutrino flux and the ability to understand systematic uncertainties.

7.3.2 Beam spill structure

The time structure of the beam extracted from the Main Injector, and hence of the neutrino beam, is an important parameter for both NuMI experiments, COSMOS and MINOS. Some of the relevant points are:

- a) Use of slow resonant extraction minimizes the potential pileup in both the COSMOS and MINOS near-hall neutrino detectors and in some of the beam monitors.
- b) The alternative, offered by the Main Injector extraction group, of a single-turn extraction of the Main Injector beam taking about 11 μsec , offers the advantage of less severe requirements on some of the beam components and the possibility of a “triggerless” data acquisition system (as discussed in Section 4.5.2).

COSMOS has determined that, because of pileup problems, alternate b) is unacceptable. A recent development is an extraction scheme suggested by Martin [35], which combines the advantages of a) and b):

- c) Complete individual bunches would be extracted using a single “kick”, with the spacing between successive extracted bunches giving a total spill duration of about 0.5-1.0 msec. Since there are about 500 bunches in the Main Injector, even a 0.5 msec spill length would give a 1 μsec bunch-to-bunch spacing. Two events in successive bunches would be resolved comfortably even with Iarocci tubes. In this case, about 10% of the events would be accompanied by another event in the same bunch in the MINOS near detector. Those events could be separated using spatial criteria or simply rejected without any bias. The low duty cycle would allow triggerless readout of the data after each bunch. In addition, precise knowledge of neutrino arrival time could give some discrimination against neutron interactions. This solution is acceptable to the COSMOS collaboration.

This “ping” extraction scheme is very attractive and there is an interest in our Collaboration to work with the Fermilab Accelerator Division to see whether this scheme can be realized. Because the proposal is relatively new, it will be at least a few months before we can understand if this extraction method is workable.

7.3.3 Lithium lens development

A lithium lens has been the primary focusing element in the Tevatron antiproton source, and since 1986 several different lenses in that system have cumulatively operated for some 40 million pulses. Therefore, the practicality of using a lithium lens as a beam focusing device is now well established.

In the MINOS Proposal a lithium lens was incorporated into the NBB design as the first focusing element. More recent studies indicate that replacing the first horn in the current three horn WBB design with a lithium lens could possibly improve parallelism, which would decrease the potential systematic error due to near/far beam differences. If further studies show that the use of a lithium lens would yield an overall improved WBB then a program should be established to push the technology of the lithium lens in two areas: a beam spill length of at least 0.5 msec and a lens radius of greater than 1 cm to improve acceptance.

7.4 The neutrino monitor detector

As will be shown in Section 7.5, the goal of near/far similarity will impose strict requirements on the near detector, since the design will be driven primarily by the far detector. There are two general areas of investigation, however, that might put quite different requirements on a detector in the near hall. These are:

- a) Detailed measurement of beam properties,
- b) Other physics experiments which could be done in the near hall.

Hence, we are seriously considering the possibility of another detector, henceforth referred to as the neutrino monitor detector, to accomplish these goals. The design of this instrument could be now driven entirely by the additional physics needs.

We elaborate on these arguments below.

Properties of the beam. The neutrino spectrum at the near and far detectors is not identical; the differences are essentially due to the fact that the primary neutrino source is a finite volume rather than a point. The differences due to this particular cause are reliably calculable. On the other hand, there will also be other neutrino sources, which we are trying to minimize *via* beam design. Neutrinos can originate, for example, from pions produced in the walls of the horns or in the walls of the hadron beam pipe. These generally will have lower energies and larger angles. In principle, our calculations can predict energy and radial distributions of these neutrinos, but it seems essential to verify the calculations as well as possible. We plan to design the neutrino monitor detector so it is optimally suited to do this.

Another example is the flux of other flavors of neutrinos. A significant fraction of ν_e 's is from muon decays. By studying their energy and radial distribution, one can confirm

experimentally the Monte Carlo calculations of this component. Thus the neutrino monitor should have a granularity that is good enough for adequate electron neutrino identification.

Other physics experiments. The Main Injector will provide a more intense neutrino beam than has been previously available. Thus new neutrino experiments might be feasible and we are currently investigating these possibilities. Three examples that might be mentioned are:

- a) Investigation of the LSND effect. The Main Injector energy and our near detector distance are ideally suited to the investigation of the $1 < (m_1^2 - m_2^2) < 10 \text{ eV}^2$ neutrino mass range. A narrow band beam, combined with a fine grained detector, should be powerful tools to study this question.
- b) The neutrino interactions in the energy range of 10 GeV are not well understood, representing, in some sense, a transition from the dominantly quasi-elastic and resonance region to the deep inelastic region. Thus it would be worthwhile to fill this experimental gap.
- c) The nuclear dependence of neutrino interactions has not been studied with a statistically significant experiment. The high flux of neutrinos at the beam monitor location would allow the use of targets with a wide range of A.

7.4.1 Neutrino monitor detector parameters

Based on the above, we can discuss briefly the zeroth order design of the neutrino monitor detector. We consider first the size. The requirement that this detector be able to study the beam imposes some constraints on its size. More specifically we want it to be able to intercept all neutrinos which would strike the far detector so that all potential sources can be studied and verified. To a very good approximation, the sources are confined to radii smaller than the radius of the beam pipe ($r < 1 \text{ m}$) and far detector neutrinos are emitted essentially parallel to the beam axis. Thus, allowing for edge effects and fiducial volume, the transverse size should be of order 3 m in both dimensions.

Alternatively, we can try to design a detector that intercepts neutrinos in the most efficient way (per unit mass of the detector). Thus one wants to limit the transverse size to the area of high neutrino flux. The solid angle subtended in the pion decay rest frame by an element of the detector is proportional to $1/(1 + \gamma^2\theta^2)^2$. Thus for $\gamma \approx 250$ (35 GeV π , 14 GeV ν) the 50% point is reached at about $\theta \approx 2.5 \text{ mr}$. For a typical decay point ($\sim 800 \text{ m}$ from the detector) this would argue for a transverse size of about 4 m plus allowance for fiducial volume, i.e., somewhat larger than obtained from the argument given in the previous paragraph. Sizes much larger than this probably are not cost effective from this point of view. If number of neutrino interactions is the figure of merit, one would prefer then to increase the length.

Regarding the length, ideally we should absorb most of the hadronic shower in the monitor detector. We assume that the near detector will be directly behind the monitor detector and thus it can absorb the tail of the hadronic shower. We might guess roughly that eight interaction lengths would be adequate: three for the interactions themselves and then five more for absorbing the showers. Three interaction lengths should be sufficient to verify that

interactions are not due to neutrons. Assuming a cross sectional area of 10 m^2 , we should observe about 10^7 neutrino interactions/year in each interaction length of the detector.

The granularity and the technology used for the active detector should be optimized for electron identification and measurement of low energy neutrino interactions. In addition, an active detector with fast timing capability would have the advantage of being able to discriminate against neutrons *via* time-of-flight if the “ping” structure of the beam is used. These requirements probably argue for liquid or solid scintillator and an absorber plate thickness of less than one radiation length. CHARM II glass or the aluminum or marble in the BNL-871 rangefinder might be suitable absorbers for this purpose.

7.5 Near/far detector differences

The search for neutrino oscillations with MINOS is performed by comparing the rates and characteristics of events in “near” and “far” detectors at two widely separated locations. This comparison is simplified, and hence a higher sensitivity is possible, if the two detectors are as similar as possible. For various reasons it is not practical to make the two detectors completely identical. We feel, however, that they should be very similar in:

- a) Active detector technology,
- b) Granularity,
- c) Material used for passive part of the detector,
- d) Average strength of the B field.

It would be acceptable if they would differ in:

- a) Overall size (in each dimension),
- b) Pattern of the B field.

Below we state very briefly the main arguments behind these statements.

Active detector technology. The quality of measurements is a sensitive function of active technology used. Thus gas detectors have lower precision for calorimetric measurements than liquid or solid scintillators and are more susceptible to tails in distributions due to delta rays, neutron recoils, etc. On the other hand, they can generally provide better spatial resolution. Our goal is to have the same quality of measurements for both hadronic showers and muons in both detectors. It would probably be impossible to achieve this with different technologies in the near and far detectors.

Granularity. Calorimetric response improves as the square root of the thickness of the passive material. Thus to achieve similar quality measurements, the same granularity should be used. More important for MINOS, electron identification, especially at low energies, deteriorates as the thickness of absorber plates is increased.

Material. One of the most precise and systematics-free measurements MINOS can make is the comparison of NC/CC ratios in the near and far detectors. At low energies, the measured energy of the hadronic system can be affected by interactions of boilloff neutrons

from the target nucleus. Thus those targets should be the same in both detectors. In addition, electron/hadron rejection depends on the ratio of the absorption length/radiation length, i.e., roughly A/Z^2 . This again argues for similar material.

B field. The precision attainable in a $\Delta p/p$ measurement, if the measurement is made by curvature, scales linearly with B. Thus it is important that the average field seen by the muons from neutrino interactions be the same in both detectors.

On the other hand, we feel that some compromises can be made in the following:

Overall size. There are no limitations on the quality of our experiment due to rate in the near detector. From this point of view the near detector can be quite small in comparison with the far detector. Very roughly, the transverse size is determined mainly by the requirement that the events of interest (i.e., the ones used for near/far comparison), which we have usually taken to be those within 25 cm radius of the beam line, have a significant amount of material around them so that leakage of muons or parts of hadronic showers are not important. The length is determined principally by the requirement that $\Delta p/p$ for muons be similar to that in the far detector. Thus the precision of curvature measurements should be similar in both detectors. The exact parameters will constitute a compromise between cost and similarity, and need to be determined by extensive Monte Carlo calculations.

Pattern of B field. At the present time, two different configurations are being considered for the near detector: a steel H magnet dipole configuration, as discussed in the proposal, and an octagon (like the far detector), reduced in size and offset from the center of the beam line so that the principal part of the beam does not go through the hole. The main argument for the octagonal toroidal geometry is that the field is focusing everywhere, whereas for the H magnet configuration the focusing is only in one plane. Again, extensive Monte Carlo calculations are needed to determine the amount of muon leakage and average $\Delta p/p$ accuracy for the two configurations. If satisfactory results are obtained for these two effects in the H magnet, then this configuration would be considered acceptable.

7.6 NuMI beam design and location of the MINOS near hall

The MINOS near hall is the underground cavern on the Fermilab site which will house the MINOS near detector (used to compare neutrino interaction characteristics there with those in the far detector), the monitor detector and, a fraction of the Soudan 2 detector, if it is decided to move part of it to the Fermilab site. These detectors are discussed in Section 7.5 below. One of the basic questions that must be answered to determine the hall's location is: What is the tradeoff between the increased cost of going further downstream to a deeper hall, separate from COSMOS, and the improved understanding of systematics resulting from this more distant location?

Unfortunately, there are no simple answers to these two questions. The answers are closely intertwined with the issues of neutrino beam simulations, active detector technology choice, beam extraction technique, and the civil construction method employed and its costs. Below we enumerate and discuss the issues that are relevant to this choice and define the work necessary to obtain all the required information.

We take it as given that the COSMOS detector will be located in a cavern some 200-250 m behind the hadron dump. The MINOS near detector could be located at that location or

further downstream; about 500 m from the hadron dump is a reasonable distance to consider. There are a number of advantages for the MINOS near detectors to be in a separate cavern further downstream. Very briefly they are:

- a) Near/far beam differences will be smaller. This statement needs to be quantified and the results of these beam calculations applied to specific oscillation tests. We see this as the major thrust of our beam simulation work during the next six months. The results will provide essential input to the location question.
- b) The rate at the near detector will be lower. Here one can gain more than the simple $1/r^2$ falloff of the neutrino flux. Since no extra shielding is needed between the COSMOS and MINOS halls, sufficient empty space could be provided in front of the MINOS detectors to reduce the rate of muons and neutrons into the detector from the neutrinos interacting in the dolomite upstream. The relative importance of this factor depends critically both on the choice of the active detector technology and on the beam spill structure.
- c) In this configuration one effectively samples the distribution of the neutrino flux at two different locations: by the COSMOS detector at 250 m and by the MINOS monitor detector at a location further downstream. At this time we do not have a quantitative understanding of the importance of this additional measurement. Again, understanding this *via* simulations will be an important focus of our work during the next six months.

On the other side of the ledger is the cost. The current plans call for one and only one access shaft, independent of the detector hall configuration. Since the additional access shaft was a major contributor to the larger cost of the two-cavern scheme in the early preliminary cost estimates, there are now grounds for optimism that the two-cavern scenario will not increase the cost significantly. Quantitative answers to these questions should be known in a few months.

We can summarize briefly our conclusions based on the discussion above. On a scale of six months we hope to have answers to several important questions:

- a) The result of simulations showing whether a significant benefit is obtained by going to a distance of 500 m or more downstream of the dump,
- b) The costs of different scenarios (one or two caverns) and the differential cost increase of moving the MINOS hall a further unit distance downstream,
- c) The feasibility of the “ping” beam extraction scheme (see Section 7.3.2) and, possibly,
- d) Some information about optimum active detector technology, even though a definite choice on that time scale seems unlikely.

It is our firm intention to make the decision on the location of the MINOS near hall on a time scale that will not compromise the timing of the NuMI civil construction bid package.

8 Experiment Optimization Planning at Lutsen

8.1 Introduction

In early June 1996 the MINOS Collaboration held a week-long workshop at a resort in Lutsen, Minnesota. The originally-planned goal of the workshop was to consider how the design of the MINOS experiment should be optimized to provide the greatest sensitivity to neutrino oscillations. Such a global view of the experiment had not been systematically considered since late 1994 when the design of the “reference detector” was frozen to allow work on the MINOS Proposal to proceed. Since that time, the detailed designs of the reference detector, instrumented with three alternative active detector technologies, and of the NuMI neutrino beam, have been explored and optimized. All of this work has shown the conceptual design of the MINOS experiment, which was described in the Proposal, to be quite powerful and flexible. The sensitivity to neutrino oscillations is likely to be excellent, and no serious technical difficulties have been encountered. After more detailed engineering work, the cost estimate given in the Proposal still seems to be valid.

Nevertheless, it seems worthwhile to stand back from our preoccupation with detailed design issues and to take a broader view of the experimental design while there is still time to make major changes. Although the discussions of the MINOS R&D program, related to the preparation of the present document, did divert some attention from the initial purpose of the workshop, a number of useful insights about the optimization of the experiment did emerge from the Lutsen meeting. The following Sections of this Chapter, written by Lutsen working group leaders, describe the Collaboration’s plan for optimizing the design of the experiment for the four oscillation tests which are potentially the most powerful.

8.2 Optimization for NC/CC and near-far tests

8.2.1 Optimization for the NC/CC test

The calculation of the NC/CC ratio was the test that has been examined in the most detail in the MINOS Proposal and during the HEPAP Subpanel review of MINOS [1, 4, 5]. To perform this test, we measure the number of charged current (CC) and neutral current (NC) events in the far detector by separating contained-vertex events based on their length. We then form the ratio

$$T^{far} = CC/(NC + CC). \quad (4)$$

(Note that the measurement of T is statistically identical to the measurement of $R=NC/CC$.) A signal for neutrino oscillations is then a difference between T^{far} and $T^{far-expected}(T^{near})$ which is calculated by measuring T in the near detector and then correcting for any near/far differences due to the beam or detector acceptances. An interesting signal would be larger than the (two year) statistical error, $\delta T = 0.0020$ and larger than the latest estimate of the systematic error, $\delta T = 0.0008$.

These studies have suggested several constraints on the designs of the far detector, of the beam and of the near detector:

1. Design considerations for the far detector:

- Large mass,
- High acceptance for CC events,
- Well understood acceptance for CC events,
- High trigger efficiency for low energy NC events,
- Well understood trigger efficiency for low energy NC events,
- Cost.

2. Design considerations for the beam:

- Large ν flux above ν_τ CC threshold,
- Alignment of the focusing elements and decay pipe,
- Stability of the neutrino yields over time,
- Uncertainties in models for the secondary particle yields before the target,
- Ability to accurately simulate the focusing devices,
- Uncertainties in the contributions from decays of hadrons produced downstream of the target (scraping),
- Cost.

3. Design considerations for the near detector:

- Size,
- Similarity of acceptance to the far detector,
- Location,
- Cost.

These design criteria for the far detector have been considered in the reference design and are also being considered in alternative detector designs. Preliminary design optimization of the beam has been described previously [36]. Over the last six months, beam design work has focused on including a variety of secondary effects, including neutrinos generated by hadron-beam “scraping”. The near detector design is discussed in Section 7.5. The reference design (as described in the MINOS Proposal) satisfies the criteria listed above. Based on our present level of understanding of the beam and detectors, we believe that, in a two year WBB run, the systematic errors on the T test will be smaller than the statistical errors. Additional studies are now underway to check this preliminary conclusion:

1. Near detector design

Previous T-test results have relied on the expectation that the near detector can be designed to have an acceptance for NC and CC events which is the same as for the far detector. This is a reasonable expectation due to a combination of three factors: the planar design of the experiment, the fiducial volume cuts at the far detector, and

the small transverse area of primary interest for the near detector. However, for a variety of reasons, the acceptances will not be identical. For example, it would be undesirable to have the hole in the toroid at the center of the near detector. Thus, other magnetic field configurations are being considered which will have implications on the acceptance. It is the uncertainties in the acceptance, not the differences *per se*, which will lead to additional systematic errors. As progress is made in near detector design, these uncertainties are being analyzed, minimized and folded into the systematic error.

2. Beam scraping

Hadron production at locations other than the primary target will lead to decay neutrinos which have not been previously considered in the beam simulations. This will lead to additional low energy neutrinos in both the near and far detectors. The collaboration is in the process of developing a GEANT-based beam Monte Carlo to take these decays into account. In general, secondary particles produced near the target or the focusing system will not lead to additional near/far differences, but particles produced near the hadron beam dump will. In addition, scraping will affect the $\nu_\mu/\bar{\nu}_\mu$ ratio in the near detector. Additional studies are now underway to determine if the uncertainties due to unexpected sources of scraping will be within present estimates of systematic error.

3. Secondary particle yields

The original, very conservative, estimate of uncertainty due to near/far beam differences was based on setting the uncertainty equal to the full effect caused by those differences [1]. Detailed study of the sources of those differences concluded that the largest effects arose from straightforward kinematics, which could be reliably calculated, and that only about 1/4 of the difference was uncertain, based on the secondary particle yields from the target [5]. This remaining uncertainty can be reduced further by using information from the radial distribution of the beam at the near detector and by using independent measurements on particle yields from the target. Both of these studies are proceeding, but given the level of systematic error remaining, they have greater implications for tests other than the T test.

4. Near detector location

We are now considering locations for the near detector which are farther downstream than the COSMOS hall. The primary motivation is to reduce near/far differences. Moving the near detector downstream makes the neutrino source more closely resemble the point source seen by the far detector. On the other hand, the ability to measure the radial distribution of the ν beam, which is an important constraint on reducing uncertainties arising from secondary particle yields, would be poorer. These tradeoffs are being actively studied together with civil-construction and financial constraints as well as the possible utilization of information from COSMOS on the radial distribution closer to the beam source.

8.2.2 Optimization for the near/far test

Measurement of the relative rates of charged current events in the near and far detectors provides a test for neutrino oscillations which is independent of the T test. However, the same factors contribute to the systematic errors, although in different ways. Our previous estimates of the systematic error on the near/far test have varied between 0.5% and 4.0%.

At the Lutsen meeting, the NC/CC and near/far working group identified the contributions to the systematic error for the near/far rate test. These included uncertainties in detector mass, acceptance and efficiencies, as well as contributions from the beam due to scraping, misalignment and uncertainties in horn currents and secondary particle yields. The group is hopeful that systematic errors will be at the low end of previous estimates. In the next few months, the Collaboration plans to put the systematic error estimates for the near/far test on the same footing as has been done previously for the T test.

8.3 Optimization for CC event energy measurement

The measurement of the energy spectrum of ν_μ charged current events is one of the most important aspects of the MINOS experiment. A clean sample of ν_μ CC events is easy to select by a cut on event length; the visible energy of a ν_μ CC event is a good measure of the energy of the interacting ν_μ , *i.e.* $E_\nu = E_{\text{vis}} = E_{\text{had}} + E_\mu$.

Use of the simple relationship between the observed and expected interaction rates as a function of E_ν :

$$\left. \frac{dn}{dE_\nu} \right|_{\text{obs}} = P_{\mu\mu}(\Delta m^2, \sin^2(2\theta)) \times \left. \frac{dn}{dE_\nu} \right|_{\text{exp}} \quad (5)$$

(where

$$P_{\mu\mu}(\Delta m^2, \sin^2(2\theta)) = 1 - \sin^2(2\theta) \sin^2(1.27\Delta m^2 L/E_\nu) \quad (6)$$

for two-flavor mixing⁴) allows a test for oscillations to be made which is independent of the mode of oscillation ($\nu_\mu \rightarrow \nu_\tau$, $\nu_\mu \rightarrow \nu_e$ or $\nu_\mu \rightarrow \nu_{\text{sterile}}$) and the normalization of the exposure of the detector [37]. As discussed in Section 6.6.1, if neutrino oscillations are convincingly detected, Δm^2 and $\sin^2(2\theta)$ can be measured by fitting $P_{\mu\mu}$ according to Equation 5.

There are two important criteria which must be satisfied before Equation 5 can be used for either the test for oscillations or a measurement of Δm^2 . The first is that the error on $dn/dE_\nu|_{\text{exp}}$ be acceptably small, the second is that E_{vis} be a sufficiently good approximation to E_ν . The expected interaction rate spectrum, $dn/dE_\nu|_{\text{exp}}$ and its error, will be predicted from a combination of beam calculations and measurements made in the near detector and beam monitors.

The accuracy of the approximation that $E_{\text{vis}} = E_\nu$ will depend upon the details of the construction of the detector and, to some extent, the active detector technology. For any ν_μ CC event, $E_{\text{vis}} = E_{\text{had}} + E_\mu$, where E_{had} will be measured calorimetrically and E_μ will either be measured by range for muons that stop in the detector, or by curvature for muons which leave the detector. The specific *detector* design issues which were studied at Lutsen were therefore:

⁴The generalization of $P_{\mu\mu}$ to three-flavor mixing is discussed in Section 6.6.

1. What is the influence of the hadronic energy resolution of the detector on the *highest* value of Δm^2 that can be measured, where the resolution of the detector integrates the observed E_ν distribution over the oscillation minima?

The effect of a finite energy resolution is expected to be important only for $\Delta m^2 > 0.1 \text{ eV}^2$.

2. What is the influence of the longitudinal granularity of the detector and the active detector technology on hadronic energy resolution?

Conventionally, hadronic energy resolution is understood to be determined by fluctuations inherent in hadronic showers and therefore is rather insensitive to the construction of a calorimeter; calorimeters with gaseous detectors for sampling the shower generally show a worse energy resolution (by a factor of ~ 1.5) than those using solid or liquid detectors. Detailed comparison between realistic detector simulations and test beam runs must be made to confirm whether or not this is the case and to establish the hadronic energy resolution of the detector.

3. Which factors influence the hadronic energy calibration, and stability of this calibration, of the detector?

It may, for example, prove necessary to weigh each steel plane in order to achieve a calibration accuracy of a few percent. Active detector inefficiencies will also need to be controlled to this level.

4. What is the influence of the granularity of the detector on the measurement of E_μ ?

The energy of the muon should always be well measured (to $\sim 6\%$) if the muon stops in the detector. For muons which leave the detector, the transverse granularity must be sufficiently fine that the E_μ resolution is dominated by multiple scattering, rather than quantization errors of the hits along the track. It may be necessary to deliberately stagger detector planes by a fraction of the readout strip width to reduce the quantization error.

5. How uniform must the magnetic field be?

If the detector is magnetized, the magnetic field must be known, stable and accurately reproducible so that $\int B \cdot dl$ is known to better than a few percent over the length of the muon track.

6. Is it necessary to magnetize the detector?

If it is decided to run with an off-axis beam or a low energy NBB the ν_μ energies are substantially lower than for an on-axis WBB. The muon energies will also, therefore, be substantially lower and a greater fraction of the muons will stop in the detector. A sufficiently high acceptance for fully measured ν_μ CC events may therefore be achievable *without* magnetizing the detector. This would simplify the construction.

Similarly, it is possible that a positive indication of neutrino oscillations will be forthcoming from the CHOOZ reactor experiment within one or two years. If this is the case, then the interesting range of Δm^2 will be in the region of a few $\times 10^{-3} \text{ eV}^2$. As

discussed in Section 6.6 measurements from MINOS would be entirely complementary to such a result although the emphasis would be in the small Δm^2 region, implying the use of lower end (5 to 10 GeV) of the neutrino energy spectrum. In this case a large fraction of the events of interest could be fully measured by muon range alone.

The working group at Lutsen had fruitful and wide ranging discussions. It concluded that significant progress had been made in quantifying near-far beam differences and set the goal of predicting the uncertainty on the expected neutrino flux, as a function of E_ν , at the far detector once the potential information from measurements made in the near detector had been fed back into the flux calculation.

The group concluded that the most important aspect of the detector to be optimized was the calibration of the energy scales. An accuracy of better than 5% on the hadronic energy scale is unlikely to be achieved and therefore there is a premium on the accuracy of the P_μ measurements. The goal of 1% systematic error on p_μ from both range and curvature measurements was specified. This translates into the requirement that $\int Bdl$, over a path length of several meters, can be known to a similar accuracy for a reconstructed muon track. (This information was passed on to the Steel Working Group at Lutsen.)

The working group expressed some concern that the planned 8 m length of the near detector was somewhat too short to cross calibrate muon momentum measurements using range or curvature and felt that further studies are required.

There was little discussion of the possibilities for a non-magnetized detector. The ability to distinguish ν_μ and $\bar{\nu}_\mu$ interactions in a magnetized detector was felt to give a useful additional constraint on the flux calculations.

8.4 Optimization for electron identification

While MINOS has focused on the possibility of $\nu_\mu \rightarrow \nu_\tau$ oscillations, the classic paradigm for neutrino oscillations is the transformation between ν_e and ν_μ . This notion, which predates the discovery of the τ lepton, has been motivated by solar neutrino experiments. Regardless of the eventual explanation of the solar puzzle, exploring this classic oscillation picture is a central goal of MINOS.

For MINOS, this means the observation of an electron from an interaction in the far detector of a neutrino which began life at Fermilab with muon flavor. Most electrons produced by charged-current ν_e interactions from $\nu_\mu \rightarrow \nu_e$ oscillations will have the full beam energy and are easy to measure, even in the coarse-grained MINOS reference detector. In the MINOS proposal, electron identification by longitudinal cuts was the most powerful test for $\nu_\mu \rightarrow \nu_e$ oscillations. This method has subsequently been used by the similarly coarse-grained CCFR experiment to set limits on $\nu_\mu \rightarrow \nu_e$ oscillations using a WBB at Fermilab [38]. Low energy electrons produced by ν_τ interactions are more difficult; this topic is discussed in Section 8.5 below.

To optimize the detector for electron detection we use several criteria: electron energy and angular resolutions as functions of energy and angle; rejection of hadronic backgrounds; and shower profile distributions. Some specific detector design considerations which will be studied during Summer 1996 with the complete GEANT-based simulation are:

- **Steel thickness**

The thickness of the steel will be varied from 2 cm to 4 cm to determine the effects of longitudinal segmentation. We will also study the impact of replacing the steel in the front 10 m of the far detector by Pb, with a thickness of 0.5 cm and 1.0 cm.

- **Transverse granularity**

We will study the use of square liquid scintillator cells, with widths of 1 cm, 2 cm and 4 cm. The reference detector Iarocci chamber response used corresponds to the description given in Section 4.2 of this document.

In both cases, the benefits of added granularity will be balanced by the higher cost per plane and thus fewer planes (for a fixed total cost) for the MINOS far detector. In addition to facilitating the study of ν_e charged current interactions, the ability to identify and analyze electron energies and angles plays a central role in the observation of τ production and decay through those decay channels containing an electron.

8.5 Optimization for explicit τ identification

The MINOS Collaboration continues to expect that the best opportunities for explicit signatures of ν_τ CC interactions will rely on statistical measurements based on kinematic properties of the final state. Previous studies have shown that, although events resulting from quasi-elastic interactions are relatively few compared to those from DIS, the ease of reconstruction of the simpler quasi-elastic events and the resolution on angle and energy of hadrons in DIS events mean that quasi-elastic events provide the best opportunities for explicit τ appearance signatures. The relevant kinematic properties of ν_τ CC events are missing transverse momentum, using either the WBB or the NBB and missing total momentum using the NBB, due to the fact that τ decays produce neutrinos. A somewhat different signature that may be available for τ appearance involves events with just a single charged pion of relatively high energy. The demands on the detector design and resolution vary depending on the particular τ decay channel, the features of the neutrino beam and the required reach in oscillation probability.

Using a detector with approximately the features of the MINOS reference detector, we anticipate that the best explicit τ appearance signatures will rely on use of the NBB and will be based on quasi-elastic interactions with the τ decaying to either a muon or an electron. Muons are the easiest particles to identify and are well measured in the reference detector, so events where virtually the only particle in the final state is a muon permit a particularly clean measurement of the event kinematics. As discussed in the MINOS Proposal, NBB events with little activity other than a muon will give a clear τ appearance signature for larger oscillation parameters. Some key issues which require further work are the elimination of a low-energy tail in the neutrino beam and understanding/reducing backgrounds arising from the low probability of relatively high-energy hadronic showers giving little or no response in the detector.

Although electrons are more difficult to identify and measure precisely than muons, the low intrinsic ν_e content of the beam means that events with τ decaying to e may offer the best opportunity for pushing τ appearance signatures to lower mixing probability. The

issues which must be understood in order to accomplish this are the probability of π^0 's being mistakenly identified as electrons, the intrinsic ν_e fraction and energy distribution in the beam (arising from decays of K's and μ 's) and the ability to use kinematic criteria to distinguish electrons produced by ν_e interactions from those produced by τ decays. Of particular relevance will be the longitudinal and transverse sampling of the detector and the effect of the active detector technology on fluctuations in the measurement of electromagnetic showers.

The production of a single, high-energy charged pion is more likely in τ decay (12% branching fraction) than in NC interactions. In addition, due to the τ mass these pions may be produced at relatively large angle compared to those coming from NC interactions. The key to identification of such events is to have a sufficient number of measurements of the pion track in the detector prior to its interaction so that it is clear that only a single particle (other than a nucleon) was produced at the primary vertex. Following the single track, the pion will interact and the energy will be measured by calorimetry. If the single track is sufficiently long, the momentum might even be measured magnetically. Since the interaction length for pions in iron is 17 cm, a typical pion will traverse 3-4 planes of the reference detector prior to interaction. This length seems marginal for identification purposes. We expect that 2 cm iron would be a significant advantage in this channel. One advantage of this signature is that it may be available using the WBB. The other signature using the WBB is the total hadronic energy distribution, but this is a more subtle and less direct signature.

In the MINOS proposal, an analysis using the Soudan 2 detector was described in which quasi-elastic events with ν_τ interactions can be identified by missing transverse momentum from measuring the muon coming from τ decay and the recoiling proton from the struck nucleus. The very-fine granularity of the Soudan 2 detector makes the clear observation of the proton possible. However, we expect that this signature is possible using thicker sampling than in Soudan 2 and we plan to study the tradeoff in absorber thickness versus detector mass (for fixed cost) using this signature. It is our anticipation that even 2 cm thick steel is probably too thick for this signature but that 1 cm thick steel may give a good signature.

All three Letters of Intent to the Gran Sasso Laboratory for long-baseline experiments using a beam from CERN (ICARUS, NOE and RICH) have stressed quasi-elastic ν_τ interactions with the τ decaying to e as their primary goal for study of neutrino oscillations. We have considered the claims made by these experiments with respect to applicability to MINOS and whether potential backgrounds and efficiencies have been considered sufficiently. It is our belief that emphasis of this signature as the primary goal of an experiment does not offer the best overall optimization of a detector for oscillation measurements. The reason for this follows from a simple calculation of the number of events available for this signature:

$$N_\tau = N_\mu \times P_{osc} \times \frac{\sigma_\tau}{\sigma_\mu} \times B.F. \times \frac{QE}{total} \times F \times M \times \epsilon, \quad (7)$$

where N_τ is the number of "identified" τ events, N_μ is the number of CC ν_μ interactions per kT in a given running period, P_{osc} is the probability that a ν_μ has oscillated into a ν_τ , σ_τ/σ_μ is the ratio of cross sections for ν_τ and ν_μ interactions averaged over the energies in the neutrino beam, $B.F.$ is the branching fraction of τ 's into the observation channel, $QE/total$ is the fraction of events which are effectively quasi-elastic, F is the fraction of the total mass which is the fiducial region, M is the total mass in kT and ϵ is the efficiency

for experimentally identifying the observation channel given the cuts necessary to eliminate significant backgrounds. Expected values for these quantities are:

- $N_\mu = 2500$ events/kT/year
- $\frac{\sigma_\tau}{\sigma_\mu} = 0.2$
- $B.F. = 0.18$ for τ decays to e
- $\frac{QE}{total} = 1/3$ for ν_τ with above σ
- $F = 0.7$
- $\epsilon = 0.7$ (probably lower).

Given these values, the expected rate of “identified” τ events for $P_{osc} = 1$ will be:

$$N_\tau = 15 \text{ events/kT/year}, \quad (8)$$

corresponding to about 300 events for a 10 kT detector running for two years. If we take 10 events with no background as the minimum necessary for a discovery, then the discovery potential in oscillation probability is just the ratio of that number of events divided by the expected number of identified events giving:

$$P_{osc} = 0.7/M/t, \quad (9)$$

where t is the running time in years. Hence, for a run of two years and mass of 600 T (relevant to ICARUS) the discovery potential would be $P_{osc} = 0.58$, for 4 kT (NOE) it would be $P_{osc} = 0.09$, for 10 kT (MINOS) it would be $P_{osc} = 0.04$ and for 25 kT (RICH) it would be $P_{osc} = 0.014$. Of course, 10 events is fewer than LSND currently has for their oscillation signature, and the assumption of no background is probably too optimistic. Our conclusion is that although such signatures may be attractive, they make sense only with very large mass detectors such as the proposed RICH detector at the Gran Sasso. However, we believe that such a detector will be significantly more expensive than presently advertised once the costing is done carefully and that it doesn't permit the same reach and features as the MINOS reference design. Hence, although one might consider such a detector as an eventual upgrade for a specific oscillation goal, it does not make sense to supplant any fraction of our current reference detector for this signature.

Our conclusions are that the granularity and mass of the current reference detector for MINOS are close to a best compromise between reach in oscillation sensitivity and τ appearance signatures. However, it is possible that thinner steel (2 cm rather than 4 cm) could offer some distinct advantages for τ appearance signatures. Since these signatures have sensitivities which are linear with the number of events, MINOS will not be able to exploit these advantages if the detector's mass is significantly reduced from the reference design. We will have quantitative answers to these optimization questions based on complete GEANT simulations of each of these τ signatures for the August 1996 MINOS collaboration meeting.

9 Soudan Site Preparation

9.1 Update on recent developments

The MINOS far detector site was described in detail in the February 1995 MINOS Proposal [1]. That document also outlined our plan for the excavation and outfitting of the new underground cavern for MINOS at Soudan. We have considerable confidence in this plan because MINOS collaborators at the University of Minnesota were also responsible for managing the excavation and outfitting of the Soudan 2 underground laboratory in 1984-1986. The site preparation plan described in the MINOS Proposal is still valid, although we have made some minor changes to the cavern design, cost estimate, and schedule. We have also begun initial preparations for the excavation, which is now planned to begin in the spring of 1998.

Some recent developments include:

- We have developed a conceptual design for the cavern based on a detailed installation plan for the MINOS reference detector. The laboratory length has been increased from 75 m to 90 m to provide a larger installation staging area, and the cross sectional area of the wide interconnecting tunnel to the existing Soudan 2 cavern has been minimized to reduce costs.
- A test bore hole has been drilled down the long axis of the proposed new cavern location and the rock cores have been analyzed. The engineer's report shows favorable geological conditions for the new laboratory.
- A plan has been developed to cut shaft hoisting costs drastically during the excavation and installation period. This involves automating hoist operation so that fewer hoist operators are required. State of Minnesota funds have been requested to pay for this hoist upgrade (see below).
- Work on the Environmental Assessment Worksheet (EAW) is progressing well. The University of Minnesota, which will manage the site preparation work, has begun discussions with the State of Minnesota Environmental Quality Board. Assuming State approval of the EAW, the University will use the EAW to help satisfy requirements of the National Environmental Protection Act (NEPA) and of the National Historical Site review.
- Only five areas of the EAW were identified which needed further work:
 1. Soudan mine bat population. A survey performed in March 1996 has satisfied concerns that threatened or endangered bat species might be disturbed by excavation work. Only common species were found.
 2. Control of sedimentation in waste water pumped from the mine during excavation.
 3. Water runoff from the pile of rock removed from the new cavern.
 4. Ionizing radiation from NuMI neutrino beam interactions.
 5. Disturbance of the Soudan Mine National Historic Site.

The last four issues are expected to be addressed in a routine fashion and should not delay the schedule or increase the cost of the excavation.

- The National Science Foundation Science and Technology Center for Astroparticle Physics at the University of California, Berkeley is considering the installation of a new apparatus at Soudan to search for dark matter. The dark matter search is about a \$2 million project (capital and operating funds) and would be supported by the NSF, the DOE, the University of California and Stanford.

9.2 Schedule and cost issues

The NuMI neutrino beam will be turned on for the first time in the summer of 2001. We plan to complete the preparation of the MINOS underground laboratory at Soudan in time to install the first third of the 10-kton far detector by that time. To accomplish this, excavation work must start in the spring of 1998. Excavation work should not begin during the winter months to avoid disturbing the hibernating bat population. As long as blasting is in progress when the bats begin hibernation, they will chose locations well away from the construction area.

After 18 months of excavation and 6 months for installation of utilities, the new underground laboratory would be ready for detector installation in the spring of 2000. The first third of the detector would be ready to operate at beam turn-on time, and the remainder of the MINOS detector would be completed in the spring of 2003. We now estimate the total detector installation period to be three years, which is somewhat longer than the 2.2 year period given in the MINOS proposal. This is based on detailed planning of the installation process, which requires one of the 600 reference-detector planes to be installed each working day. To meet this schedule, five assembly stations for the steel and detector planes will operate in parallel, requiring a longer cavern than that described in the MINOS Proposal.

This schedule requires that a construction bid package be prepared during FY 1996 and FY 1997, so that a contract can be awarded in the fall of 1997 (early FY 1998). Initial preparations for work on the bid package has already begun using \$100K of University of Minnesota funds and \$13K of (FY 1995) Fermilab funds. These funds were used for initial engineering design work and for the test bore hole along the axis of the proposed cavern location. An additional \$50K to support this work is being supplied by Fermilab in FY 1996, and we are requesting \$150K from Fermilab in FY 1997. Initial engineering work will concentrate on the civil engineering, with less time-critical electrical and mechanical engineering being deferred until 1997.

Negotiations for additional State funds to support this work are already quite advanced. The University of Minnesota has requested \$500K from the State Legislative Commission on Minnesota Resources. Responses to a presentation to the Commission were quite positive. These funds would be used to enhance public access to MINOS for educational purposes (\$100K) and to automate the Soudan mine hoist controls (\$400K), as described above. Any funds provided would be available in July 1997.

University of Minnesota personnel have also been well received during initial discussions with representatives of the Iron Range Resources and Rehabilitation Board (IRRRB) about a possible grant of \$250K to support MINOS site preparation engineering work. Represen-

tatives from St. Louis County, Minnesota Power and the Township of Breitung (in which Soudan is located) have all expressed interest and support for the project. The University has been a good neighbor in Soudan during the past 15 years of work on the Soudan 2 project and we hope to receive considerable support for this project from a variety of Iron Range interests.

There is a very real possibility that we will be able to secure significant State of Minnesota support for MINOS. However, this is likely to be a “boot-strap” process during which we must provide hard evidence that the project has firm financial support from the DOE and Fermilab. The evidence must be provided on a time scale consistent with the start of excavation work at Soudan in the spring of 1998.

We plan to propose a \$3M State contribution, conditional dollar-for-dollar on the availability of external funds (U.S. government, foreign government or other non-State, non-University funds). The State will likely require that all State and matching funds be expended in Minnesota. Over the extended construction period of the MINOS experiment there will be no difficulty in matching the requested State funds. The critical period will be in the initial stages of the project because the excavation work must be completed before the expenditure of installation funds can begin. Since the total cost of the excavation work will require the proposed \$3M State contribution to be supplemented by more than \$2M in other funds, we expect that a firm commitment of these non-State funds must be made during FY 1998 in order for the excavation contract to be signed in late 1997. Most of this \$2M “pledge” would not actually be spent in FY 1998, but some solid assurance must be provided to the University of Minnesota in order for the work to proceed.

Table 26 summarizes the site-related supplemental costs described in this Chapter.

Activity	\$K
FY 1995:	
Initial cavern design, cost estimate (Allocated by Fermilab)	13
FY 1996:	
Conceptual design engineering (Allocated by Fermilab)	50
FY 1997:	
Excavation bid-package engineering (Requested from Fermilab)	150
FY 1998:	
Excavation contract “pledge” (Actual expenditures spread over FY98 and FY99)	2,000

Table 26: Summary of supplemental site-related costs for FY 1995 (in FY 1995 dollars) and FY 1996-8 (in FY 1996 dollars).

10 Cost Estimates and Schedules

10.1 Summary of FY 1996-1998 funding requirements

Table 27 contains a summary of the supplemental funding needs which have been presented in detail elsewhere in this document. The total funding required for the full MINOS R&D program, for FY 1995-98, is \$2.753M. This total includes the \$105K received in FY 1995, \$213K for Soudan site design work, and \$280K for simulations postdoc positions. The current total is comparable to the total R&D cost estimate of \$2.732M (in FY 1995 dollars) which was presented to the Lehman Subcommittee in June 1995 [3]. (The Ref. [3] R&D cost did not include the site design funds, which were covered under the Soudan Hall Preparation cost estimate.)

The total construction funding required in FY 1998 is \$3.324M, which is substantially less than the \$4.455M total FY 1998 construction funds in Ref. [3]. This difference is mainly due to the \$1.124M in estimated foreign contributions which are included in the current FY 1998 budget. Note that the FY 1998 construction cost for Near Detector Systems (\$164K for design engineering work) has no associated R&D cost, and is therefore not described elsewhere in this document.

10.2 Updated MINOS cost estimate

Table 28 shows a summary of the current cost estimate for the MINOS experiment. This Table includes several changes to the previous MINOS cost estimate, given in Ref. [3] and presented to the Lehman Subcommittee of the HEPAP Subpanel in June 1995:

- The WBS organization has been modified so that each Level 2 task can be effectively supervised by a single Level 2 Manager.
- All costs have been escalated to FY 1996 dollars.
- The contingency for the steel cost has been increased (Lehman Subcommittee recommendation).
- The far detector installation time has been increased (Lehman Subcommittee recommendation).
- The EDIA estimate for Far Detector Systems has been increased (Lehman Subcommittee recommendation).
- The EDIA estimate for Near Detector Systems has been increased (Lehman Subcommittee recommendation).
- The engineering cost estimate for Electronics has been increased (Lehman Subcommittee recommendation).

The cost estimates given in Table 28 are still preliminary, and will continue to be updated as the design of the experiment becomes more detailed and as more reliable component costs

Activity	FY95	FY96	FY97	FY98
R&D funds:				
Iarocci	15	57	333	0
RPC's	25	28	259	0
Scintillator	22	28	380	0
Test beams	0	5	60	180
Electronics	12	0	150	100
Steel, magnet	26	60	513	0
Simulations	5	27	255	0
Soudan site design	13	50	150	0
Construction funds:				
Far detector systems	0	0	0	493
Near detector systems	0	0	0	164
Far detector structures	0	0	0	292
Near detector structures	0	0	0	173
Active detector factories	0	0	0	2054
Russian contributions	0	0	0	-279
Chinese contributions	0	0	0	-279
Electronics engineering	0	0	0	1272
UK contributions	0	0	0	-566
Total costs	118	255	2100	3604

Table 27: Summary of MINOS supplemental R&D and construction costs for FY 1995 (in FY 1995 dollars) and FY 1996-8 (in FY 1996 dollars). FY 1998 construction cost estimates assume the reference detector technology.

become available. This cost estimate assumes that the “Reference Detector” technologies are used for the active detector elements, as described in Chapter 4, and for the steel plane fabrication, as described in Chapter 5. The overall cost of the MINOS detector will be constrained to be less than or equal to the Lehman Subcommittee estimate [6] of \$50.722M in FY 1995 dollars (for example, by adjusting the mass of the far detector). Not included in this total detector cost estimate are the Lehman Subcommittee estimates for WBS 1.1 (Soudan hall preparation at \$5.555M), WBS 1.8 (Detector R&D program at \$2.732M), or WBS 1.9 (Soudan 2 Near Detector at \$1.163M).

Contributions from overseas collaborators are shown as a separate line in Table 28. The cost estimates in the main body of the Table assume that all construction work is performed in the U.S. We estimate that value-equivalent contributions from collaborators in the U.K., Russia, and China will total \$1.1M in FY 1998 and approximately \$2M per year for each of the next four years of the construction period.

The revised WBS organization, which is used in the EXCEL spreadsheet record of this cost estimate, is outlined below.

WBS 1.1 Soudan Excavation and Hall Preparation

- Managed by the University of Minnesota.
- The State of Minnesota is being requested to contribute \$3.75M to help pay for the Soudan site excavation costs.
- Level 2 Manager: Marvin Marshak.

WBS 1.2 Far Detector Systems

- Includes steel and detector installation.
- Level 2 Manager: Bill Miller (acting).

WBS 1.3 Near Detector Systems

- This task has no associated R&D costs, and is not described in this document.
- Includes steel and detector installation.
- Level 2 Manager: Jenny Thomas.

WBS 1.4 Far Detector Structures

- Includes steel planes, magnet, support structure.
- Level 2 Manager: Doug Wright (acting).

WBS 1.5 Near Detector Structures

- Includes steel planes, magnet, support structure.
- Level 2 Manager: Doug Wright (acting).

WBS 1.6 Active Detector Elements

- Includes near and far detector chambers (Reference Detector).
- Level 2 Manager: Doug Michael.

WBS 1.7 Electronics

- Includes near and far detector trigger and readout electronics.
- Level 2 Manager: Jonathan Thron (acting).

WBS 1.8 Detector R&D

- Includes R&D for active detectors, electronics, and steel.
- Level 2 Manager: Ken Heller.

WBS 1.9 Soudan 2 Detector

- This task is under Collaboration review, and is not described in this document.
- Includes the Soudan 2 near detector and its electronics.
- Level 2 Manager: Jonathan Thron (acting).

FY	95	96	97	98	99	00	01	02	03	Tot
Activity:										
Far Det Systems	0	0	0	0.5	1.9	2.0	3.1	3.1	2.3	12.9
Near Det Systems	0	0	0	0.1	0.6	1.1	1.3	0	0	3.1
Far Det Struct	0	0	0	0.3	3.0	4.0	4.0	2.9	0	14.2
Near Det Struct	0	0	0	0.2	0.3	0.9	1.2	0	0	2.6
Active Detector	0	0	0	2.0	2.3	3.8	3.8	2.7	0	14.6
Electronics	0	0	0	1.3	1.0	2.3	2.4	1.8	0	8.8
Subtotal	0	0	0	4.4	9.1	14.1	15.8	10.5	2.3	56.2
Foreign Contrib	0	0	0	1.1	2.0	2.0	2.0	2.0	0	9.1
US Construc tot	0	0	0	3.3	7.1	12.1	13.8	8.5	2.3	47.1
Other costs:										
R&D	0.1	0.3	2.1	0.3	0	0	0	0	0	2.8
Soudan hall prep	0	0	0	3.3	1.0	1.6	0	0	0	5.9

Table 28: Summary of the cost estimate and funding profile for the MINOS experiment, excluding NuMI beam and civil construction costs at Fermilab (in millions of FY 1996 dollars).

10.3 Schedule

Figure 11 shows the overall schedule for the design and construction of the NuMI neutrino beam, MINOS far detector, and Soudan site work. Technical Design Reports (TDR's) for the MINOS detector and the NuMI beam technical components are both scheduled for completion in October 1997. Chapter 9 describes the schedule for the near-term Soudan site preparation work in detail.

MINOS Timelines

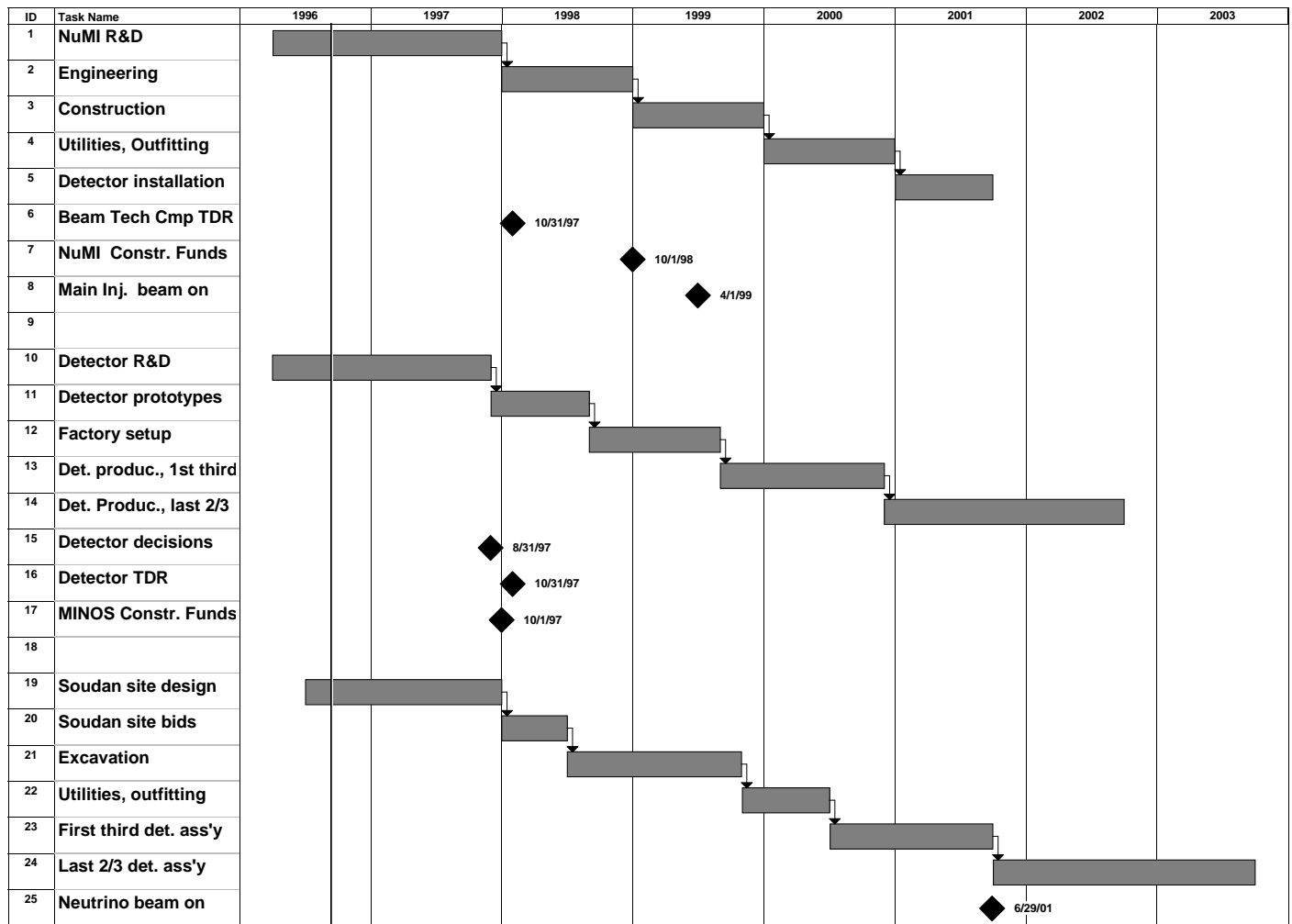


Figure 11: Overall design and construction schedule for the MINOS experiment. The time scale shown is in fiscal years.

11 MINOS Collaboration R&D Effort

11.1 Current collaborator activities

- **Argonne:** Beam, Electronics, Iarocci, Steel/magnet
- **Boston College:** NuMI civil construction
- **Caltech:** RPC's, Test beam
- **Columbia:** Beam, Electronics
- **Dubna:** Iarocci, Simulations
- **Fermilab:** Beam, Near detector, Scintillator, Simulations
- **IHEP-Beijing:** Iarocci, RPC's, Steel
- **Indiana:** Scintillator, Simulations
- **ITEP-Moscow:** Scintillator, Simulations, Test beam calorimeter
- **Lebedev:** Simulations, Test beam calorimeter
- **Livermore:** RPC's, Simulations, Steel/magnet
- **Minnesota:** Soudan site, Scintillator, Simulations, Steel
- **PNPI-St.Petersburg:** Electronics, Iarocci
- **Oak Ridge:** Electronics
- **Oxford:** Electronics, Near detector, Simulations
- **Rutherford:** Electronics, Installation, RPC's, Simulations, Steel
- **Stanford:** Simulations
- **Sussex:** Electronics, Simulations
- **Texas A&M:** Scintillator
- **Texas-Austin:** Scintillator, Simulations
- **Tufts:** Beam, Iarocci, Scintillator, Simulations, Steel/magnet
- **Western Washington:** Installation

Notes on institutional activities:

- Much FY 1996 R&D is being paid for by institutional funds
 - Institutional funds are highly leveraged by supplemental funds
 - Fermilab is supporting Chinese and Russian visitors
- Possible new collaborators – discussions under way
 - Efremov Sci. Res. Inst., St. Petersburg, Russia: Steel
 - ITEP-Moscow: possible expansion of original MINOS group
 - IHEP-Protvino: Neutrino beam, simulations, scintillator
 - Univ. of Melbourne, with other Australian groups: initial discussions
- Possible overseas production of chambers and steel
 - Potential savings from cheap overseas labor costs
 - Extensive Iarocci chamber experience in China, Russia
 - Possible chamber production scenario: US/Russia/China = 1/1/1
 - Russian steel used for several recent US HEP detectors
 - Possible steel production scenario: US/Russia = 1/1
 - Design/production optimization will be different from US:
parallel R&D programs for mass production techniques

11.2 Current MINOS collaborator effort

This Section lists the names and institutional effort levels of all collaboration personnel who are currently (June 1996) working on the MINOS experiment. The names shown below are different from those on the “official” MINOS collaborator list because (1) technical support people who are not on the collaborator list are shown, and (2) only those collaborators who are actively working on MINOS now are included.

Active MINOS collaborators:

- **Argonne:**
I. Ambats, D. Ayres, L. Balka, J. Dawson, T. Fields, M. Goodman, N. Hill, D. Jankowski, E. May, L. Price, P. Schoessow, R. Talaga, K. Thompson, J. Thron, L. Turner
- **Boston College:**
T. Toohig
- **Caltech:**
J. Hanson, D. Michael, L. Mossbarger, A. Silverfarb
- **Columbia:**
W. Choi, A. Gara, Y. Ho, W. Lee, W. Sippach, X. Zhang

- **Dubna:**
G. Alexeev, V. Anosov, V. Brudanin, G. Chelkov, V. Cherpurnov, B. Fialovski, Y. Gornushkin, M. Ignatenko, G. Karpenko, N. Khovansky, Z. Krumstein, V. Malychev, A. Nozdrin, A. Olchevski, I. Pisarev, I. Prokhorov, A. Rozdestvenskiy, T. Rudenko, N. Russakovich, A. Sadovsky, M. Sapozhnikov, Yu. Sedykh, A. Sissakian, L. Tkatchev, V. Tokmenin, V. Tretyak, L. Vertogradov
- **Fermilab:**
R. Bernstein, D. Bogert, D. Cossairt, W. Freeman, J. Hylan, D. Johnson, A. Malensek, P. Martin, G. Mitselmakher, J. Morfin, S. O'Day, A. Para, R. Rameika, A.L. Read, W. Smart, A. Wehmann, J.C. Yun
- **IHEP-Beijing:**
Y. Chen, J. Guo, B. Shen, L. Wang, M. Wang, X. Xia, Y. Xu, W. Yan
- **Indiana:**
R. Hatcher, R. Heinz, L. Miller, S. Mufson
- **ITEP-Moscow:**
A. Arefiev, Y. Jivalov, I. Malutin, V. Mitrofanov, V. Smotriyev, I. Trostin, V. Utkina
- **Lebedev:**
V. Bulatov, V. Ermilova, E. Kuznetsov, B. Lomonosov, G. Merzon, L. Pervov, V. Rybov, V. Tsarev
- **Livermore:**
E. Ables, O. Alford, R. Bionta, O. Fackler, M. Fowler, E. Hartouni, T. Ladran, M. Libkind, H. Olsan, L. Ott, E. Parker, A. Posey, J. Swan, M. Walter, M. Wang, D. Wright
- **Minnesota:**
T. Berg, P. Border, T. Chase, H. Courant, P. Cushman, K. Heller, M. Marshak, D. Maxam, W. Miller, J. Nelson, E. Peterson, K. Ruddick, R. Rusack, M. Schub
- **PNPI-St.Petersburg:**
L. Bakanov, V. Bogdanov, V. Britov, N. Bondar, G. Gavrilov, E. Ivanov, V. Ivochkin, V. Jakutovich, M. Jarmarkin, S. Kovalenko, V. Kozlov, A. Krivshich, I. Parchenko, V. Tarakanov, V. Zhivaev
- **Oak Ridge:**
C. Britton, W. Bryan
- **Oxford:**
S. Berry, J. Cobb, H. Gallagher, G. Harris, C. Hunter, D. Petyt, P. Shield, J. Thomas, R. Wastie, N. West
- **Rutherford:**
G.J. Alner, R. Cotton, R. Edgecock, G. Grayer, P. Litchfield, G. Pearce

- **Stanford:**
G. Irwin, S. Wojcicki
- **Sussex:**
J. Byrne, P. Dawber, K. Green, P. Harris, R. White
- **Texas A&M:**
A. David, M. Drew, R. Webb
- **Texas-Austin:**
K. Lang, M. Proga
- **Tufts:**
T. Kafka, W. Mann, R. Milburn, W. Oliver, J. Schneps
- **Western Washington:**
W.L. Barrett

Table 29 summarizes the current full time equivalent (FTE) effort levels at MINOS collaborating institutions. The “Physicist” category includes physicists, postdocs, computer scientists, and Ph.D. thesis students.

Institution	Physicist	Engineer	Technical
Argonne	3.5	0.3	1.5
Boston College	0.3	0	0
Caltech	0.7	0	0.7
Columbia	0.7	0.1	0
Dubna	3.8	0.9	0.5
Fermilab	8.1	0	1.5
IHEP-Beijing	1.2	0.7	1.2
Indiana	3.4	0	0
ITEP-Moscow	0.4	0.4	0.6
Lebedev	0.6	0.6	0.4
Livermore	1.5	1.3	1.2
Minnesota	2.5	0.7	0.7
PNPI-St.Petersburg	1.5	2.8	0.6
Oak Ridge	0	0.3	0
Oxford	2.3	1.5	2.5
Rutherford	2.1	0.3	0
Stanford	1.0	0	0
Sussex	0.4	0.2	0
Texas A&M	0.7	0	0.1
Texas-Austin	0.4	0	0.5
Tufts	1.3	0	0.2
W. Washington	0.3	0	0
Totals:	36.7	10.1	12.2

Table 29: Current FTE effort levels at MINOS collaborating institutions.

References

- [1] The MINOS Collaboration, "P-875: A Long-baseline Neutrino Oscillation Experiment at Fermilab," Fermilab report NuMI-L-63, February 1995.
- [2] The MINOS Collaboration, "Addendum to P-875: A Long-baseline Neutrino Oscillation Experiment at Fermilab," Fermilab report NuMI-L-79, April 1995.
- [3] R.A. Rameika, "Fermilab Neutrino Oscillation Program, Cost and Schedule Data," Fermilab report NuMI-90, May 1995.
- [4] The MINOS Collaboration, "MINOS Answers to HEPAP Subpanel Questions," Fermilab report NuMI-L-96, June 9, 1995.
- [5] The Fermilab NuMI Group and the MINOS Collaboration, "Fermilab Answers to HEPAP Subpanel Supplemental Questions," Fermilab report NuMI-L-100, July 14, 1995.
- [6] Report of the High Energy Physics Advisory Panel, Subpanel on Accelerator-based Neutrino Oscillation Experiments, U.S. Department of Energy report DOE/ER-0662, September 1995.
- [7] The MINOS Collaboration, "MINOS Detector R&D Plan," Fermilab report NuMI-L-130, January 5, 1996.
- [8] P.F. Harrison, D.H. Perkins and W.G. Scott, *Phys. Lett* **B349**, 137 (1995).
- [9] *Nuclear Instruments and Methods* **A366**, 263 (1996).
- [10] M. Libkind, "Design Description (including costs) for MINOS Steel," Fermilab report NuMI-L-103, May 17, 1995.
- [11] M. Libkind and J. Swan, "Basis of Estimate: MINOS magnet coils, far detector (Feb. 14, 1995); MINOS magnet coils, near detector (March 18, 1995); MINOS steel, far detector (April 19, 1995); MINOS steel, near detector (April 18, 1995)," Fermilab report NuMI-L-104.
- [12] H.M. Gallagher and M.C. Goodman, "Tau neutrino cross sections," Fermilab report NuMI-112, 1995.
- [13] M. R. Adams *et al.*, *Z. Phys. C.* **67**, 403 (1995).
- [14] J. Morfin, Private Communication.
- [15] D. Rein and L. Seghal, *Ann. Physics (NY)*, **133**, 79 (1981).
- [16] R. P. Feynman, M. Kislinger, and F. Ravndal, *Phys. Rev.* **D3**, 2706 (1971).
- [17] S. L. Adler, *Annals of Physics*, **50**, 189 (1968).
- [18] G. L. Fogli and G. Nardulli, *Nuclear Physics* **B160**, 116 (1979).

- [19] P. Lipari *et al.*, ROMA Preprint No. 1072, (1994).
- [20] Giles Barr, Ph. D. Thesis, Oxford University, (1987).
- [21] Z. Koba, H. B. Nielsen, P. Olesen, Nuclear Physics **B40**, 317 (1972).
- [22] T. Sjöstrand, Computer Physics Commun. **39**, 347 (1986).
- [23] T. Sjöstrand and M. Bengtsson, Computer Physics Commun. **43**, 367 (1987).
- [24] G. Ingleman and T. Sjöstrand, Phys. Rep. **97**, 31 (1983).
- [25] S. A. Rabinowitz *et al.*, Phys. Rev. Lett **70**, 134 (1993); C. Foudas *et al.* Phys. Rev. Lett., 1207 (1990); B. Strongin *et al.* Phys. Rev. **D43**, 2057 (1990); H. Abramowicz *et al.* Z. Phys. **C15**, 19 (1982).
- [26] H. C. Ballagh *et al.* Phys. Rev. **D24**, 7 (1981); M. Murtagh *et al.* Phys. Rev. Lett. **42**, 1721 (1979).
- [27] R. Brock, private communication. Also see R. Phillips, Nucl. Phys. *B212*, 109 (1983).
- [28] W. Allison *et al.*, "Update to Fermilab Proposal P-822; Proposal for a Long Baseline Neutrino Oscillation Experiment from Fermilab to Soudan," Fermilab report NuMI-L-4, March 8, 1994.
- [29] David A. Petyt, "A consistent three-generation approach to MINOS analysis," NuMI-L-129, December 1995.
- [30] A. DeRújula *et al.*, Nucl. Phys. **B168**, 54 (1980).
- [31] V. Barger, K. Wishnant and R.J.N. Phillips, Phys. Rev. **D22**, 1636 (1980).
- [32] J.H. Cobb, "Errors on Δm^2 and $\sin^2(2\theta)$ from CC energy measurements," NuMI-L-88, May 1995
- [33] G.L. Fogli, E. Lisi and G. Scioscia, Phys. Rev. **D52**, 5334 (1995).
- [34] C. Athanassopoulous *et al.*, Phys. Rev. Lett. **75**, 2650 (1995).
- [35] P. Martin and J. Johnstone, Main Injector technical note, in preparation.
- [36] D.A Crane *et al.*, "Status report: Technical design of neutrino beams for the Main Injector (NuMI)," Fermilab report NuMI-B-92, June 1995.
- [37] J.H. Cobb, "A method for the detection of neutrino oscillations in a long baseline experiment using energy measurements of ν_μ charged current events," Nuclear Instruments and Methods **A373**, 501 (1996).
- [38] Janet Conrad and the CCFR collaboration, private communication; presented at the Indianapolis APS meeting and the Fermilab User's Meeting. They refer to this as the "eta" test.